SUPERCRITICAL FLUID EXTRACTION OF MINERALS IN MARTIAN SOILS

By

Tong Wang

Dissertation

Submitted to the Faculty of the

Graduate School of Vanderbilt University

in partial fulfillment of the requirements for

the degree of

DOCTOR OF PHILOSOPHY

in

Chemical Engineering

December, 2005

Nashville, Tennessee

Approved:

Professor Kenneth A. Debelak

Professor John A. Roth

Professor G. Kane Jennings

Professor Alan R. Bowers

Professor Bridget R. Rogers

To my Mother and Father

Whose love is always with me

ACKNOWLEDGEMENTS

I would like to express my sincere appreciation to my advisor, Dr. Kenneth A. Debelak and Dr. John A. Roth, for the guidance, patience and leadership during my doctoral studies at Vanderbilt. They always treated me with kindness and respect in my studies and research work. I appreciate their time and knowledge. They have played an important role in shaping my understanding of the research field.

I thank my outstanding doctoral committee members, Dr. G. Kane Jennings, Dr. Bridget R. Rogers and Dr. Alan R. Bowers for they good advice and suggestions for my research.

I want to thank the faculty and staff from the Vanderbilt University Chemical Engineering Department. In particular, Margarita Talavera and Mary Gilleran have been provided me with information, help and support throughout my time in Vanderbilt. Thanks to all of my colleagues who have helped me during my stay here. I also thank all my friends who provide their help and support as they can.

Finally, I acknowledge that I am much indebted to my dear parents and other family for their love and support in my academic pursuit as well as in my life journey. I could not have been possible to finish any work without their support and encouragement. I hope that someday I can return to them the unquestioning love and selflessness that they have given me.

TABLE OF CONTENTS

LIST OF TABLES

LIST OF FIGURES

NOMENCLATURE

a	Parameter in a cubic equation of state
b	Parameter in a cubic equation of state
c	Molar concentration
c_p	Constant-pressure molar heat capacity
ε	Error of nonlinear least square
E	Enhancement factor
f	Fugacity; function
H	Enthalpy
k_{12}	Interaction coefficient
n	Number of moles
P	Pressure
R	Gas constant
S	Sum of the residuals
t	Extraction time
T	Temperature
v	Molar volume
V	Total volume
Y	Mole fraction
Z	Compressibility factor

Greek Symbols

φ	Fugacity coefficient

ω Acentric factor

Subscripts

c Critical property

i Component i

j Component j

Superscripts

F Supercritical fluid phase

G Gas phase

PureS Pure solid

S Solid phase

Sat Saturated property

Abbreviations

AA Atomic absorption spectrometer

AXPS The mobile alpha proton x-ray spectrometer

DSC Differential Scanning Calorimetry

EOS Equation of state

JSC Mars-1 A Mars simulant soil from the Johnson space flight center

LLE liquid- liquid equilibria

MLLS Marquardt-Levenberg least squares method

PR Peng-Robinson equation of state

SFE Supercritical fluid extraction

SCF A supercritical fluid

SRK Soave-Redlick-Kwong equation of state

TGA Thermo gravimetric analyses

VLE Vapor-liquid equilibria

VLLE Vapor-liquid-liquid equilibria

XRF X-Ray-Fluorescence

CHAPTER I

INTRODUCTION

Mars is the fourth planet from the Sun. It is more like Earth than any other body in our solar system. It has polar ice caps, seasons, an atmosphere with clouds, winds and dust storms, and a solid rocky surface. Compared to other planets in our solar system, Mars is the only place that humans can support a possible settlement in the future. The Mars Exploration Program is a science-driven program that seeks to understand whether Mars was, or can be, a habitable world. Among all discoveries about Mars, one stands out above all others: the possible presence of liquid water on Mars. Water is key because almost everywhere we find water on Earth, we find life. Even if Mars is devoid of present life, however, we ourselves might become the "life on Mars". Humans could travel there one day in the future. When astronauts first go to Mars, it will be difficult for them to bring everything they need to survive. For supporting life on Mars, in-situ resources must be recovered. This will tremendously lower the weight of manned ships, and thus the cost.

The Viking Lander missions have provided data of the composition on Martian soils. The chemical analysis of Martian soil has been reported in several publications [1,2,3,4]. Table 1.1 shows the elemental concentration of Martian soil determined by the Viking Lander X-Ray fluorescence spectrometers [3]. Two landing sites of Viking 1 and Viking 2 were about 6500 km apart from each other. The Viking X-ray fluorescence spectrometers cannot detect elements of atomic number less than 12. Therefore, some of

the important elements in mineral formation such as C, N and Na cannot be detected. The most recent data on the chemical composition of Martian soils come from the mobile alpha proton x-ray spectrometer (AXPS) on board the rover of the Mars pathfinder [9]. These data are shown in Table 1.1. The Mars Pathfinder mission measured the chemical composition of six soils and five rocks at the Ares Vallis landing site. The soil analyses show similarity to those determined by the Viking missions. All soil samples have been normalized to 44% by weight of silica. Their high concentration of iron is reported as Fe_2O_3. Aluminum and magnesium are low compared to the amounts of most basalts found on the earth and moon. The mineralogical composition is dominated by the silicate minerals (80%) [4]. Since the concentration of S and Cl is relatively high, the Martian soil might contain a high amount of sulfate and chloride salts. The composition profile of Martian soil is different from that found on the earth. It is a challenging task to extract useful materials from in-situ resources on Mars.

Table 1.1: Chemical composition of Martian regolith and simulated JSC Mars-1

	Viking Lander I [3]	**Viking Lander II** [3]	**A-4, Soil After deploy** [9]	**A-5, Soil Next to Yogi** [9]	**JSC Mars-1** [8]
SiO_2	44	43	48±2.4	47.9±2.4	43.7
TiO_2	0.62	0.54	1.4±0.2	0.9±0.1	0.65
Al_2O_3	7.3	7	9.1±0.9	8.7±0.9	23.4
Fe_2O_3/FeO	17.5	17.3	14.4±1.4	17.3±1.7	15.3
MgO	6	6	8.3±1.2	7.5±1.1	3.4
CaO	5.7	5.7	5.6±0.8	6.5±1.0	6.2
K_2O	<0.5	<0.5	0.2±0.1	0.3±0.1	0.6
SO_3	6.7	7.9	6.5±1.3	5.6±1.1	Not analyzed
Cl	0.8	0.4	0.6±0.2	0.6±0.2	Not analyzed
Other	2	2			
Total	91	90			

Supercritical fluid extraction (SFE) has become an increasingly popular technique for the extraction and recovery of a wide range of organometallic and inorganic analyses. Many investigators have studied the solvent behavior of supercritical fluids. The solvating strength of a supercritical fluid is directly related to the density. The density of the supercritical fluid can be varied by controlling the pressure and temperature. Supercritical fluids have densities and solvating properties similar to liquid solvents, but have extremely rapid diffusion characteristics and viscosities closer to those of gases. We wish to take advantage of these solvating properties to recover minerals from the Martian surface soils and its igneous crust. Carbon dioxide in the Martian atmosphere can be used as the solvent. Carbon dioxide, the most common supercritical fluid, is an excellent alternative solvent to common organic solvents. It has many advantages including enhanced diffusivity (mass transfer), chemical stability, and ease of sample separation. The Martian atmosphere is composed mostly of carbon dioxide (~ 95.3%) and could therefore provide an in-situ source of carbon dioxide as a supercritical solvent. It may be feasible to use supercritical carbon dioxide to recover minerals from Martian soils.

This research includes three parts. The first part is screening for soluble species in supercritical carbon dioxide. We would like to know what kind of minerals in Martian soil could be extracted in supercritical carbon dioxide. The screening samples include the JSC Mars-1, the simulated Martian regolith, and some inorganic compounds such as metal sulfates, chlorides, carbonates, nitrates and oxides. Samples of the simulant JSC Mars-1 were obtained from the Johnson space flight center. Allen et al. [8] have developed a simulant of the regolith of Mars for support of scientific research, engineering studies, and education. The simulant, JSC Mars-1, was collected from Pu’u

Nene cinder cone, located in the saddle between Mauna Loa and Mauna Kea volcanoes on the Island of Hawaii. The chemical composition of this material is given in the Table 1.1. The chemical composition of the JSC Mars-1 determined by X-Ray fluorescence is similar to the Martian soil [6,7]. Additional compounds were prepared based on current knowledge of the composition of Martian soils [8].

The second part is a study focused on dehydration properties of several species such as ferrous sulfate and calcium sulfate. Recent data [10] obtained by the Gamma-Ray Spectrometer on the Mars Odyssey probe have identified two regions near the poles that are enriched in hydrogen. In the upper layer, hydrogen is present in the form of physically or chemically bound water. The upper layer may be mixed with a middle layer, since ice is not stable in the middle layer. In the deeper layer, ice may be the only reasonable phase in which hydrogen is present. Hydrated species could be present on the upper and middle layer of Mars. The Martian soils could contain large quantities of hydrated compounds, e.g., ferrous sulfate and calcium sulfate. This is inferred from a high concentration [4] (nearly 12%) of sulfate salts and a high concentration of iron and calcium in the Martian surface. We focused on the dehydration properties of ferrous sulfate and calcium sulfate. The results of the screening for soluble species of simulated Martian regolith and inorganic samples show that the hydrated compounds have significant weight change when extracted in supercritical carbon dioxide. Therefore, it may be possible to extract the physically or chemically bound water from hydrated compounds using supercritical carbon dioxide. We did further tests on ferrous sulfate and calcium sulfate to determine the temperatures at which waters of hydration can be removed and to estimate the bond energy in the dehydration process.

In the third part, we used a surfactant (a high performance perfluoropolyether) and water to enhance the solubility of metals in supercritical carbon dioxide. Direct extraction of metal ions by supercritical carbon dioxide is known to be highly inefficient because of the charge neutralization requirement and the weak solute-solubility in pure supercritical carbon dioxide [11,12,13,14]. Yazdi and Beckman [15] have shown that adding highly fluorinated ligands can enhance the solubility of metal complexes. By addition of a complex agent into the supercritical phase, the metal ion charge can be neutralized and the lipophilic groups can be introduced to the metal-complex system. The addition of a complex agent makes the solubilization of the metal complex into the supercritical carbon dioxide possible. The surfactant we chose is a high performance perfluoropolyether ammonium carboxylate (PFPE-NH_4). This perfluoropolyether surfactant has a long nonpolar organic chain which helps make it soluble in the supercritical carbon dioxide. There are a number of fluorine atoms attached at different positions along the chain. These help the surfactant to trap the metal ions in the supercritical phase. Experimentation focused on two issues. One is to study how the experimental conditions (extraction pressure, extraction temperature, amount of surfactant, amount of water) affect the metal complex solubility in supercritical CO_2. The other is to determine the solubility of cupric nitrate trihydrate and magnesium chloride hexahydrate at best extraction conditions as a function of pressure.

Solubility is a function of pressure and temperature. It indicates the relative extractability of a substance and sets the limit of extractability. Therefore, solubility is one of the keys to achieve quantitative extraction in a reasonable time using a minimum amount of fluid. An accurate metal-chelate complex solubility database has become more

and more important. However, it is not practical to obtain the solubility data over all pressures and temperatures. Therefore, we modeled the solubility of metal-chelate components in supercritical carbon dioxide. A thermodynamic model consisting of the mixing rules and the Peng-Robinson equation of state was used to correlate the experimental data. Interaction parameter and other modeling constants were determined by regressing the experimental data using standard statistical methods. The goal is to predict the solubility of metal complex in supercritical carbon dioxide at varying operating conditions.

References

1. Jan Osburg, *Space Missions to Mars: Past, Present and Future*. Research Paper, Georgia Institute of Technology School of Aerospace Engineering. Atlanta, GA, 1998.

2. David R. Williams. (1977). Viking Mission to Mars, Viking Project Information. *The Journal of Geophysical Research*, **1997**, 82, 28.

3. Clark B.C.,A.K.Baird, R.J. Weldon,, D. M. Tsuaki, L. Schnabel, and M. P. Candelaria. Chemical Composition of Martian Fines. *J. Geophys.* **1982**, 87, 10059-10067.

4. Stroker C.R., *The Physical and Chemical Properties and Resource Potential of Martian Surface Soils*. Resources of near-earth space.Univ. of Arizona press. **1993**, 659-708.

5. James F. Bell III., *Iron, Sulfate, Carbonate, and Hydrated Minerals on Mars*. Geochemical Society Special publication No. 5., **1996**.

6. Rieder R, T. Economou, H. Wanke, A. Turkevich, J. Crisp. The Chemical Composition of Martian Soil and Rocks Returned by the Mobile Aipha Proton X-ray Spectrometer: Preliminary Results from the X-ray Mode. *Science*, **1997**, 278, 1771-1774.

7. Klaus S. Lackner, Christopher. H. Wendt. Carbon Dioxide Disposal in Carbonate Minerals. *Energy* , **1995**, 20, 1153-1170.

8. Carlton C. Allen, Richard V. Morris, and David J. Lindstrom, *JSC Mars-1: Martian Regolith Simulant*. NASA Johnson Space Flight Center, Houston,TX , **1997**.

9. Rieder R, T. Economou, H. Wänke, * A. Turkevich, J. Crisp, J. Brückner, G. Dreibus, H. Y. McSween Jr. The Chemical Composition of Martian Soil and Rocks Returned by the Mobile Alpha Proton X-ray Spectrometer: Preliminary Results from the X-ray Mode. *Science*, **1997**, 278**,**1771-1774.

10. Boynton WV, Feldman WC, Squyres SW, Prettyman TH. Distribution of Hydrogen in the Near Surface of Mars: Evidence for Subsurface Ice Deposits. *Science*, **2002**, 297, Issue 5578, 81-85.

11. Laintz, K. E., Yu, J., Wai, C. M., Smith, R. D. Separation of Metal Ions with Sodium Bis(trifluoroethyl)dithiocarbamate Chelation and Supercritical Fluid Chromatography. *Analytical Chemistry*, **1992**, 64, 311-315.

12. Laintz, K. E., Wai, C. M., Yonker, C. R., Smith, R. D. Extraction of Metal Ions from Liquid and Solid Materials by Supercritical Carbon Dioxide. *Analytical Chemistry*, **1992**, 64, 2875-2878.

13. Lin, Y., Wai, C. M., Jean, F. M., Brauer, R. D.. Supercritical Fluid Extraction of Thorium and Uranium Ions from Solid and Liquid Materials with Fluorinated Diketone and Tributyl Phospate. *Environ. Sci. Technol*, **1994**, 28, 1190-1193.

14. Lin, Y., Brauer, R. D., Laintz, K. E., Wai, C. M.. Supercritical Fluid Extraction of Lanthanides and Actinides from Solid Materials with Fluorinated Diketone. *Analytical Chemistry*, **1993**, 65, 2549-2551.

15. Ali V. Yazdi and Eric J. Beckman. Design of Highly CO_2-Soluble Chelating Agents. 2. Effect of Chelate Structure and Process Parameters on Extraction Efficiency. *Ind. Eng. Chem. Res, **1997**,* 36 (6), 2368 -2374.

CHAPTER II

LITERRATURE REVIEW AND THERMODYNAMIC THEORY OF SUPERCRITICAL EXTRACTION

Literature review of supercritical extraction

Background of supercritical extraction

A supercritical fluid (SCF) is “any substance, the temperature and pressure of which are higher than its critical values, and which has a density close to or higher than its critical density” [1]. The boundary of gas-liquid disappears when both pressure and temperature exceed their critical values. A typical pressure-temperature phase diagram for a pure component shows that it passes directly from a liquid phase to a gas phase without phase separation simply by taking a path through the supercritical region of the phase diagram, the carbon dioxide -phase diagram is shown in Figure 2.1 [2].

A substance becomes a supercritical fluid (SCF) when compressed to a pressure and elevated to a temperature greater than that of its critical point (see Figure 2.1). The density of gas increases as the pressure increases. The density of the liquid decreases because of thermal expansion as the temperature increases. At the critical point, the density of gas and liquid become identical as the pressure and temperature increase. The difference between gas phase and liquid phase disappears, and a supercritical fluid is formed. Although a supercritical fluid (SCF) is a single phase, it exhibits properties of both liquid phase and gas phase. Supercritical fluid has density and solvating properties similar to a liquid. Solubility increases with density and pressure; thus, SCFs have a high

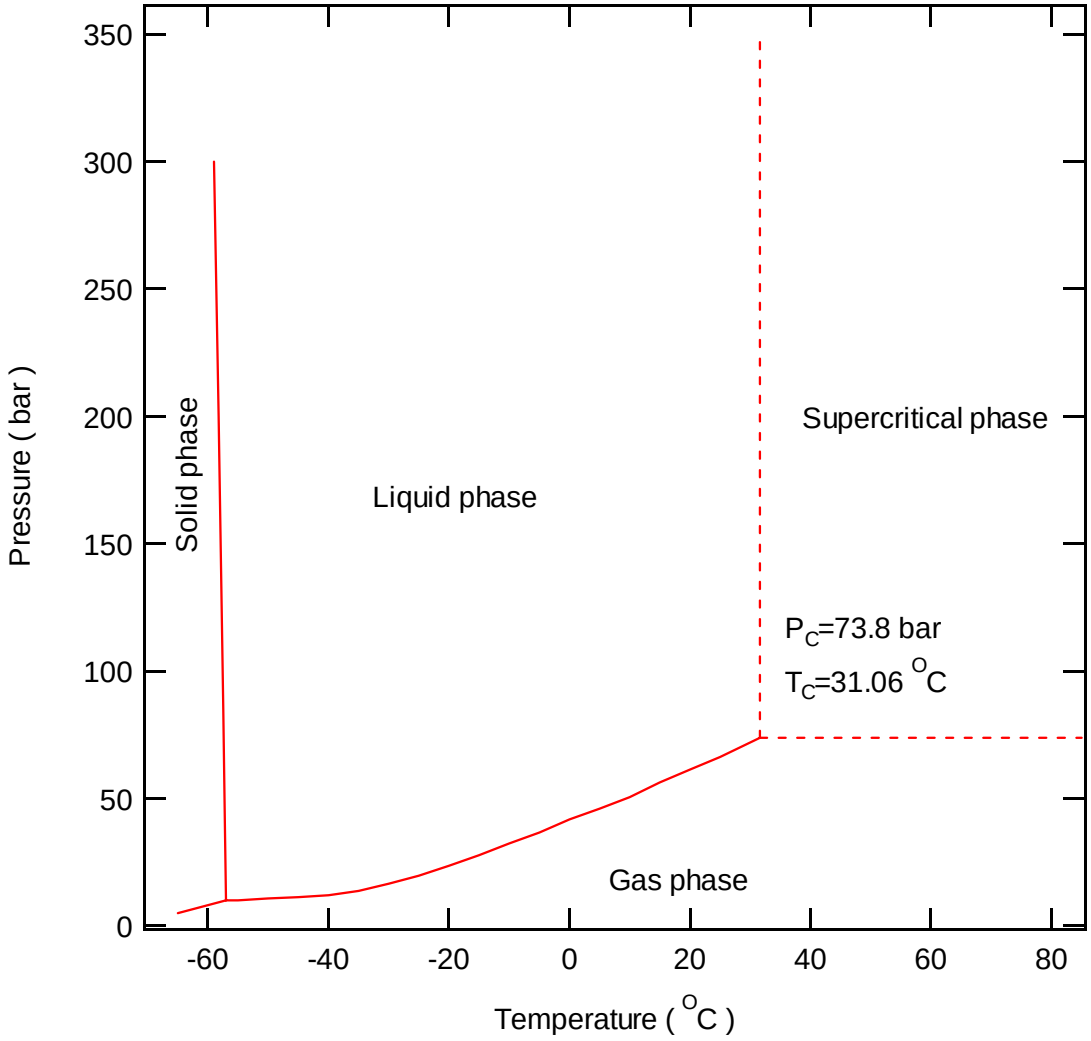

Figure 2.1: P-T phase diagram for carbon dioxide [2].

absorption capacity. Supercritical fluids also have extremely high diffusivity and low viscosity properties closer to gases. These properties promote high mass transfer rates between a solute and a supercritical fluid.

In 1879, Hannay and Hogarth [3] first discovered that solid solubility increased significantly in supercritical fluid by studying the solubility of cobalt (II) chloride, iron (III) chloride, potassium bromide, and potassium iodide in supercritical ethanol (Tc=243°C Tp=63 atm). They also found that decreasing the pressure around critical pressure caused the solutes to precipitate significantly as a “snow”.

Zhuse [4] reported the first industrial application in 1951. The food and beverage industry was the first to make commercial use of supercritical carbon dioxide extraction. Replacing conventional organic solvents with SCFs in extraction procedures is a major advancement in today's pollution prevention programs. Supercritical fluid extraction can be used for waste separation and minimization, as well as solvent recycling. Other advantages of supercritical extraction include high efficiency, high extraction rates and greater selectivity. In 1970, Zosel [5] reported the decaffeination of green coffee with carbon dioxide. This was a significant development in supercritical extraction. The application of supercritical carbon dioxide in the food industry is widely used for extraction of organics. Table 2.1 shows some typical industrial supercritical extraction processes [4-6].

The process of supercritical fluid extraction is relatively simple. The extraction system usually consists of an extractor, controller, and pump. A fluid is pumped through the extractor from its storage vessel. The system controller maintains the pressure and temperature. The pressure and temperature are increased to the compound's supercritical

conditions in the extractor. A continuous stream of the SCF is supplied to the extractor where it absorbs the contaminant. The solvent and solute stream travel to the expansion vessel. Here, as the pressure decreases, the solubility of the solute decreases and the two components separate. The contaminant is collected and the extracting fluid is recycled back to the storage tank for reuse.

Table 2.1: Fundamentals and applications of supercritical fluid technology

Application scope	Supercritical fluid	Industrial condition, T (^oC)	Industrial condition, P (Mpa)
Lemon oil extraction	CO_2	40	30
Nicotine extraction	CO_2	50~70	15~30
Hops extraction	CO_2	45~55	31.9~40.5
Coffee decaffination	CO_2	90	16.2~22.3
Lipid extraction from bean, sunflower	CO_2	35~75	20.7~62.0
Essence extraction from black pepper	CO_2	30~50	150~300
Oil extraction from almond	CO_2	40	60
Oil extraction from fennel and cinnamon	CO_2	40	8~9
Flavoring extraction from pineapple	CO_2	0~40	8~20
Oil extraction from corn	Propane	50	35
Coal extraction/liquidation	Benzene	350~400	10
Asphaltum from petroleum	Propane	100	9.1~11.1
Waste residue refine	CO_2	32~55	7.4~55.2
Petroleum resideue extraction	Propane	140	11.1~12.2

Properties of supercritical fluids

The carbon dioxide pressure-temperature phase diagram, a typical diagram for a pure component, is shown in Figure 2.1. There are three lines---melting line, boiling line and liquid line. These lines define the regions corresponding to the gas, liquid and solid. Each line represents the equilibrium state of the gas-liquid, liquid-solid and gas-solid phase. The boiling line starts at the triple point and ends at the critical point. Table 2.2

gives the Tc, Pc and boiling point for some typical supercritical fluids [7,10]. Supercritical fluids have the properties of both a liquid and a gas. Supercritical fluids have densities similar to liquids. Therefore, supercritical fluids have a relatively high liquid-like density. In general, the solubility of a compound in a supercritical fluid is related to its vapor pressure and density. Solubility increases with density and pressure, thus, supercritical fluids have a high absorption capacity. Supercritical fluids also have rapid diffusion and low viscosity close to those of gases. The gas-like properties allow for high mass transfer rates between a solute and a supercritical fluid. Table 2.3 shows the typical values for the density, viscosity, and diffusivity coefficients of a gas, supercritical fluid, and liquid by order of magnitude [8].

Table 2.2: Critical data for selected substances [7, 10].

Gas	Boiling point (K)	Supercritical temperature Tc (K)	Supercritical pressure Pc (Mpa)
CO_2	194.7	304.2	7.38
C_2H_4	161.4	282.4	5.13
NO	121.4	180	6.48
C_2H_6	184.5	305.4	4.94
$CClF_3$		28.9	3.71
C_3H_8	231.1	369.8	4.26
H_2O	373.15	647.3	21.83
NH_3		405.6	11.25
H_2S		373.5	8.89

Table 2.3: Properties of supercritical fluids vs. gases and liquids [8].

	Gas	Supercritical fluid	Liquid
Density (g/cm^3)	10^{-3}	0.1 ~ 1	1
Diffusion coefficient (cm^2/s)	10^{-1}	$10^{-3} \sim 10^{-4}$	$< 10^{-5}$
Viscosity (g/cm.s)	10^{-4}	$10^{-3} \sim 10^{-4}$	10^{-2}

The most important property for a supercritical fluid is the density. The higher the supercritical fluids density, the higher the solubility. This behavior is illustrated in Figure 2.2 [9]. At the low temperature of 310 K, the density changes dramatically around the critical pressure. Above 310 K, the change becomes small with increasing temperature. This means the property of density can be controlled by both pressure and temperature around critical temperature and critical pressure. Reducing the pressure decreases the solubility of the solute very quickly and the solute can be separated very easily by reducing the pressure.

The temperatures normally employed for supercritical fluid are in the range of room temperature to 200°C as shown in Table 2.2. The materials to be used for supercritical fluid have more available with lower critical temperature. From Table 2.2 we observe that carbon dioxide is a suitable substance for use as a supercritical fluid. Supercritical extraction has high efficiency, high extraction rates and greater selectivity. A major advantage of supercritical carbon dioxide extraction is that conventional organic solvents can be replaced by supercritical carbon dioxide in extraction procedures. Its non-toxic and non-combustible properties make it environmentally friendly. This is a major advancement in today's pollution prevention programs. Supercritical carbon dioxide has a higher density than most of the other supercritical fluids. But supercritical carbon dioxide has a lower critical temperature and pressure than most of the others. Therefore, supercritical carbon dioxide extraction energy costs are lower than those of other fluids. Supercritical carbon dioxide is also commercially available in high purity. Therefore, supercritical carbon dioxide is a popular and inexpensive solvent used in supercritical extraction.

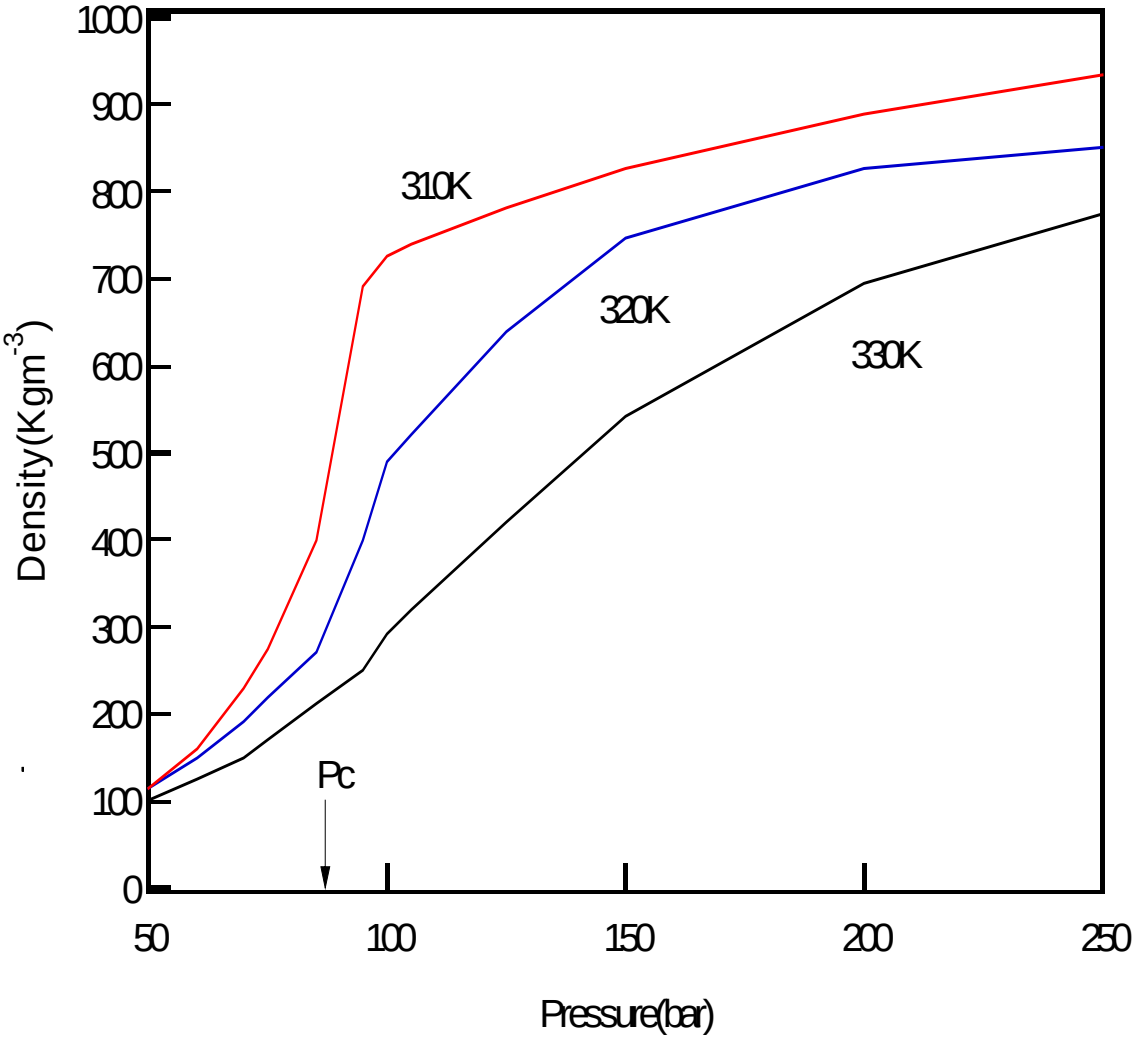

Figure 2.2: Density-pressure isotherms for carbon dioxide [9].

Literature review of solubility of organic material in supercritical carbon dioxide

The solubility of solutes in supercritical fluids is very important to establish the technical and economic feasibility of any supercritical fluid extraction process and separation operations. A large number of investigations on solubility have been made in recent years. The experimental data and methods have been reported in several review articles [11-17]. Knapp et al. (1981)[11] reviewed the high-pressure phase-equilibrium data covering the period from 1900 to 1980. Fornari et al. (1990)[13] reviewed the phase-equilibrium data covering the period from 1978 to 1987. Bartle et al. [14] reviewed the solubility of solids and liquids of low volatility in supercritical carbon dioxide that have been published through 1989. Bartle [14] included experimental solubility in supercritical carbon dioxide, the temperature and pressure ranges of the experimental process, the experimental method, and references to the data sources. Dohrn and Brunner [15] give an overview about high-pressure phase equilibrium data that have been published from 1988 to 1993, including vapor-liquid equilibria (VLE), liquid- liquid equilibria (LLE), vapor-liquid-liquid equilibria (VLLE), and the solubility of high-boiling substances in supercritical fluids. Lucien and Foster [16] reviewed the solubility of solid mixtures in supercritical carbon dioxide. They indicated that the solubility of a solid that mixed with a second solid might be enhanced significantly compared to its binary systems. They gave an extensive compilation of solubility enhancement data of solid mixtures. For most S-V equilibrium systems, they found that the solubility enhancement could be explained in terms of an entrainer effect. For S-L-V equilibrium, the solubility enhancement depends heavily on which specie is present as an excess solid phase.

Literature review of solubility of inorganic material in supercritical carbon dioxide

Most of the investigations on solubility have been concerned with organic systems. Solubility data for inorganic systems have been reported less frequently. Tolley and Tester [18] used supercritical carbon dioxide in extractive metallurgy. They determined the solubility of titanium tetrachloride ($TiCl_4$) in supercritical carbon dioxide, as shown in Figure 2.3. Titanium tetrachloride is highly soluble in supercritical carbon dioxide. Solubility initially decreases as the pressure rises from ambient pressure to near the supercritical pressure, and then it increases dramatically as the pressure rises around the supercritical point. As the pressure was increased above 1500 psig, titanium tetrachloride and carbon dioxide were found to be completely miscible at any combination of temperature and pressure.

In some cases, however, direct extraction of metal ions by supercritical carbon dioxide is known to be highly inefficient because of the charge neutralization requirement and the weak solute-soluble in pure supercritical carbon dioxide [19-22]. The metal ions must be present as electrically neutral complexes to be extracted by supercritical carbon dioxide. Laintz et al. [23] first reported the use supercritical fluids modified by the addition of complex agents in extraction of metal ions from liquid and solid materials. This has opened up a new area of research for the use of supercritical fluids as solvents.

The currently modification of supercritical fluids focuses on three potential applications including environmental treatment, metallurgical processing, and electronic materials/ceramics production. The solubility of the metal-chelate complex in the supercritical fluid is the most important property. It needs to be determined to develop

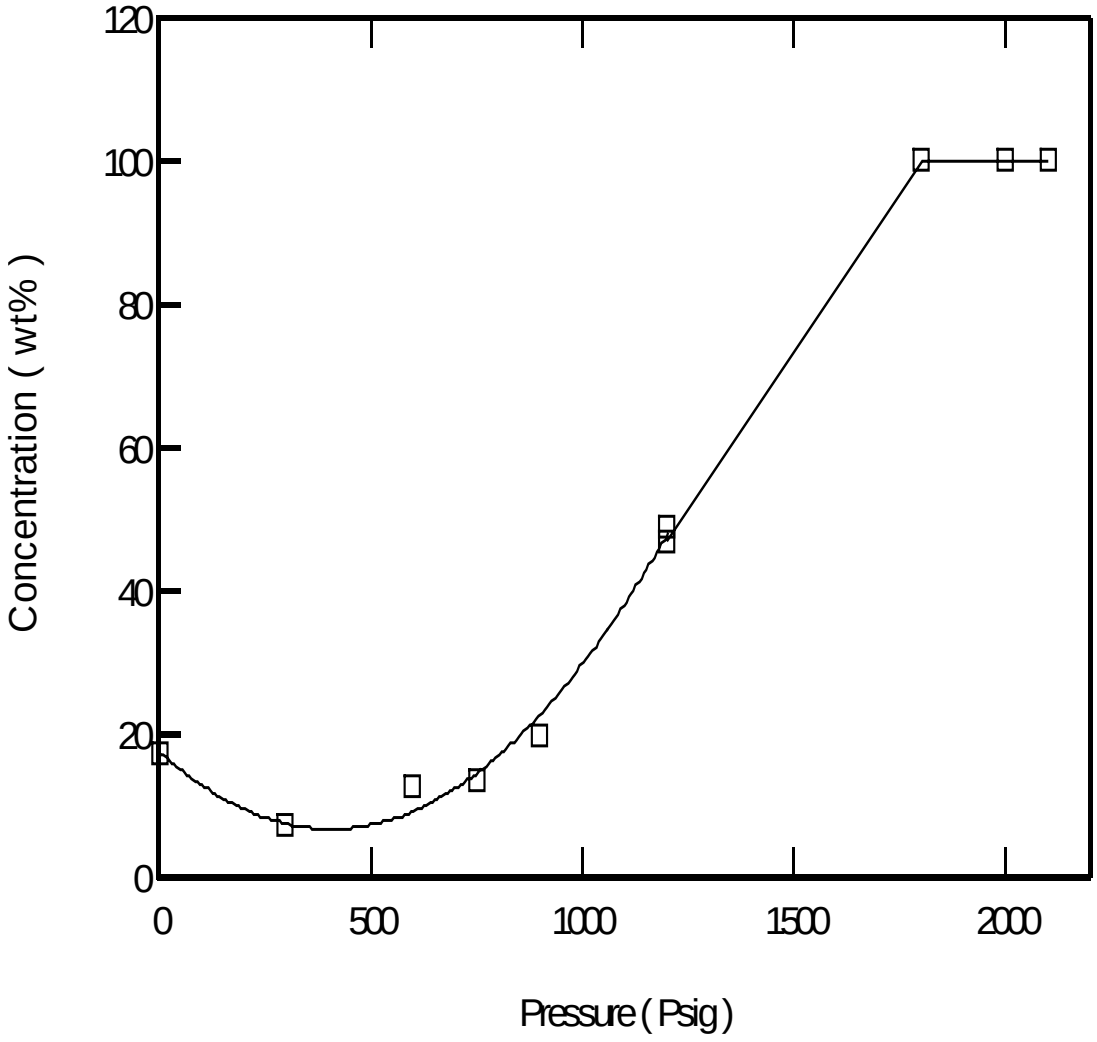

Figure 2-3. $TiCl_4$ solubility in supercritical carbon dioxide at 56°C [18].

any of extraction technologies. Metal complex solubility and metal extraction using chelating agents have recently been widely investigated [24-32].

Solubility is a function of pressure and temperature. It indicates the relative extractability of a substance and sets the limit of extractability. Therefore, solubility is one of the keys to achieve quantitative extraction in a reasonable time using a minimum amount of fluid. An accurate metal-chelate complex solubility database has become more and more important. In recent studies, the solubility is focused on the metal-chelate complex solubility rather than the solubility of the chelating agent itself. The metal-chelate complex solubility rather than the solubility of the chelating agent itself would be the limiting factor. The chelate is more soluble in supercritical fluid because the chelate is organic.

A widely used chelating agent is diethyl dithiocarbamate (DDC), which forms stable complexes with over 40 metals and nonmetals. Yazdi and Beckman [33] have shown that adding highly fluorinated ligands enhances the solubility of metal complexes. The metal recovery efficiencies approach 87%. Laintz [34] showed that the solubility was enhanced by several orders of magnitude by substituting fluorine for hydrogen in the ligand. Lin et al. [21,22] has shown that the presence of a small amount of water would increase significantly the metal-chelate complex solubility in modified supercritical carbon dioxide. Jonston et al. [41] and Eastoe et al. [42] first demonstrated that a perlluoropolyether ammonium carboxylate surfactant was effective in forming water microemulsion droplets (< 10 nm in diameter) in supercritical carbon dioxide. However, the affect of this small amount of water on the solubility of the metal complex is not well understood.

Experimental methods of measuring the solubility in supercritical carbon dioxide

There are many ways to measure the solubility in supercritical fluids. All these methods can be divided into two classifications depending on how the compositions are determined. One is the analytical method or direct sampling method, and the other is the synthetic method or indirect method. The analytical method requires chemical analysis to determine the composition of the coexisting phases at equilibrium. The synthetic method or indirect method involves an indirect determination of equilibrium composition without sampling. The idea of this method is to prepare a mixture of known composition and then investigate the phase behavior in an equilibrium cell.

Most techniques used for measuring solubility of solid components in supercritical fluids are analytical methods. These methods can be classified into four different categories depending on the analysis methods: a) gravimetric methods, b) chromatographic methods, c) spectroscopic methods, d) miscellaneous methods [13].

A gravimetric method is most widely used for investigation of solubility in supercritical fluids. The basic idea is to reach a coexisting equilibrium phase in an extraction cell. The procedure includes passing the supercritical fluid through the sample, dropping the pressure to precipitate the solute, and weighing the sample. A schematic diagram of a basic system is shown in Figure 2.4 [14]. A typical experiment involved setting the flow and allowing the system to reach a steady state. A preweighted trap or cell is introduced to the system while the rate of flow of carbon dioxide is monitored. The cell was reweighted and the total mass of carbon dioxide passed the cell in the period was calculated. The solubility can be obtained in terms of mole fraction. Experimental errors are quoted in the range of 3-5% for solubility data.

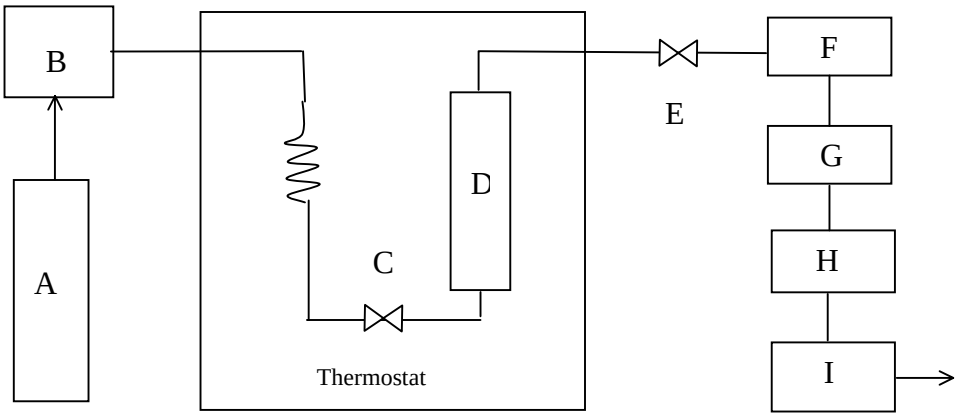

Figure 2.4: Schematic diagram of the gravimetric method (A: CO_2 cylinders; B: CO_2 pump; C: supply valve; D: extraction cell; E: vent valve; F: analyte valve; G: restrictor and restrictor fitting; H: collection vessel; I: flow meter).

Thermodynamic theory of supercritical extraction

Thermodynamic basis

For solid-supercritical fluid equilibrium, we have the following equilibrium relations for component i:

$$f_i^F = f_i^S \; ; \; T_i^F = T_i^S \; ; P_i^F = P_i^S \tag{2-1}$$

where f_i^F is the fugacity of component i in the supercritical fluid phase and f_i^S is that in the solid phase. For the binary system, the supercritical fluid phase fugacity, recalling its definition is:

$$f_2^F = P \, \phi_2^F \, y_2 \tag{2-2}$$

where P is pressure, ϕ_2^F is the fugacity coefficient and y_2 is the solubility (mole fraction) in a supercritical fluid.

Because we assume that the solid solute is pure, the fugacity of solute in the solid state f_2^S is equal to the pure solid fugacity f_2^{PureS}. The fugacity of component 2 is given by:

$$f_2^S = f_2^{pureS} = p_2^{Sat} \phi_2^S \left(\int_{p_2^{Sat}}^{p} \frac{v_2^S}{RT} dp \right) \tag{2-3}$$

Where p_2^{Sat} is the saturated vapor pressure, ϕ_2^S is the fugacity coefficient at saturation pressure, R is the gas constant, T is the temperature, and v_2^S is the solid-state molar volume of the solute.

Assuming that the molar volume of solid-state solute is constant over the pressure range, and the saturated vapor of the solid solute vapor system behaves are ideal gases,

we can derive as:

$$y_2 = \frac{f_2^F}{p\phi_2^F} = \frac{f_2^G}{p\phi_2^F} = \frac{p_2^{Sat}\phi_2^S}{p\phi_2^F}\exp(\int_{p_2^{Sat}}^{p}\frac{v_2^S}{RT}dp) = \frac{p_2^{Sat}}{p}\frac{1}{\phi_2^F}[\frac{v_2^S(p-p_2^{Sat})}{RT}] \quad (2\text{-}4)$$

where the supercritical fluid phase fugacity coefficient at saturation pressure has been set equal to unity and *P*, *T* are the system pressure and temperature.

The saturated vapor pressure and solid molar volume are physical properties of the pure solid phase. Therefore, the solid solubility in supercritical fluid is primarily a function of system pressure, temperature, solid compound physical properties, and the fugacity coefficient of the solid phase in the supercritical fluid. Finally we define an enhancement factor *E* as follows:

$$E = \frac{1}{\phi_2^F}[\frac{v_2^S(p-p_2^{Sat})}{RT}] \quad (2\text{-}5)$$

Equation (2-4) then becomes:

$$y_2 = \frac{p_2^{Sat}}{p}E \quad (2\text{-}6)$$

The enhancement factor, *E*, is nearly always greater than unity and $E \to 1$ as $p \to p_2^{Sat}$.

Equation of state

Fugacity coefficients can be calculated by the following equation [35]:

$$\ln \phi_2^F = \frac{1}{RT}\int_v^\infty [(\frac{\partial p}{\partial n_i})_{T,V,n_{i\neq j}} - \frac{RT}{V}]dv - \ln Z \quad (2\text{-}7)$$

where *Z* is the compressibility factor.

The empirical equations of state methods provide one of the most useful techniques in the high-pressure phase equilibrium calculation. The cubic equations of state such as the Soave-Redlick-Kwong (SRK) equation or the Peng-Robinson (PR) equation are widely used to evaluate the fugacity coefficient.

There are more than one hundred empirical equations of state that have been published. All these empirical equation can be divided into two classes: cubic equations of state and multiple parameter equations of state. Cubic equations usually have two or three parameters and are derived from the Van der Waal equation. Some multiple parameter equations have more than 20 parameters. The evolution of cubic equation of state is: Van der Waal (1873) — Redlick-Kwong (1949) — Wilson (1965) — Soave (1972) — Peng-Robinson (1976). The evolution of multiple parameter equation of state is: Beattie-Bridgeman (1928) — Benedice-Webb-Rubin (1940-1942) — Starling (1971) — Starling-Han (1972).

In 1873, Van der Waal developed an equation that can describe the volumetric properties of a fluid:

$$p = \frac{RT}{v-b} - \frac{a}{v^2}$$

$$a = \frac{27}{64}\left(\frac{RT_C}{P_C}\right)^2$$

$$b = \frac{1}{8}\frac{RT_C}{P_C} \qquad (2\text{-}8)$$

where v is the molar volume of the mixture, a and b are constants that depend on composition, Tc is critical temperature and Pc is critical pressure. The equation of Van

der Waal gives only an approximate description of gas-phase properties, but it was a major contribution for the comparison of later cubic equations of state.

The Redlich-Kwong EOS (1949) is a modification of the Van der Waal EOS. Like many early investigations, Redlick-Kwong modified the pressure, and developed a new equation of state in 1949 [35]:

$$p = \frac{RT}{v-b} - \frac{a}{T^{0.5}v(v+b)}$$

$$a = 0.42748\frac{R^2 T_C^{2.5}}{P_C}$$

$$b = 0.08664\frac{RT_C}{P_C} \qquad (2\text{-}9)$$

The Soave-Redlich-Kwong EOS was the first modification of the simple Redlich-Kwong EOS. Soave [36] modified the Redlick-Kwong equation by defining the parameter, *a*, was a function of *Tr* and ω. The pressure curve could be well reproduced after this modification. The EOS requires three input parameters per pure compound *Tc*, *Pc* and ω.

$$p = \frac{RT}{v-b} - \frac{a(T)}{v(v+b)}$$

$$a(T) = a(T_c)\alpha(T)$$

$$a(T_C) = 0.42748\frac{(RT_C)^2}{p_C}$$

$$\alpha(T) = [1 + (0.480 + 1.574\omega - 0.176\omega^2)(1 - \sqrt{T/T_C})]^2$$

$$b = 0.08664 \frac{R T_C}{P_C} \tag{2-10}$$

The disadvantage of Redlick-Kwong and Soave-Redlick-Kwong equations of state is that the equations cannot predict the density of liquid accurately. Peng and Robinson [37] developed the Peng-Robinson EOS to overcome this disadvantage in 1976 by a modified Redlick-Kwong equation. The Peng-Robinson EOS is the EOS most widely used in chemical engineering thermodynamics. It gives slightly better predications of liquid densities than the Soave-Redlich-Kwong EOS [38].

$$p = \frac{RT}{v-b} - \frac{a(T)}{v(v+b)+b(v-b)}$$

$$a(T) = a(T_C)\alpha(T)$$

$$a(T_C) = 0.45724 \frac{(R T_C)^2}{P_C}$$

$$\alpha(T) = [1+\beta(1-\sqrt{T/T_C})]^2$$

$$\beta = 0.37464 + 1.54226\omega - 0.26992\omega^2 \qquad 0 \le \omega \le 0.5$$

$$b = 0.07780 \frac{R\ T_C}{P_C} \tag{2-11}$$

Solubility calculation

The solubility of a material in supercritical fluid is essential for evaluating the viability of a minerals extraction recovery process. The cubic equations of state, Soave-Redlick-Kwong equation or Peng-Robinson equation, have most widely used in predictions of solubility in supercritical fluid. However, the interaction parameters have been determined mostly by fitting the experimental solubility data. It gives better

predictions only after proper use of mixing rules and the assignment of the interaction parameters. Carleson et al [39] have recently developed a group contribution method to predict interaction parameters in the absence of experimental data. Brennecke and Eckert [40] reviewed the various equations of state and concluded that the Peng-Robinson EOS may be as good as more complicated equations.

The mixture parameters, *a* and *b*, are related to the pure component terms a_i and b_i by

$$a = \sum_{i=1}^{n} \sum_{j=1}^{n} x_i x_j a_{ij}$$

$$a_{ij} = (1 - k_{ij})(a_i a_j)^{1/2}, i \neq j$$

$$b = \sum_{i-1}^{n} x_i b_i$$

$$a_{ii} = a_i \qquad (2\text{-}12)$$

Using mixing rules and the Peng-Robinson EOS for a binary system, the fugacity coefficient for component in a mixture can be related by

$$\ln \varphi_2 = \frac{b_2}{b}\left(\frac{Pv}{RT} - 1\right) - \ln \frac{P(v-b)}{RT} - \frac{a}{2\sqrt{2}bRT}\left[\frac{2(y_1 a_{12} + y_2 a_{22})}{a} - \frac{b_2}{b}\right] \ln \frac{v + (1+\sqrt{2})b}{v + (1-\sqrt{2})b} \qquad (2\text{-}13)$$

Recalling equation 2-4, the solid solubility, y_2, in supercritical fluid is primarily a function of system pressure, temperature, solid compound physical properties, and the fugacity coefficient of the solid phase in the supercritical fluid:

$$y_2 = \frac{p_2^{Sat}}{p} \frac{1}{\phi_2^F} \left[\frac{v_2^S (p - p_2^{Sat})}{RT}\right] \qquad (2\text{-}14)$$

References

1. Jawwad A. Darr and Martyn Poliakoff. New Directions in Inorganic and Metal-organic Coordination Chemistry in Supercritical Fluids. *Chemical Review,* **1999**, *99*, 495-541.

2. McHugh M.A. and V. Krukonis, *Supercritical Fluid Extraction. Principles and Practice*. Butterworths, Boston, **1986**.

3. Michael E. Paulaitis, Johan M. L. Penninger, Ralph D. Gray. *Chemical Engineering at Supercritical Fluid Conditions*, Ann Arbor Science Publishers, **1983**.

4. Zosel, K. Angew. Separation with Supercritical Gases: Practical Applications. *Chem. Int. Ed., Engl*, **1978**, 17, 701.

5. Keith W. Hutchenson, Neil R. Foster, *Innovations in Supercritical Fluids:Science and Technology.* American Chemical Society. Washington, DC, **1995**.

6. Frank V. Bright and Mary Ellen P. McNally. *Supercritical Fluid Technology*: *Theoretical and Applied Approaches to Analytical Chemistry*. ACS Symposium Series, **1992**.

7. John M. Prausnitz, Rudiger N. Lichtenthaler, Edmundo Gomes Azevedo, *Molecular Thermodynamics of Fluid-phase Equlibria*. Prentice Hall PTR.P845, **1999**.

8. Keith W. Hutchenson, Neil R. Foster, *Innovations in Supercritical Fluids Science and Technology.* American chemical society. Washington, DC, **1995**.

9. J. R. Williams and A. A. Clifford, *Supercritical Fluid Methods and Protocols*. Human Press, Totowa. New jersey, **1997**.

10. Jawwad A. Darr and Martyn Poliakoff.. New Directions in Inorganic and Metal-Organic Coordination Chemistry in Supercritical Fluids. *Chem. Rev.*, **1999**, 99, 495-541.

11. Knapp, H., Doring, R. Oellrich, L., Plocker, U. and Prausnitz, J. M.. *Vapor-Liquid Equilibria for Low Boiling Substances*. DECHEMA Chemistry Data Series, Frankfurt, **1982**.

12. U. K. Deiters, G. M. Schnelder. High-pressure Phase Equilibria: Experimental Methods. *Fluid Phase Equilibria*, **1986**, 29, 145-160.

13. Fornari, R. E., Alessi, P., & Kikic, I.. High-pressure Fluid Phase Equilibria: Experimental Methods and Systems Investigated (1978-1987), *Fluid phase Equilibria*, **1990**, 57, 1-33.

14. K. D. Bartle, A. A. Clifford, S. A. Jafar, and G. F., Shilstone, Solubilities of Solids and Liquids of Low Volatility in Supercritical Carbon Dioxide. *J. Phys. Chem. Ref. Data*, **1991**, 20(4), 713-756.

15. Ralf Dohrn, Gerd Brunner, High-Pressure Fluid-phase Equilibrium: Experimental Methods and Systems Investigated (1988-1993). *Fluid Phase Equilibrium*, **1995**, 106, 213-282.

16. Frank, P. Lucien, Neil R. Foster. Solubilites of Solid Mixtures in Supercritical Carbon Dioxide: a Review. *Journal of Supercritical Fluids*, **2000**, 17, 111-134.

17. Can Erkey. Supercritical Carbon Dioxide Extraction of Metals Fro-aqueous Solutions: a Review. *Journal of Supercritical Fluids*, **2000**, 17, 259-287.

18. Tolley W. K, Tester L. S., *Supercritical CO_2 Solubility of TiCl4*. Report of Investigations, **1989**.

19. Laintz, K. E., Yu, J., Wai, C. M., Smith, R. D. Separation of Metal Ions with Sodium Bis(trifluoroethyl)dithiocarbamate Chelation and Supercritical Fluid Chromatography. *Anal. Chem*., **1992**, 64, 311-315.

20. Laintz, K. E., Wai, C. M., Yonker, C. R., Smith, R. D. Extraction of Metal Ions from Liquid and Solid Materials by Supercritical Carbon Dioxide. *Anal. Chem.* **1992**, 64, 2875-2878.

21. Lin, Y., Wai, C. M., Jean, F. M., Brauer, R. D., Supercritical Fluid Extraction of Thorium and Uranium Ions from Solid and Liquid Materials with Fluorinated Diketone and Tributyl Phospate. *Environ. Sci. Technol*, **1994**, 28, 1190-1193.

22. Lin, Y., Brauer, R. D., Laintz, K. E., Wai, C. M., Supercritical Fluid Extraction of Lanthanides and Actinides from Solid Materials with Fluorinated Diketone. *Anal. Chem*, **1993**, 65, 2549-2551.

23. Neil G. Smart, Carleson T., Kast T., et al., Solubility of Chelating Agents and Metal-containing Compound in Supercritical Fluid Carbon Dioxide. *Talanta*, **1997**, *44*, 137-150.

24. Ozel MZ. Bartle KD, Clifford AA, Buford MD., Extraction, Solubility and Stability of Metal Complexes Using Stainless Steel Supercritical Fluid Extraction System. *Analytica Chimica Acta*, **2000**, 417, 177-184.

25. Burford MD, Ozel MZ, Clifford AA, Bartle KD, et al., Extraction and Recovery of Metals Using Supercritical Fluid with Chelating Agents. *Analyst*, **1999**, 124, 609-614.

26. Cowey CM, Bartle KD, Burford MD, Clifford AA, et al., Solubility of Ferrocene and a Nickel Complex in Supercritical Fluids. *J. Chem. Eng. Data*, **1995**, 40, 1217-1221.

27. Glennon JD, Hutchinson S, Walker A, Harris SJ, McSweeney CC. New Fluorinated Hydroxamic Acid Reagents for the Extraction of Metal Ions with Supercritical CO_2. *Journal of Chromatography A*, **1997**, 770, 85-91.

28. Cross W, Akgerman A., Erkey C. (1996). Determination of Metal-chelate Complex Solubilities in Supercritical Carbon Dioxide. *Ind. Eng. Chem. Res*., **1996**, 35, 1765-1770.

29. Murphy JM, Erkey C. Copper (II) Removal from Aqueous Solutions by Chelation in Supercritical Carbon Dioxide Using Fluorinated B-diketones. *Ind.Eng. Chem. Res*., **1997**, 36, 5371-5376.

30. Wai CM, Wang S, Yu JJ. Solubility Parameters and Solubilities of Metal Dithiocarbamates in Supercritical Carbon Dioxide. *Anal. Chem*., **1996**, 68, 3516-3519.

31. Murphy JM, Erkey C., Thermodynamics of Extraction of Copper (II) from Aqueous Solutions by Chelation in Supercritical Carbon Dioxide. *Environ. Sci. Technol* , **1997**, 31, 1674-1679.

32. Meguro Y, Iso S, Yoshida Z., Correlation Between Extraction Equilibrium of Uranium (VI) and Density of CO_2 Medium in a HNO3/Supercritical CO_2-Tributyl Phosphate System. *Anal. Chem*., **1998**, 70, 1262-1267.

33. Yazdi, A V., Beckman,E. J., Design of Highly CO_2-Soluble Chelating Agents II. Effect of Chelate Structure and Process Parameters on Extraction Efficiency. *Ind.Eng. Chem.*, **1997**, 36, 2368 E.

34. Laintz KE, Wai C.M, Yonder CR, Smith RD., Extraction of Metal Ions from Liquid and Solid Materials by Supercritical Carbon Dioxide. *Anal. Chem*., **1992**, 64, 2875-2878.

35. Redlick O. and J. N. Kwong., The Thermodynamics of Solutions. V. An Equation of State. Fugacities of Gaseous Solution. *Chem. Rev.*,**1949**, 44, 233.

36. Soave.G., Equilibrium Constants from a Modified Redlich-Kwong Equation of State. *Chem. Eng. Sci*., **1972**, 27, 1197.

37. Peng D.Y. and D. B. Robinson., A New Two Constant Equation of State. *Ind. Eng. Chem*., 1976, 15, 59.

38. http://www.tu-harburg.de/vt2/pe2000/Dokumentation/PE2000_Kap7A1.htm

39. Carleson, T. E., S. Chancre, C. Way, L. S.S. Huang. *Group Contribution Method for Estimating Solubility of Selected Hydrocarbons Solutes in Supercritical Carbon Dioxide* Supercritical Fluid Engineering Science, Ed. E. Koran and J. F. Brennecke, ACS Symposium Series 514, CH.24, **1993**.

40. Brennecke, J. F. and C. A. Eckert. (1989). Phase Equilibria for Supercritical Fluid Process Design. *AICHE J*., **1989**, 35(9), 1409.

41 K.P.Johnston, K.L.Harrison, M.J.Clarke, S.M.Howdel, M.P.Heitz, F.V.Bright, C.Carlier and T.W.Randolph, *Science*, **1996**, 271,624.

42 J.Eastoe, B.M.H.Cazelles, D.C.Steytler, J.D.Holmes, A.R.Pitt, T.J.Wear and P.K.Heenan, *Langmuir*, **1997**, 13, 6980.

CHAPTER III

SCREENING FOR SOLUBLE SPECIES IN SIMULATED MARTIAN REGOLITH AND INORGANIC SAMPLES

Introduction

To extract the useful minerals in Martian soil via supercritical carbon dioxide, we need to know the chemical composition of the regolith and geological formations on Mars. What is the mineralogy of the rocks and soils on Mars? The present knowledge of the chemistry and mineralogy of the Martian surface rocks and soils is very limited. The most direct data were obtained by the two Viking Landers and the mobile alpha proton x-ray spectrometer (AXPS) on board the rover of the Mars pathfinder. The chemical analysis of Martian soil from Viking Landers has been reported in several publications [1-4]. Two landing sites of Viking 1 and Viking 2 were about 6500 km apart from each other. The chemical composition of soil analyzed by X-Ray-Fluorescence (XRF) was found to be almost identical. The Viking X-ray fluorescence spectrometers cannot detect elements of atomic number less than 12. Therefore, some of the important elements in mineral formation such as C, N and Na cannot be detected. The recent data on the chemical composition of Martian soils come from the mobile alpha proton x-ray spectrometer (AXPS) on board the rover of the Mars pathfinder [5]. All these data indicate silicates predominate the Martian soil. Iron (ranging from 16% to 19% Fe as Fe_2O_3) is in abundance as well as sulfur and chlorine. Viking also revealed that the soils are highly magnetic, possibly resulting from 1-7 wt% of a strongly magnetic component like maghemite (Fe_2O_3) dispersed as a pigment throughout the surface particles [6]. The

mineralogical composition is also dominated by the silicate minerals, which may include weathered, igneous silicates including pyroxenes, feldspars, magnetite, glass of igneous composition, and sectite clays of various compositions [4].

We plan to investigate the solubility properties of inorganic minerals that may be present in the Martian surface. The samples in this screening include metal chlorides, sulfates, and hydrated sulfates, nitrates, carbonates, and oxides. They are prepared based on the composition of current knowledge of Martian soils [7].

We also will investigate the solubility properties of the simulant JSC Mars-1 in supercritical CO_2. The simulant, JSC Mars-1, was obtained from the Johnson Space Flight Center, and is a simulant of the regolith of Mars for support of scientific research, engineering studies, and education. The chemical composition of the JSC Mars-1 determined by X-Ray fluorescence was similar to the Martian soil [8, 9].

Materials and Methods

The JSC Mars-1 simulated Martian regolith was obtained from the Johnson space flight center. Gypsum ($CaSO_4 \cdot 2H_2O$) was obtained from Acros Organics. Iron heptahydrate ($FeSO_4 \cdot 7H_2O$) was obtained from J. T. Baker Chemical Co. The following were obtained from Fisher Scientific: NH_4HF_2, $CoCl_2 \cdot 6H_2O$, $CuSO_4 \cdot 5H_2O$, $FeCl_2 \cdot 4H_2O$, $CaCl_2$, $AgNO_3$, NH_4SO_4, NaI, $MnSO_4 \cdot 5H_2O$, Ni $(NO_3)_2 \cdot 5H_2O$, $Fe(NH_4)_2(SO_4)_2 \cdot 12H_2O$, $Fe(NO_3)_3 \cdot 9H_2O$, $Fe(NH_4)_2(SO_4)_2 \cdot 6H_2O$, Serpentine ($Mg_3Si_2O_5(OH)_4$), $K_2Cr_2O_7$, $(NH_4)_2MoO_4$, $CuCl_2$ and $CuCl_2 \cdot 2H_2O$. The carbon dioxide was obtained from J&M Cylinder Gases, Inc.

The extractions were performed using an ISCO SFX220 supercritical fluid extraction system, which is shown in Figure 3.1. It consists of an extractor, a controller, and one D series syringes pump. The supercritical carbon dioxide is pumped through the extraction cell at a flow rate of about 1 ml/min. The system controller maintains constant pressure and temperature. The temperature range investigated is 35°C to 145°C and the pressure range is 50 bar to 280 bar. Approximately one gram of sample was weighed and placed in the extraction cell. The extraction cell was weighed before and after extraction to detect mass change of samples.

The JSC Mars-1 simulant Martian regolith samples were put in standard TGA experiment to study the weight change of the material as a function of temperature. A TA Instruments TGA 2960 was used for thermo gravimetric analyses. A typical procedure for the TGA includes setting the flow rate of nitrogen at 120 ml/min, mounting the platinum sample tray, adjusting the zero point, and then putting 8 to15 mg samples in the sample tray. The samples were analyzed at constant heating rate (10°C/min) and constant temperature (35°C and 120°C).

Differential Scanning Calorimetry was performed on a TA Instruments DSC 2920. The samples were analyzed in aluminum pans with special hermetic pan lids that have a laser cut vent hole. The sample's weight was 4 to 6 mg in a nitrogen atmosphere using a nitrogen flow rate is 90 ml/min. An essential procedure for the differential scanning calorimeter is the preparation of two samples: the simulated Martian regolith and a reference. They are put on the raised platforms inside the DSC cell. A heating rate of 10°C/min was used in these experiments.

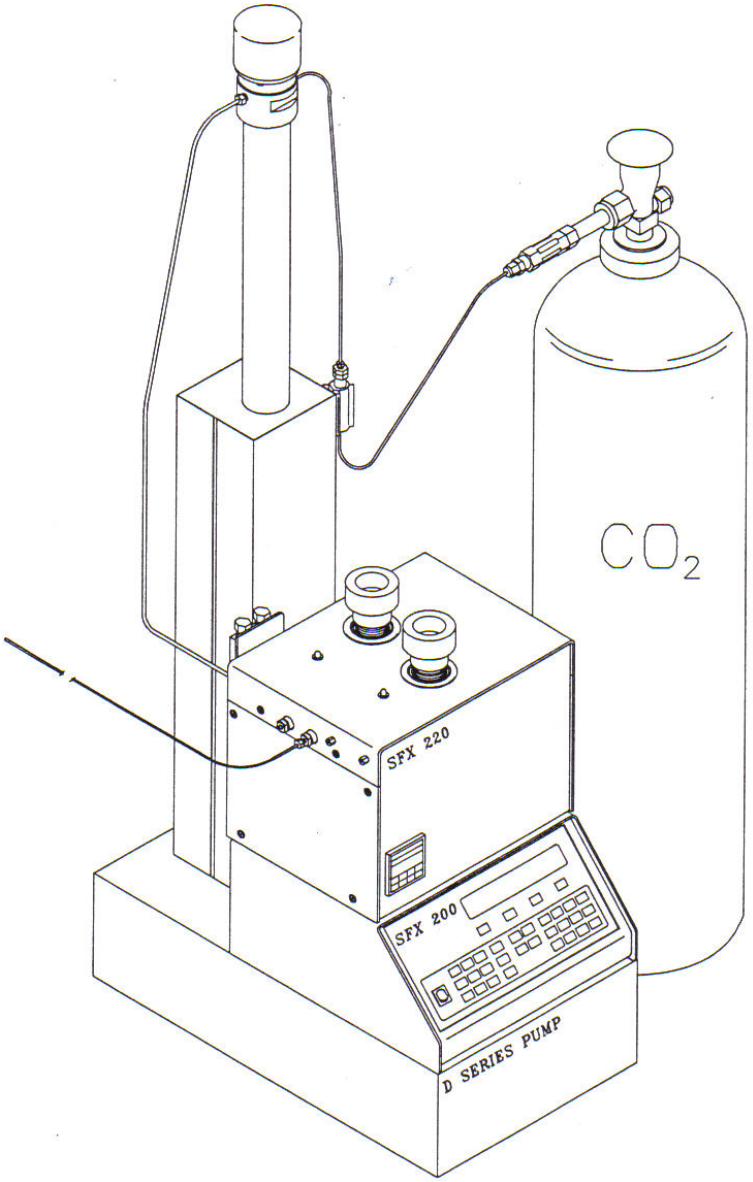

Figure 3.1: Schematic diagram of the extraction system.

Results and discussion

Figure 3.2 shows the weight change of simulated Martian regolith in supercritical fluid at different temperatures. Between 50 and 150 bar, simulated Martian regolith weight loss increases with increasing pressure. Weight loss does not increase significantly with further increase the pressure. At 35°C, the weight loss of simulated Martian regolith increases from 4% to 6% with increasing pressure. The weight loss increases from 12% to 14% at 120°C. Temperature is an important factor which influences weight loss of simulated Martian regolith.

Thermal Gravimetric Analysis (TGA) results for the simulated Martian regolith are shown in Figure 3.3. The simulated Martian regolith was analyzed at constant temperature for 60 minutes. The experimental temperatures were 35°C and 120°C. There is no chemical reaction during the thermal gravimetric analysis process at this temperature. A plateau is reached after 10 to 15 minutes at each temperature. No further weight change occurs with increasing time. The weight loss is approximately 1% and 7% at 35°C and 120°C, respectively. Comparing the weight loss of the extraction process to that of the thermal process shows that the weight loss is approximately 2% and 7% more in supercritical extraction process than in the thermal process at 35°C and 120°C, respectively. A higher weight loss in the extraction process indicates that it may be possible to recover useful minerals from the Martian soils by a supercritical extraction process.

Differential Scanning Calorimetry (DSC) was also run on the simulated Martian regolith. The results are shown in Figure 3.4. There is one peak present between 50°C and 300°C. The maximum heat flow is reached at 140°C. The enthalpy of this peak is

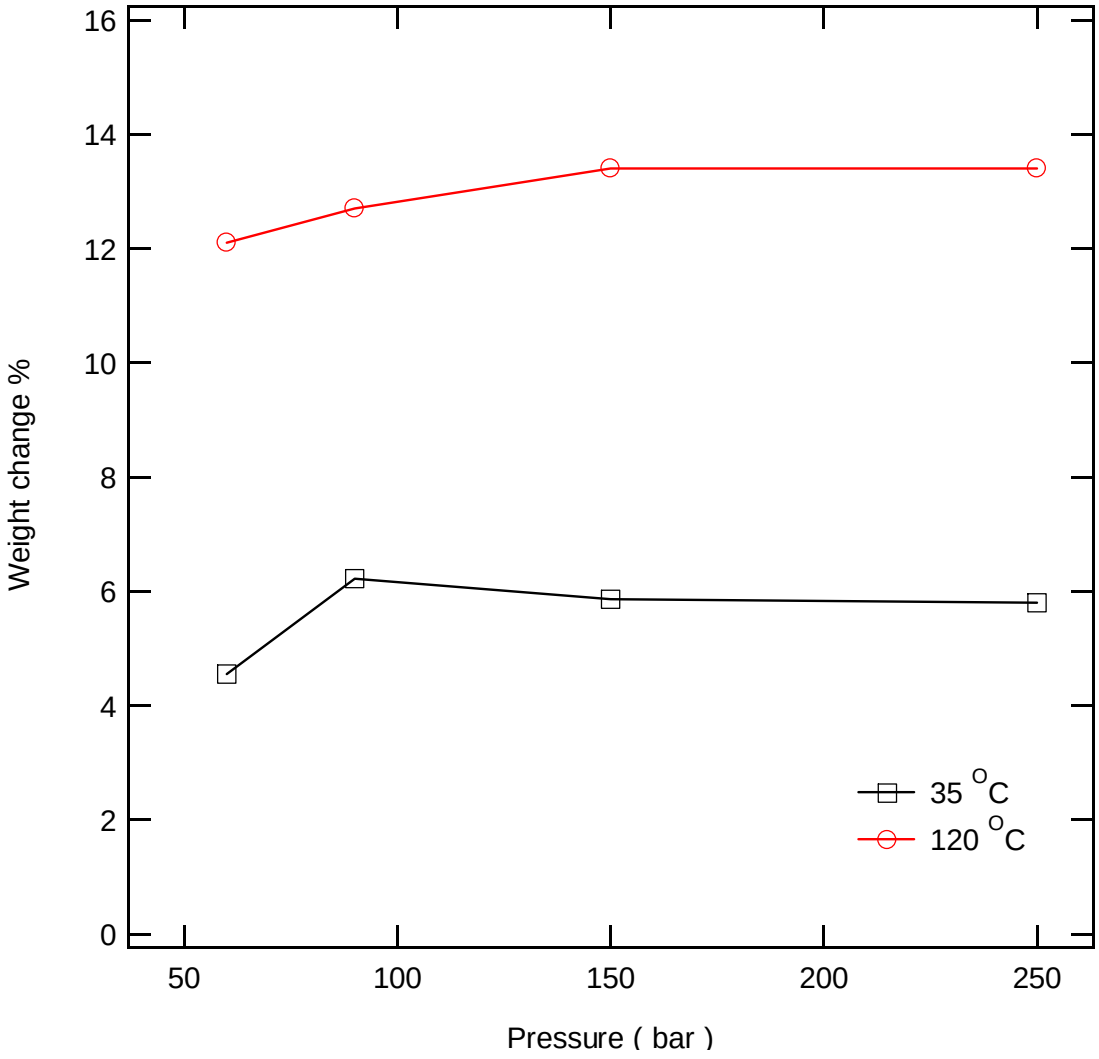

Figure 3.2: Weight change of simulated Martian regolith at different conditions in supercritical carbon dioxide extraction.

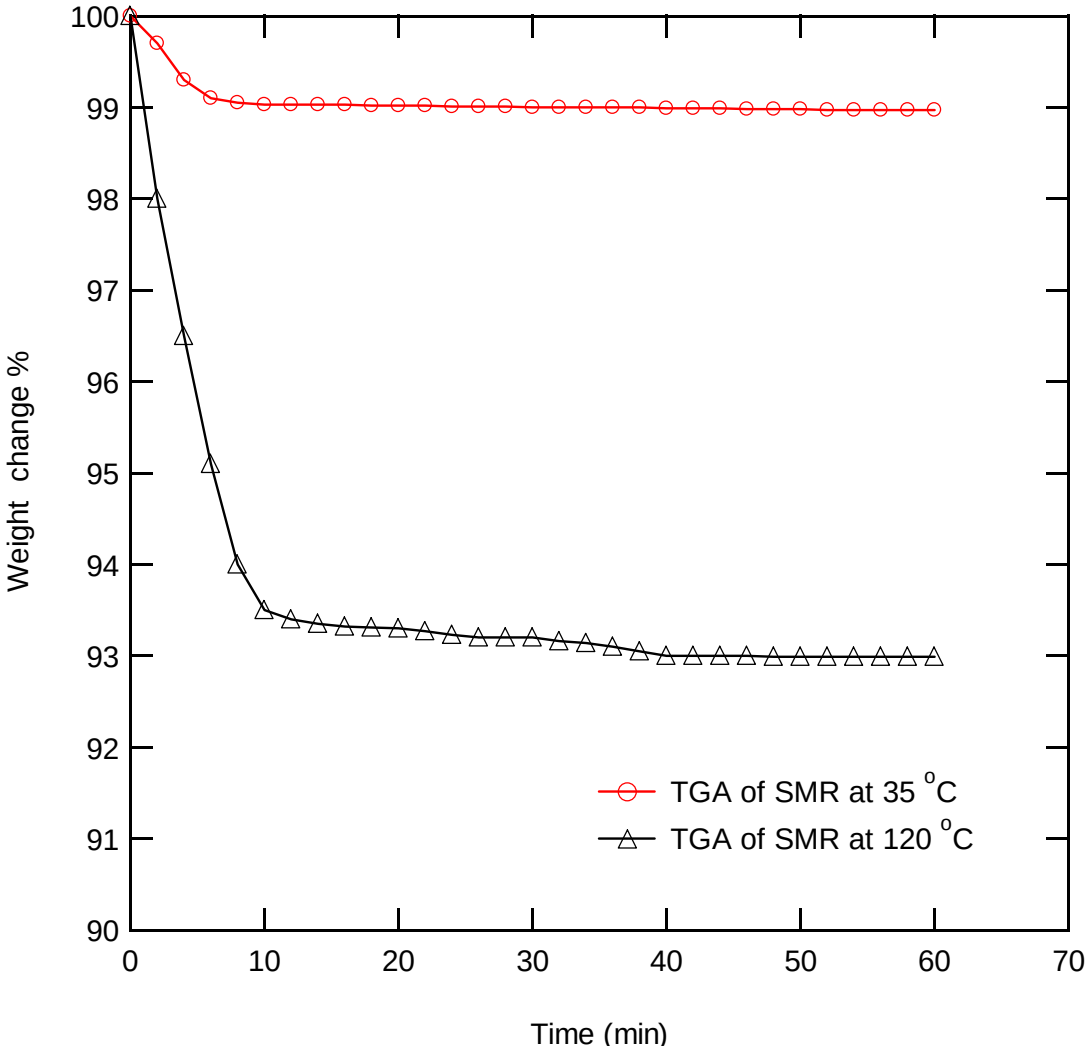

Figure 3.3: Weight loss results of simulated Martian regolith at different temperature.

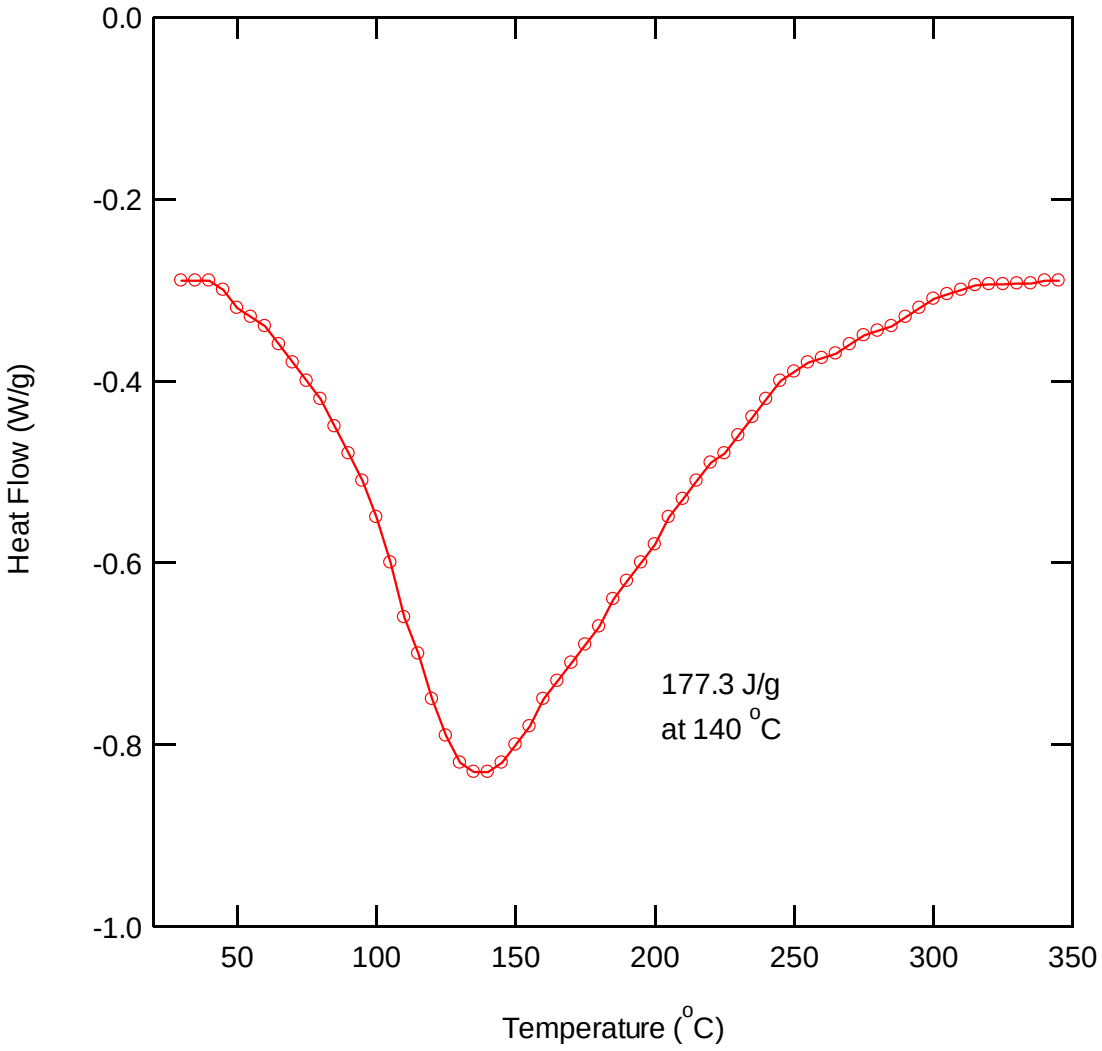

Figure 3.4: DSC thermograph of simulated Martian regolith.

177.3 J/g. This peak might result from the dehydration, vaporization, or a combination of latent heats of structure rearrangement.

We screened for soluble species of some inorganic compounds that may be present in the Martian surface. All samples chosen were based on the current knowledge of the composition of Martian soils. The screening samples include metal chlorides, sulfates, and hydrated sulfates, nitrates, carbonates, and oxides. Table 3.1 lists the solubility screening results for all compounds. The results show no appreciable extraction for $CaCl_2$, $AgNO_3$, NH_4SO_4, NaI, $K_2Cr_2O_7$, $(NH_4)_2MoO_4$, $CuCl_2$ and $FeCl_3$. It can be seen that all the hydrated compounds show significant weight change. This confirmed that it is possible to recover water from the hydrated compounds. Recovering water is significantly useful, since water can be used to support life on Mars. The water can also be broken into hydrogen and oxygen. Hydrogen can be used as rocket fuel and oxygen can be used for breathing by the astronauts or as an oxidizer.

Table 3.1: Results for screening for soluble species of inorganic compounds in supercritical carbon dioxide.

Significant weight change	No significant weight change
NH_4HF_2	$CaCl_2$
$CoCl_2 \cdot 6H_2O$	$AgNO_3$
$CuSO_4 \cdot 5H_2O$	NH_4SO_4
$FeCl_2 \cdot 4H_2O$	NaI
$MnSO_4 \cdot 5H_2O$	$K_2Cr_2O_7$
$Ni(NO_3)_2 \cdot 5H_2O$	$(NH_4)_2MoO_4$
$Fe(NH_4)_2(SO_4)_2 \cdot 12H_2O$	$CuCl_2$
$FeSO_4 \cdot 7H_2O$	$FeCl_3$
$Fe(NO_3)_3 \cdot 9H_2O$	
$Fe(NH_4)_2(SO_4)_2 \cdot 6H_2O$	
$CaSO_4 \cdot 2H_2O$	
Serpentine ($Mg_3Si_2O_5(OH)_4$)	
Simulated Martian Regolith	

Figure 3.5 shows the weight change of three ferrous hydrated compounds at 35°C. All the samples have slightly more weight loss with pressure increasing between 50 and 150 bar. No significant weight change occurs when the pressure is higher than 150 bar. Weight loss of $FeSO_4 \cdot 7H_2O$ is the greatest among the three samples. About 35% of the $FeSO_4.7H_2O$ was removed at high pressure.

Figures 3.6 and 3.7 show the comparison of weight change between carbon dioxide extraction at 200 bar and thermal heating at 1 bar for $FeSO_4 \cdot 7H_2O$ and $Fe(NH_4)_2(SO_4)_2 \cdot 6H_2O$. The weight loss increases with increasing temperature in both the extraction and thermal heating process for these two compounds. The extraction process removes slightly more water than just thermal heating, especially for $Fe(NH_4)_2(SO_4)_2 \cdot 6H_2O$. At room temperature (25°C) there is no weight loss for $Fe(NH_4)_2(SO_4)_2 \cdot 6H_2O$. Using the extraction process at 25°C, the weight loss is about 20%.

It is known that hydrated compounds can lose water molecules at various temperatures. More water molecules are removed at high temperature. Thermal dehydration of ferrous sulfate and $Fe(NH_4)_2(SO_4)_2 \cdot 6H_2O$ has been studied by a number of investigators [10-12]. $FeSO_4 \cdot 7H_2O$, and $Fe(NH_4)_2(SO_4)_2 \cdot 6H_2O$ do not dehydration at given experimental temperature. The extraction process produces more weight loss than the thermal heating process. There is no chemical reaction nor decomposition in either process. Direct extraction of metal ions by supercritical carbon dioxide is known to be highly inefficient. The weight loss only results from the dehydration. This indicates that a supercritical extraction process can recover water from hydrated species more efficiently

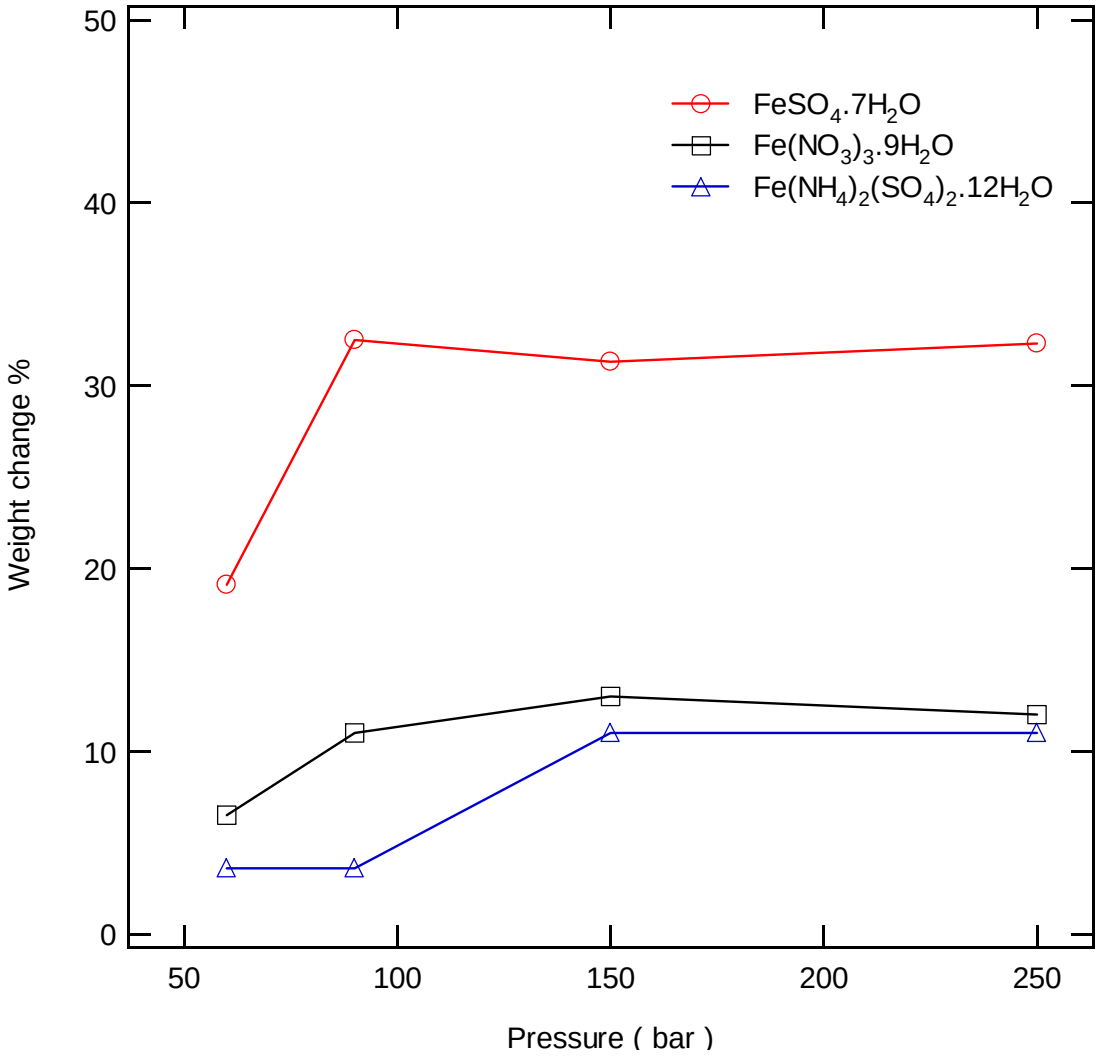

Figure 3.5: Weight change of some ferrous hydrated compounds with pressure at 35^{o}C.

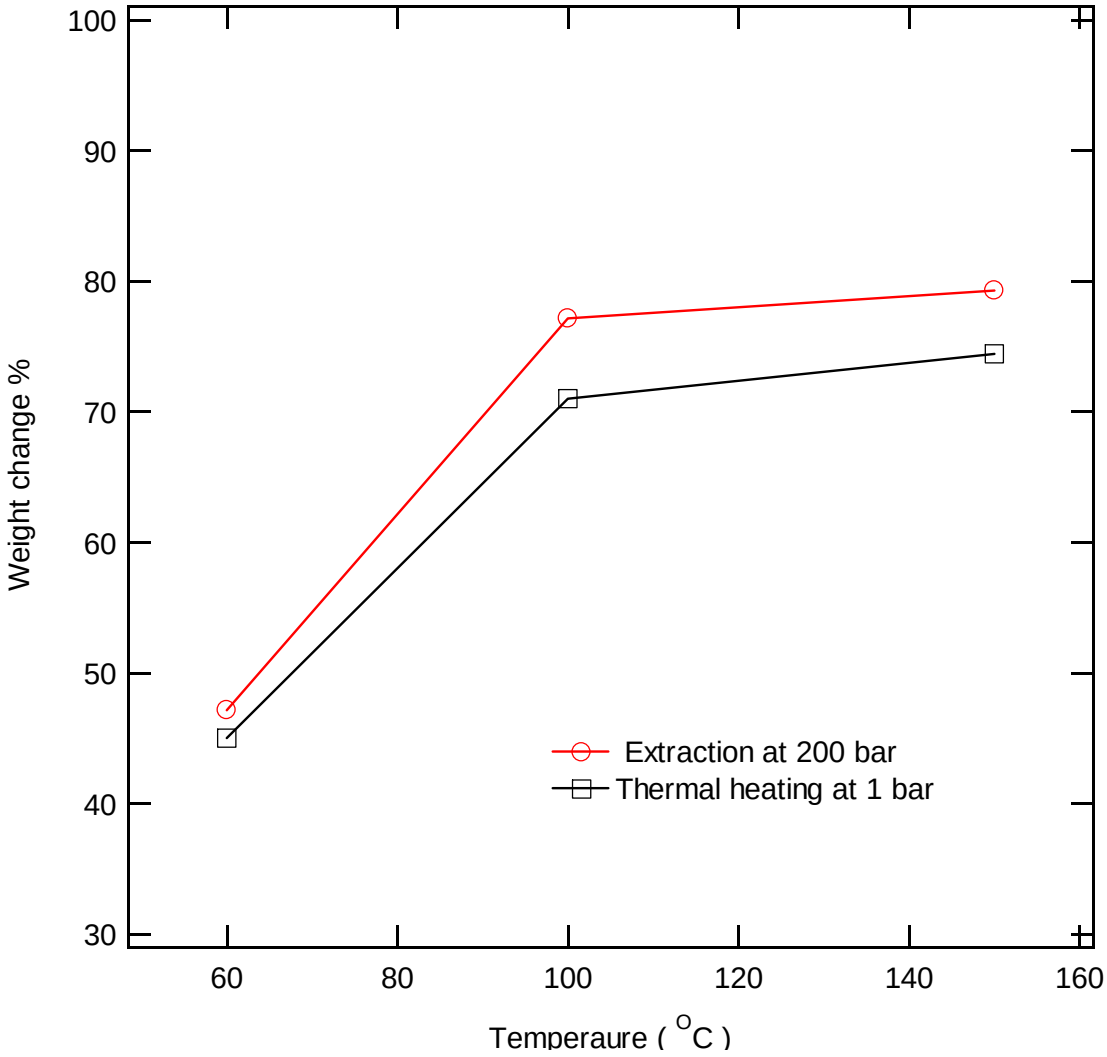

Figure 3.6: Comparison of weight change of $FeSO_4 \cdot 7H_2O$ between extraction and thermal heating.

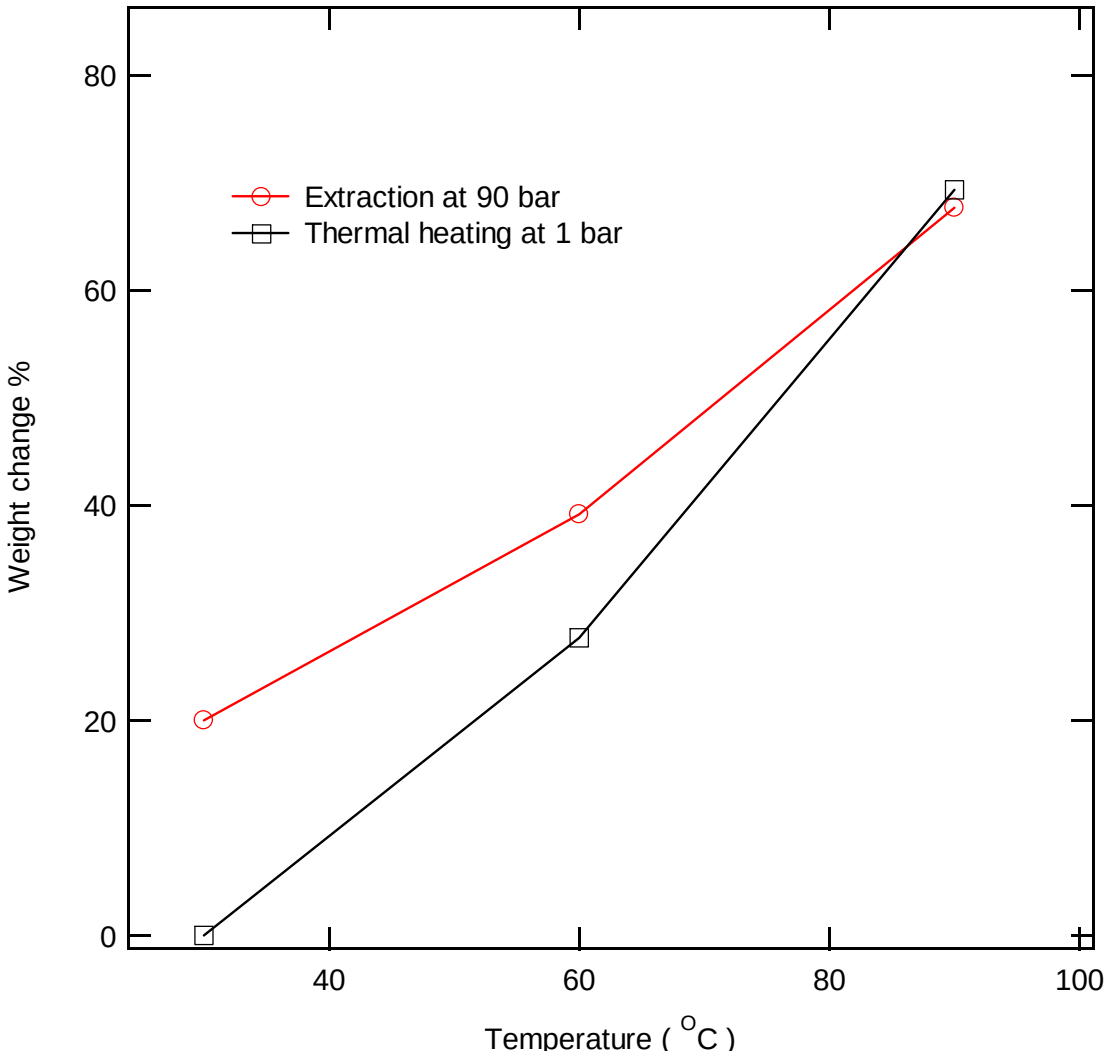

Figure 3.7: Comparison of weight change of $Fe(NH_4)_2(SO_4)_2 \cdot 6H_2O$ between extraction and thermal heating.

than thermal heating process. The dehydration process is a reversible process. The weight loss is a constant value at the thermodynamic equilibrium condition. But a dehydration process will proceed if the water molecules are removed. We know that water is soluble in supercritical carbon dioxide up to about 5-6%(mole fraction)[13]. Therefore, an extraction process in supercritical carbon dioxide exhibits more weight loss than a corresponding thermal heating process.

Serpentine, magnesium silicate hydroxide, is composed of magnesium, silicon and oxygen. It is a major rock-forming mineral and is found as a constituent in many metamorphic and weathered igneous rocks on earth. It is actually a general name applied to several members of a polymorphic group. Its chemical formula is $(Mg)_3Si_2O_5(OH)_4$. Serpentine reacts with carbon dioxide at proper conditions as follows [14]:

$$Mg_3Si_2O_5(OH)_4 + 3CO_2 = 3MgCO_3 + 2SiO_2 + 2H_2O \qquad (3\text{-}1)$$

Figure 3.8 shows the weight change of serpentine at different temperatures and pressures. The weight change is 3% at 120^{o}C and 140^{o}C. If the reaction of 3-1 occurs, a weight change would result.

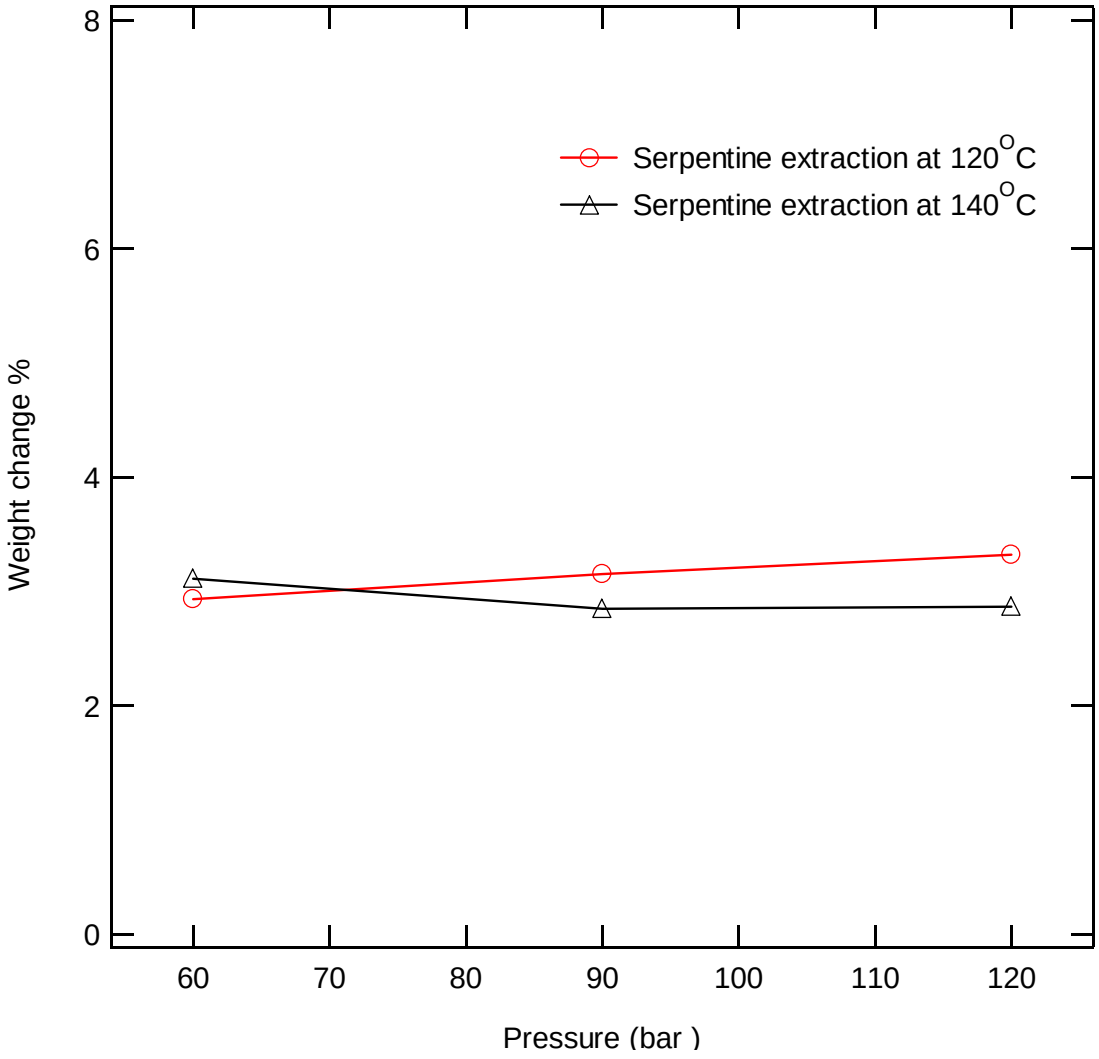

Figure 3.8: Weight change of serpentine with pressure at different temperature.

References

1. Jan Osburg. *Space Missions to Mars: Past, Present and Future*. Research Paper, Georgia Institute of Technology School of Aerospace Engineering. Atlanta, GA., **1998**.

2. David R. Williams, Viking Mission to Mars, Viking Project Information. *The Journal of Geophysical Research*, **1977**, 82, 28.

3. Clark B.C.,A.K.Baird, R.J. Weldon,, D. M. Tsuaki, L. Schnabel, and M. P. Candelaria. Chemical Composition of Martian Fines. *J. Geophys*, **1982**, **87**, 10059-10067.

4. Stroker C.R., *The Physical and Chemical Properties and Resource Potential of Martian Surface Soils*. Resources of Near-earth Space, University of Arizona. press.659-708,**1993**.

5. Rieder R, T. Economou, H. Wänke, * A. Turkevich, J. Crisp, J. Brückner, G. Dreibus, H. Y. McSween Jr. The Chemical Composition of Martian Soil and Rocks Returned by the Mobile Alpha Proton X-ray Spectrometer: Preliminary Results from the X-ray Mode. *Science*, **1997**, 278, 1771-1774.

6. Bell III, J.F. *Nature and Origin of Martian Surface Materials*. Cornell University, Department of Astronomy, Ithaca NY 14853, **1996.**

7. Carlton C. Allen, Richard V. Morris, and David J. Lindstrom. *JSC Mars-1: Martian Regolith Simulant*. NASA Johnson Space Flight Center, Houston,TX, **1997**.

8. Rieder R, T. Economou, H. Wanke, A. Turkevich, J. Crisp. (1997). The Chemical Composition of Martian Soil and Rocks Returned by the Mobile Aipha Proton X-ray Spectrometer: Preliminary Results from the X-ray Mode. *Science*,**1997**, 278, 1771-1774.

9. Klaus S. Lackner, Christopher. H. Wendt. Carbon Dioxide Disposal in Carbonate Minerals. *Energy*, **1995**, 20, 1153-1170.

10. J. E. Macintyre. *Dictionary of Inorganic Compounds*. London. New York, Chapman & Hall, **1992**.

11. Diev. N. P., Abstract of Dehydration of Ferrous Sulfate, *Phys. Chem. Miner*.,**1995**,23,263-275.

12. Rodionov, A.I., Zapol'skii, A.K., Yakushev, V.I., Fedoritenko, I.I. Dehydration of Ferrous Sulfate Heptahydrate. *Inst. Im. D. I. Mendeleeva*, **1979**, 109, 51.

13. Takenouchi,S., Kennedy G.C., The Binary System H_2O-CO_2 at High Temperature and Pressure. *Am.Sci*., **1964**, 262,1055.

14. Ron Zevenhoven, Mineral Carbonation for Long-term CO_2 Storage:an Exergy Analysis. *Int.J. Thermodynamics,* **2004**, **7**, 23.

CHAPTER IV

DEHYDRATION STUDY OF FERROUS SULFATE AND CALCIUM SULFATE

Introduction

The results of solubility screening of simulated Martian regolith and inorganic samples show that the hydrated compounds have significant weight change when extracted in supercritical carbon dioxide. This indicates that it is possible to recover water from hydrated compounds using supercritical carbon dioxide. We ran further tests on ferrous sulfate and calcium sulfate to determine their dehydration behavior in supercritical carbon dioxide.

Based on the current knowledge of the composition of Martian soils [1, 2], nearly 20% of the Martian surface contains ferrous minerals. Although no hydrated compounds have been identified, it is accepted that Mars was once wet. One possible place the water went was into hydrated compounds. For that reason we chose to study the dehydration of candidate hydrated iron compound, iron heptahydrate [$FeSO_4 \cdot 7H_2O$]. It is a blue-green, monoclinic, and odorless crystals or granules [3]. Thermal dehydration of ferrous sulfate has been studied by a number of investigators. Diev [4] considered that the true structure of heptahydrate is $(FeSO_4 \cdot H_2O) \cdot 6H_2O$ and heptahydrate can be easily dehydrated to the monohydrate in 5-7 min and to $FeSO_4$ in 120 min by heating it at 200°C. Rodionov [5] studied the dehydration of $FeSO_4 \cdot 7H_2O$ in air atmosphere. His results showed that $FeSO_4 \cdot 7H_2O$ dehydrated in the temperature range 40-100°C and simultaneously formed $Fe(OH)SO_4$. With further heating treatment in the temperature range 300-400°C,

$Fe(OH)SO_4$ would lose H_2O and form $FeSO_4$. Kanri [6] et al. investigated the dehydration of $FeSO_4 \cdot 7H_2O$ under nitrogen atmosphere and indicated the mechanism of the thermal dehydration of ferrous sulfate heptahydrate to anhydrous according to the following equations [7]:

$$FeSO_4 \cdot 7H_2O = FeSO_4 \cdot 4\,H_2O + 3\,H_2O \quad (4\text{-}1)$$

$$FeSO_4 \cdot 4\,H_2O = FeSO_4 \cdot H_2O + 3\,H_2O \quad (4\text{-}2)$$

$$FeSO_4 \cdot H_2O = FeSO_4 + H_2O \quad (4\text{-}3)$$

Ferrous sulfate heptahydrate dehydrated to $FeSO_4 \cdot 4H_2O$ first and then $FeSO_4 \cdot 4H_2O$ dehydrated to $FeSO_4 \cdot H_2O$ from room temperature to 150°C. $FeSO_4 \cdot H_2O$ was the final product at 150°C. The anhydrous ferrous sulfate was obtained at temperatures higher than 225°C. Results indicated that dehydration rate was almost independent of the flow rate of nitrogen. The conversion of tetrahydrated to monohydrated ferrous sulfate was more temperature sensitive than that of heptahydrated to tetrahydrated ferrous sulfate.

About 5% of the Martian surface contains calcium minerals. A common calcium hydrated compound is gypsum. It is a soft, transparent mineral composed of crystallized calcium sulfate ($CaSO_4$). Le Chatelier was the first to study the hydration mechanisms of gypsum. The dehydration of gypsum is carried out by following steps [8, 9]

$$CaSO_4 \cdot 2H_2O = CaSO_4 \cdot 0.5H_2O + 1.5\,H_2O \quad (4\text{-}4)$$

$$CaSO_4 \cdot 0.5H_2O = CaSO_4 + 0.5\,H_2O \quad (4\text{-}5)$$

The dehydration begins at approximately 80°C (176°F). The heat delivered to the gypsum at this time removed off water molecules and vaporized the water. Heating gypsum above approximately 150°C (302°F) causes 75% of the water (1.5 water molecules) contained

in its chemical structure to be lost. After 1.5 water molecules are lost and the temperature of the gypsum is further increased, all the water will be removed.

The object of this part is to determine the temperatures at which waters of hydration are removed and the enthalpy values for the various dehydration steps. The theoretical thermal value for various dehydration steps was calculated using the heats of formation of various hydrates of the compound and water. We compared the dehydration behavior to the thermal heating processes and the supercritical extraction processes.

Materials and Methods

Materials

Calcium sulfate ($CaSO_4 \cdot 2H_2O$) was supplied from Acros Organics. Ferrous sulfate ($FeSO_4 \cdot 7H_2O$) was supplied from J. T. Baker Chemical Co. The other materials were purchased from Fisher Scientific Co. The carbon dioxide was obtained from J& M Cylinder Gases, Inc.

Apparatus

The ferrous sulfate ($FeSO_4 \cdot 7H_2O$) samples and calcium sulfate ($CaSO_4 \cdot 2H_2O$) were heated in nitrogen atmosphere at different heating rates. Thermogravimetric analysis (TGA) and differential scanning calorimetry (DSC) were used to study the dehydration using a TA Instruments model Q600 SDT.

To study the behavior of dehydration in supercritical carbon dioxide, we took our extracted sample from the extractor and examine them immediately via DSC without re-

exposing the sample to the atmosphere. Extractions were performed in a 10 mL stainless cell using a Isco 220 Supercritical Fluid System with a model 260D Syringe Pump.

Results and Discussion

Dehydration Study of Ferrous Sulfate ($FeSO_4 \cdot 7H_2O$)

Figure 4.1 shows the percent weight remaining versus temperature, and Figure 4.2 shows the dehydration rate versus temperature. As shown in Figure 4.1, there are three plateaus. This indicated a three-step process for the ferrous sulfate dehydration. The weight loss of 19.7% found in 40-80°C can be explained as the first dehydration step that loses three water molecules. A mass loss of 19.0% found in the 100-150°C temperature range can be assigned to the second dehydration step that loses another three water molecules. The weight loss of 5.7% found in the high temperature range (200-350°C) is explained as the third dehydration step. Figure 4.2 clearly shows the rate of dehydration of each step.

The TGA result shows that the ferrous sulfate gives off water in the following relative molar sequence: 3-3-1. The TGA results at different heating rate indicated that slower heating rate lead to each dehydration step moving to lower temperatures range. All the samples at all heating rates showed that the dehydration of ferrous sulfate took place in three stages. At a fast heating rate (10°C/min), the dehydration from $FeSO_4 \cdot 7H_2O$ to $FeSO_4 \cdot 4H_2O$ does not completely finish, and continues combined with the dehydration from $FeSO_4 \cdot 4H_2O$ to $FeSO_4 \cdot H_2O$. All of the above result in less weight

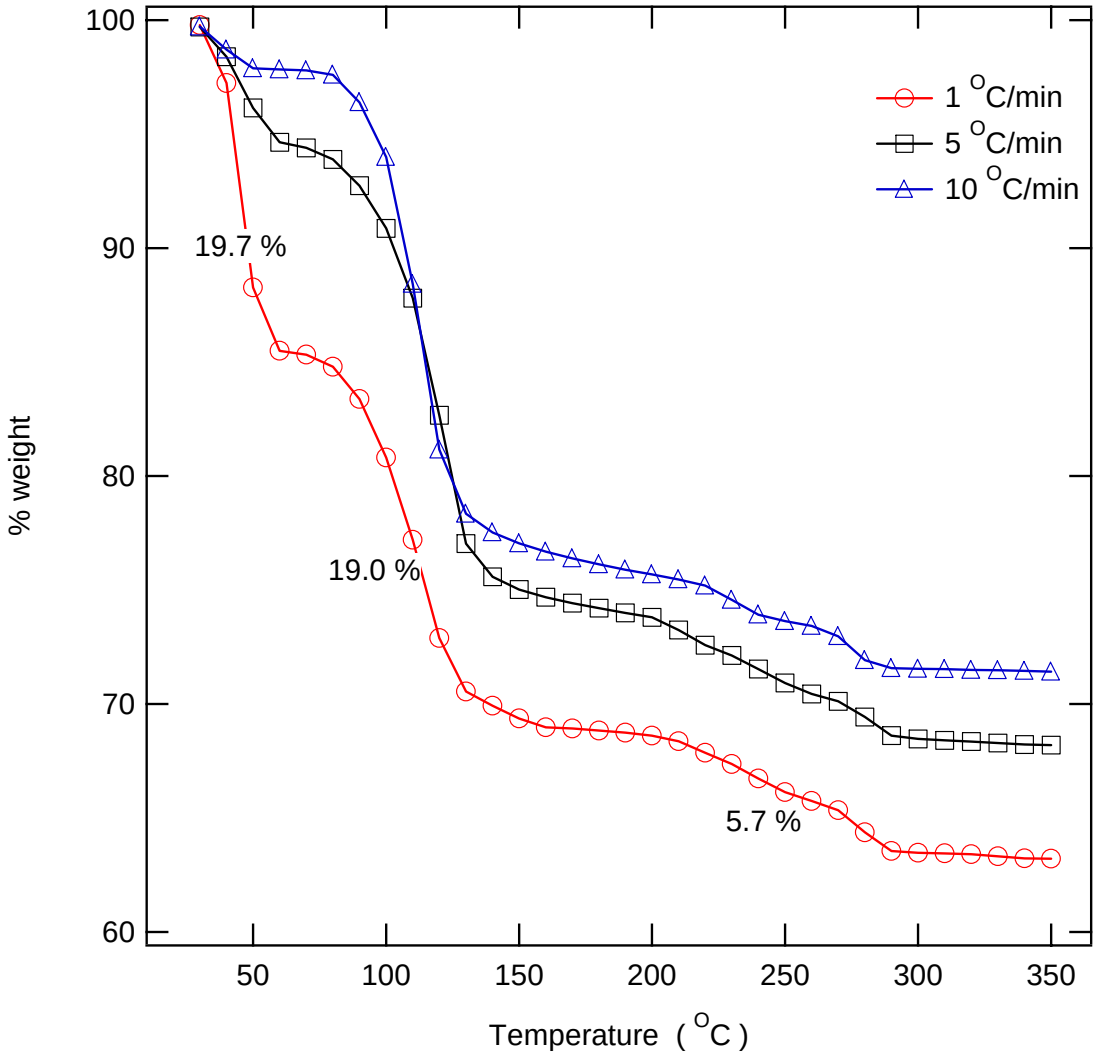

Figure 4.1: TGA results of the ferrous sulfate at different heating rates.

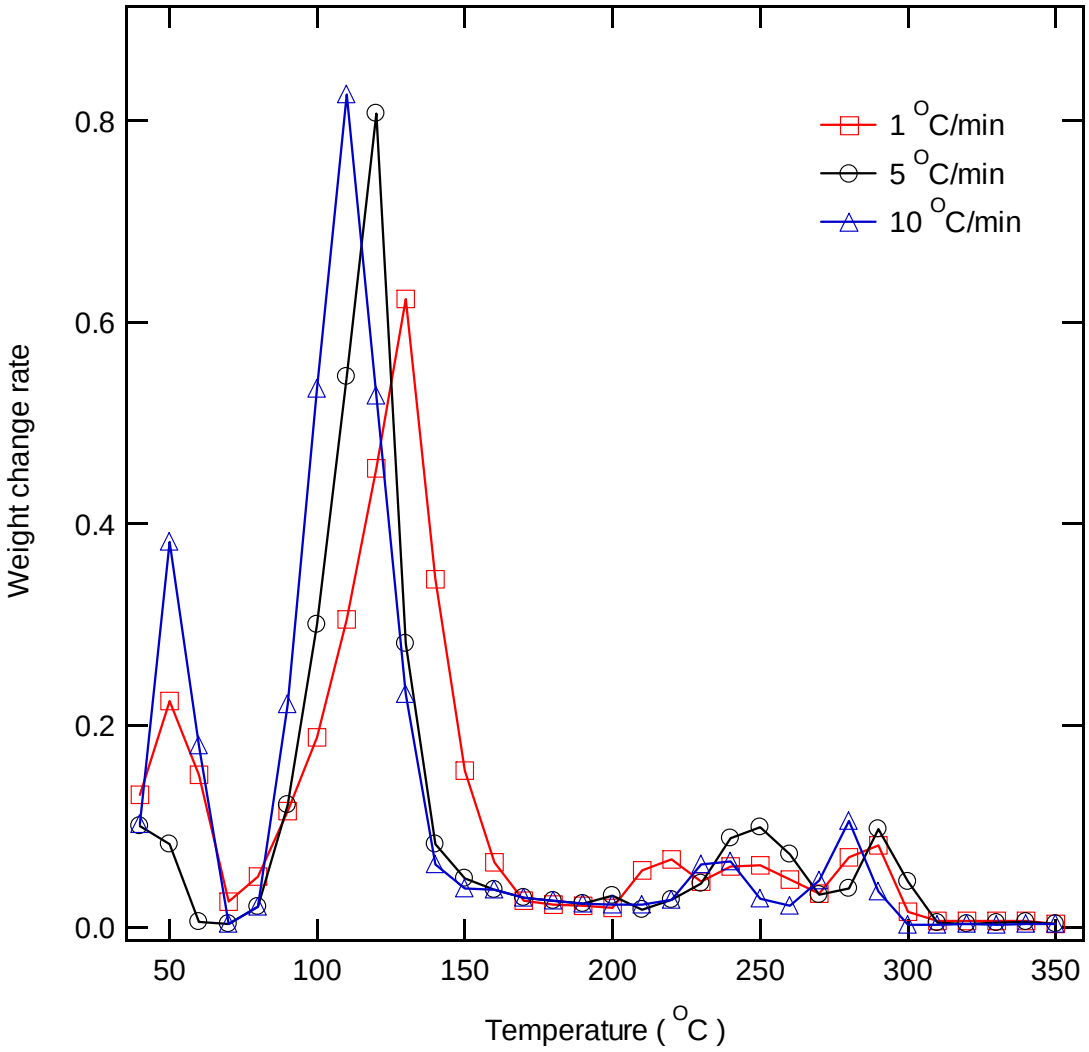

Figure 4.2: Dehydration rate of ferrous sulfate at different heating rates

loss at low temperature range and accordingly more weight loss at high temperature. The optimum TGA heating rate for ferrous sulfate was found to be 1°C/min.

The enthalpy values for the various dehydration steps were calculated from thermodynamic data and compared with the experimental results. The heats required for the various dehydration steps were estimated using the heats of formation and heat capacities of water and the various hydrates of ferrous sulfate. The heats of formation and molar heat capacity of various compounds are shown in Table 4.1. The heat of formation and molar heat capacity of $FeSO_4 \cdot H_2O$ were not available. The available data for $FeSO_4 \cdot 7H_2O$, $FeSO_4 \cdot 4H_2O$ and $FeSO_4$ were plotted and extrapolated to get the unknown value for $FeSO_4 \cdot H_2O$. A line of best fit was obtained based on $FeSO_4 \cdot 7H_2O$, $FeSO_4 \cdot 4H_2O$ and $FeSO_4$ for both the heats of formation and molar heat capacity as shown at Figure 4.3. The heats of formation (-1231.8 kJ/mol) and molar heat capacity (135.4 J/mol·K) of $FeSO_4 \cdot H_2O$ were estimated from these graphs.

Table 4.1: Heats of formation and heat capacity for various compounds [10, 11].

Compound	Heats of formation 25°C (kJ/mol)	Heat capacity at constant pressure (J/mol·K)
$FeSO_4 \cdot 7H_2O$	-3012.6	401.2
$FeSO_4 \cdot 4H_2O$	-2129.1	265.85
$FeSO_4 \cdot H_2O$	Not available	Not available
$FeSO_4$	-932.2	91.96
H_2O (l)	-258.84	75.30
H_2O (g)	-241.83	33.58
$CaSO_4 \cdot 2H_2O$	-2022.6	186.0
$CaSO_4 \cdot 0.5H_2O$	-1576.7	119.4
$CaSO_4$	-1425.2	99.0

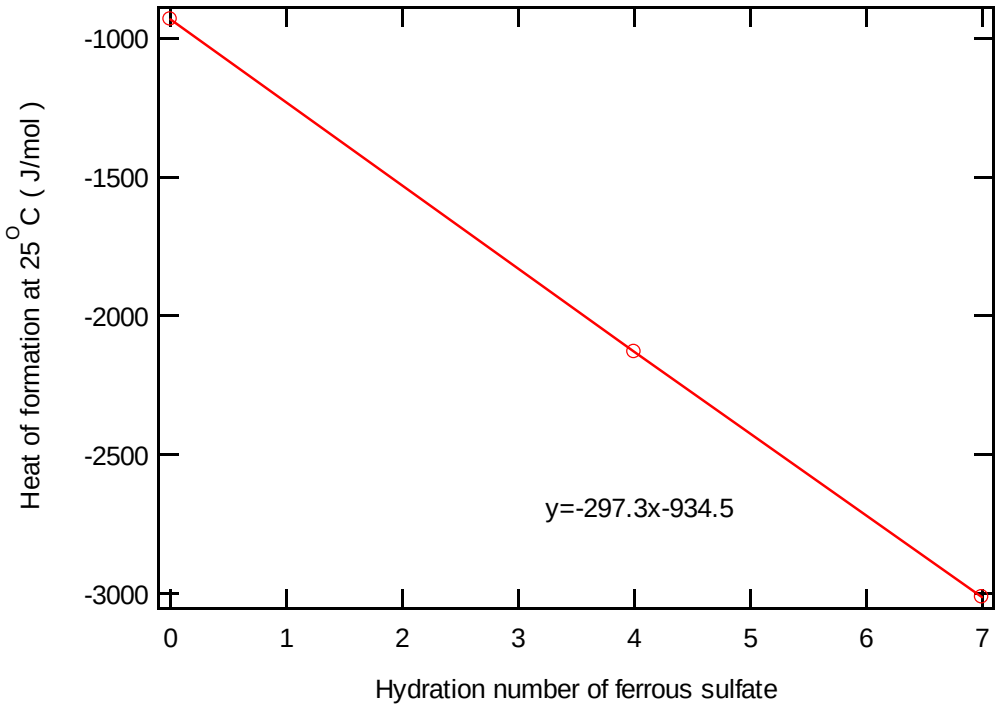

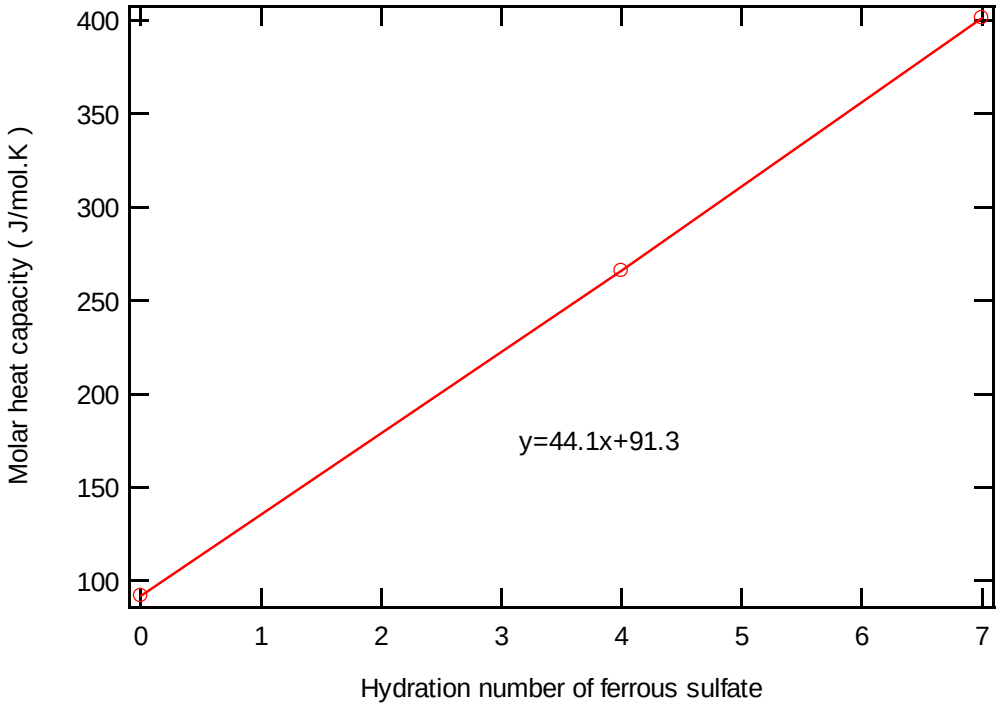

Figure 4.3: Heats of formation and molar heat capacity of ferrous sulfate

The enthalpy of dehydration for each step can be calculated at the temperature that is the peak maximum temperature on the DSC thermograph. The total enthalpy change in going from $FeSO_4 \cdot 7H_2O$ to $FeSO_4$ is 400.8 kJ/mol. This value is combined with the enthalpy of vaporization for water. The enthalpy to transition from one hydrate to another is 159.8 kJ/mol, 178.3 kJ/mol and 62.7 kJ/mol corresponding to each dehydration step.

Figure 4.4 shows the DSC thermograph for ferrous sulfate using a closed DSC pan with a pin hole and using open pan at a heating rate of 10°C /min. The onset, end point, and the maximum temperature are labeled. Three sigmoidal baselines were used to determine the enthalpy for each step. The total enthalpy to transition from $FeSO_4 \cdot 7H_2O$ to $FeSO_4$ is 316.3 kJ/mol. The enthalpies to transition from one hydrate to another are 86.9 kJ/mol, 171.3 kJ/mol and 58 kJ/mol.

The experimental result for total enthalpy is -21.1% lower than the theoretical thermal value at a heating rate of 10°C/min. The dehydration enthalpy for each step is –45.6%, -4% and –7% lower than the calculated values. While comparing each dehydration step, we found that the difference at the first step is the biggest (-45.6%) and smallest at the second step. We assume the first peak in the DSC thermograph represents the removal of the first three water molecules. This step of dehydration from $FeSO_4 \cdot 7H_2O$ to $FeSO_4 \cdot 4H_2O$ took place at temperature lower than 100°C. The water from this step is not completely evaporated during the dehydration process. However, the calculated value of enthalpy in this step includes the enthalpy of water vaporization. The calculated value of enthalpy at this step is 96.5 kJ/mol not excluding the enthalpy for the vaporization of water. The experimental result (86.9 kJ/mol) is much closer to this value.

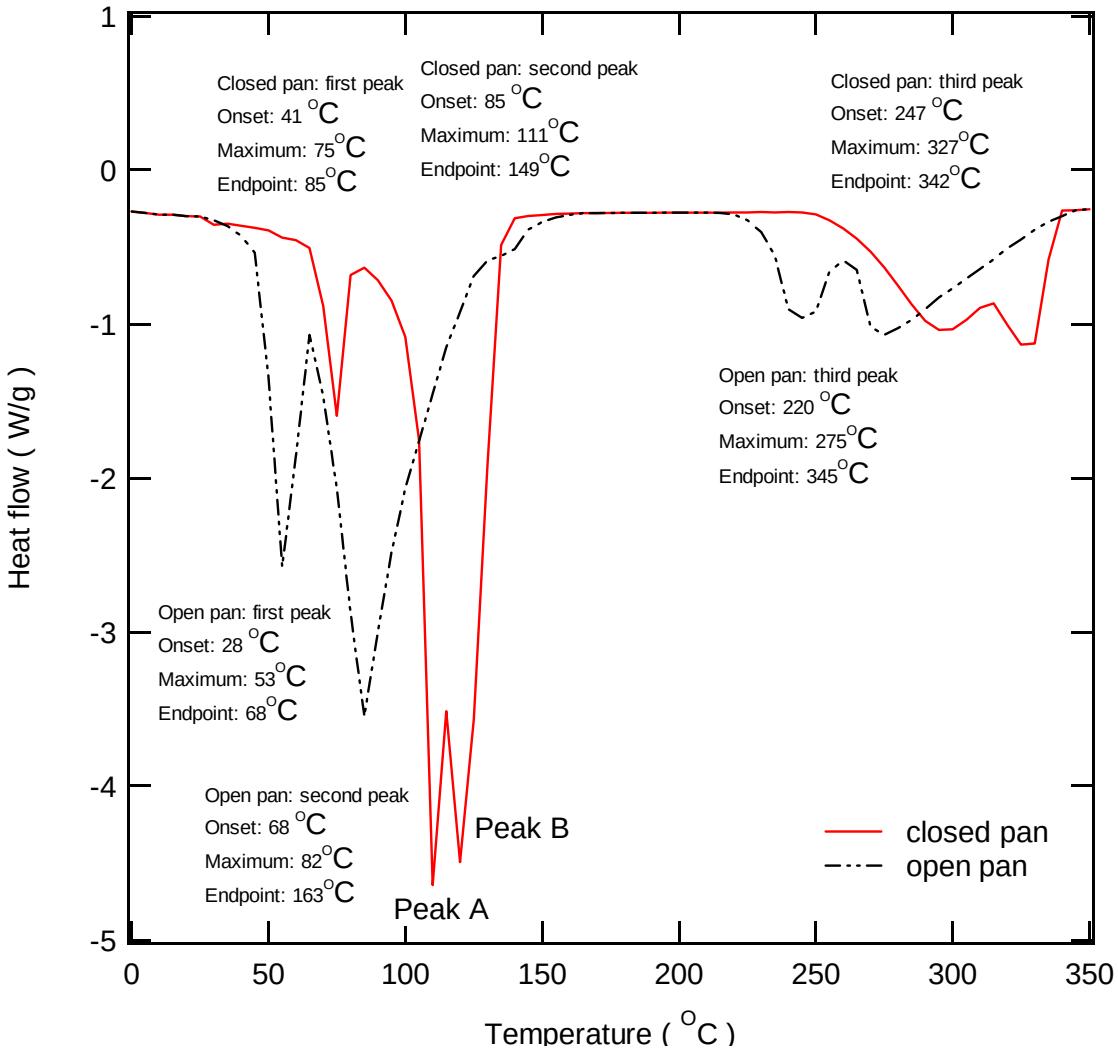

Figure 4.4: DSC thermograph for ferrous sulfate using closed pan and open pan with a heating rate of 10°C /min.

The second step of dehydration from $FeSO_4 \cdot 4H_2O$ to $FeSO_4 \cdot H_2O$ took place over a temperature range from 100°C to 150°C. Water generated by this dehydration step vaporized immediately followed by the dehydration. At the same time, water from the first dehydration step is vaporized at the beginning of this step. So the second peak in the DSC thermograph might represent the removal of the three water molecules and vaporization of six water molecules. The calculated value of enthalpy for this step is 227.3 kJ/mol if the enthalpy for the vaporization of six water molecules is included. The DSC experimental result for the second step is -21.6% lower than the theoretical thermal value.

We can also observe that two peaks are combined to form the second peak when using a closed DSC pan with a pinhole. Peak A represents the enthalpy of dehydration from $FeSO_4 \cdot 4H_2O$ to $FeSO_4 \cdot H_2O$ and the enthalpy of vaporization for three water molecules generated by the first dehydration step. Peak B represents the enthalpy of vaporization of three water molecules generated by the second dehydration step.

The third step of dehydration from $FeSO_4 \cdot H_2O$ to $FeSO_4$ took place over a temperature range from 200°C to 300°C. One water molecular generated by this dehydration step vaporized immediately followed by dehydration. So the enthalpy of third peak of DSC thermograph corresponds to the total enthalpy of dehydration of water and vaporization of water.

The DSC thermograph for ferrous sulfate using open DSC pan at a heating rate of 10°C /min is shown in Figure 4.4. Three sigmoidal baselines were used to determine the enthalpy for each step. The enthalpies to transition from one hydrate to another are 103.2 kJ/mol, 121.7 kJ/mol and 61.1 kJ/mol. The total enthalpy to transition from $FeSO_4 \cdot 7H_2O$

to $FeSO_4$ is 286 kJ/mol. The experimental value for the enthalpy of dehydration for each step and total its enthalpy values are –35.4%, -31.8%, -2.5% and –28.6% different from the values calculated by the heats of formation and molar heat capacity of various compounds. The peak of dehydration and vaporization overlap completely when the open DSC pan was used. The open pan DSC method cannot resolve the second peak in the thermogram into a dehydration peak and water vaporization peak whereas the closed pan method can.

The enthalpy values from the experimental results for both closed DSC pan and open DSC pan have more than –20% difference from the theoretical thermal value. Part of the reason for this difference is because the peak for each dehydration step cannot be completely separated. The end point of each peak does not return to the horizontal baseline. As a result peak area will be less when using sigmoidal baseline correction. The thermographs were analyzed again using horizontal baselines assuming the end point of peaks return to the baseline. A summary of results is provided in Table 4.2. The enthalpy of each dehydration step measured experimentally in this analysis is higher than that using a sigmoidal baseline. The total enthalpy measured experimentally is within 10% of the calculated values from the heats of formation and molar heat capacity of various compounds for both closed DSC pan and open DSC pan. Comparison of both the total enthalpy and the enthalpy for the individual steps show that the analysis with horizontal baseline is more accurate than the analysis with sigmoidal baseline, especially for the open DSC pan, where the total enthalpy measured experimentally is 383 kJ/mol. This experimental result is close to the calculated value (-4.4% difference).

Table 4.2: Summary of the DSC results for ferrous sulfate

Experimental condition	Enthalpy of 1st step (kJ/mol)	Enthalpy of 2nd step (kJ/mol)	Enthalpy of 3rd step (kJ/mol)	Total Enthalpy (kJ/mol)
Calculated enthalpy from thermal data [10,11]	159.8	178.3	62.70	400.83
DSC data using closed pan at a heating rate of 10°C /min (analysis with sigmoidal baseline)	86.9	171.26	58	316.3
% Difference compared with calculated value	-45.6%	-4%	-7%	-21.1%
DSC data using open pan at a heating rate of 10°C /min (analysis with sigmoidal baseline)	103.2	121.7	61.1	286.0
% Difference compared with calculated value	-35.4%	-31.8%	-2.5%	-28.6%
DSC data using closed pan at a heating rate of 10°C /min (analysis with horizontal baseline)	102.6	205.5	58.7	366.8
% Difference compared with calculated value	-35.8%	15.3%	-2.5%	-8.5%
DSC data using open pan at a heating rate of 10°C /min (analysis with horizontal baseline)	138.7	181.5	62.8	383.4
% Difference compared with calculated value	-13.2%	1.8%	1.75%	-4.4%
DSC data using open pan at a heating rate of 2.5°C /min (analysis with sigmoidal baseline), particle size less 325 mesh	116.5	142.3	64.5	323.4
% Difference compared with calculated value	-27.1%	-20.2%	2.9%	-19.3%
DSC data using open pan at a heating rate of 2.5°C /min (analysis with horizontal baseline), particle size less 325 mesh	145.7	180.4	64.8	390.9
% Difference compared with calculated value	-8.8%	1.2%	3.4%	-2.5%

The ferrous sulfate samples were treated in nitrogen atmosphere using different heating rates. The results demonstrate that the peak resolution is highest in the range of 2 to 10°C/min. A low heating rate provides a slightly better result in this range

Different particle sizes of ferrous sulfate samples were run in DSC using an open pan. All experiments were analyzed using a heating rate of 2.5°C/min. We have focused on three particle sizes of the ground ferrous sulfate. The largest particle size is great than 100 mesh. The middle particle size is from 170-230 mesh and the small particle size is less than 325 mesh. Experimental results are provided in Table 4-2. Our data show that the enthalpy measured experimentally for small particle size was slightly better than big size as compared to thermograph. The reason might be the crystal size of samples might affect heat transfer during DSC analysis. The heat transfer may not be uniform for the particles of different size. Dehydration might occur at different bulk temperatures for the different particle sizes. Another reason is the big size crystals might not dehydrate completely during the first and second dehydration step that take place in very narrow temperature range. The experimental DSC thermograph for the smallest particle size was found to give better resolution.

Figures 4.5, 4.6, and 4.7 were the DSC thermographs that compare the dehydration behavior under thermal heating and supercritical extraction. The thermal heating samples were prepared by heating the $FeSO_4 \cdot 7H_2O$ at constant temperature for 30 min. The extraction samples were prepared by extracting the $FeSO_4 \cdot 7H_2O$ at 120 bar for 30 min. The temperature 32^oC is the same in both processes. The extracted samples were analyzed immediately via DSC without re-exposing the sample to the atmosphere. Figure 4.5 is the DSC thermograph for the extraction sample and thermal heating sample at 32°C

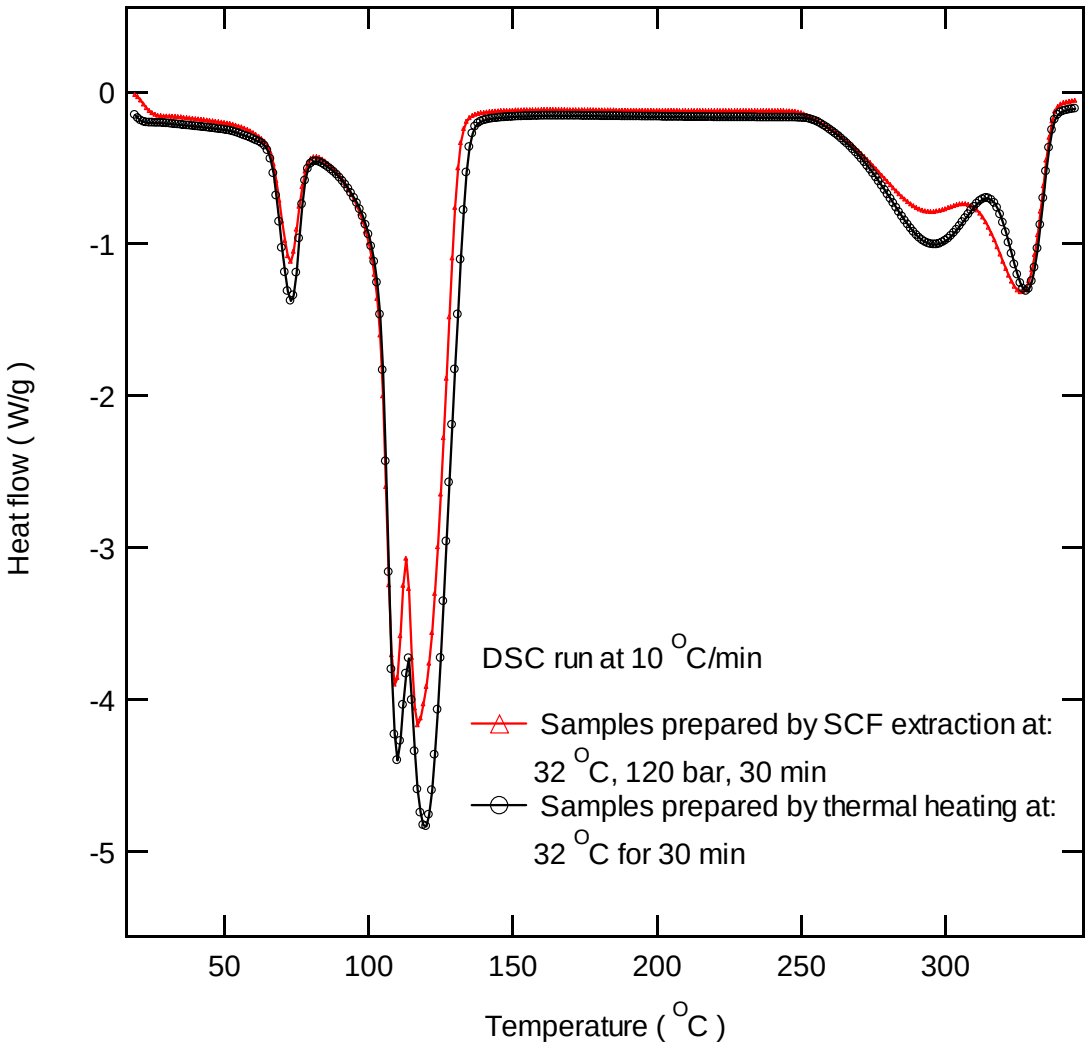

Figure 4.5: DSC thermograph comparison of thermal heating and supercritical extraction at 32°C.

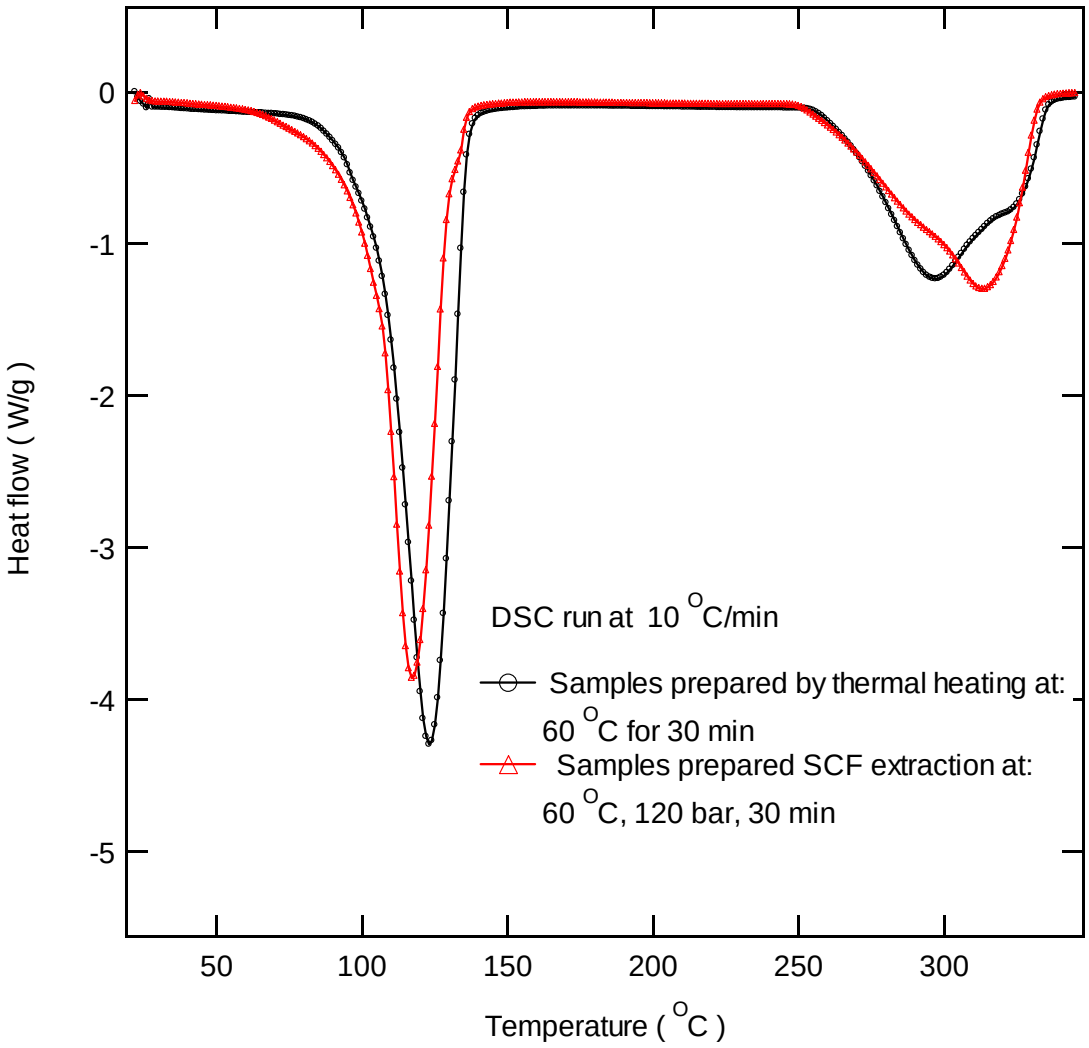

Figure 4.6: DSC thermograph comparison of thermal heating and supercritical extraction at 60°C.

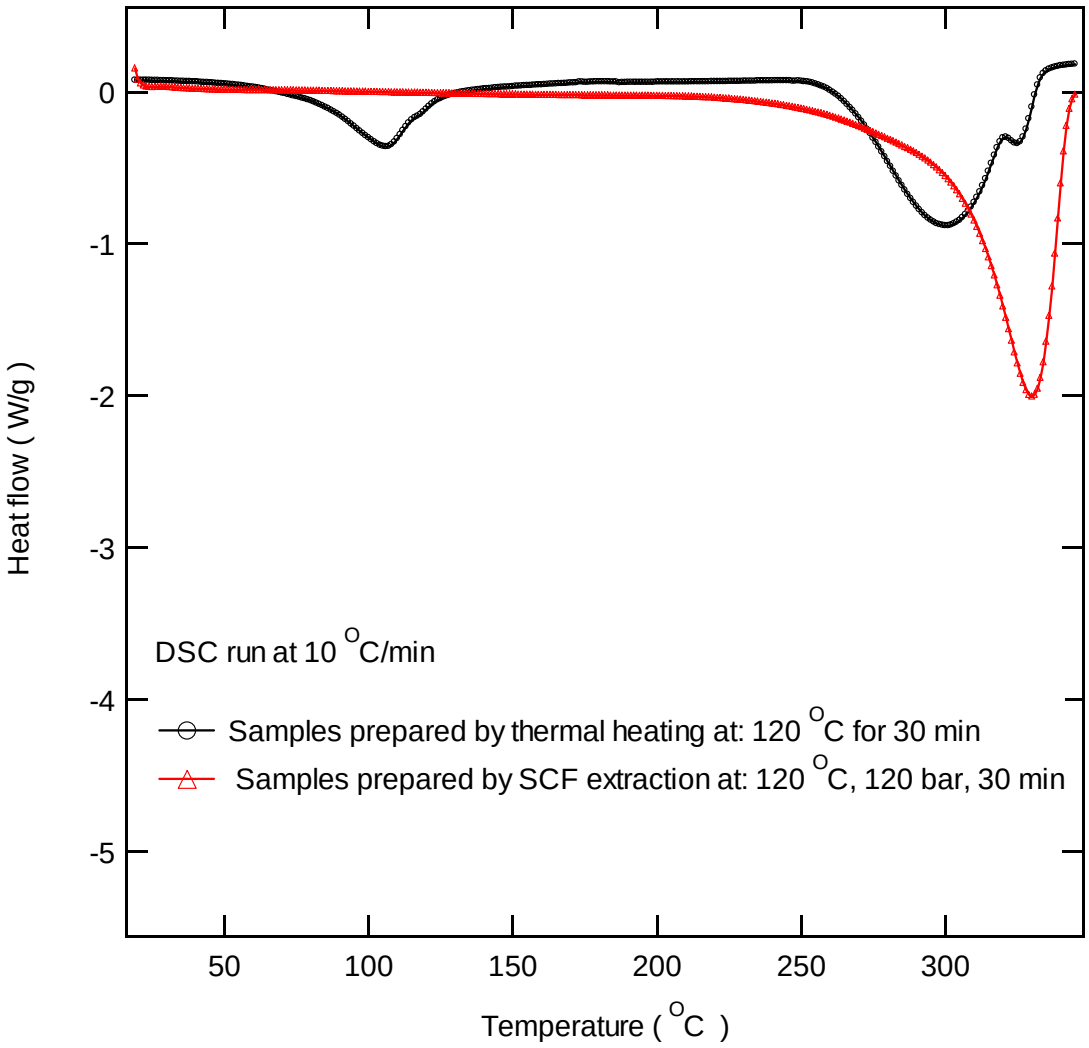

Figure 4.7: DSC thermograph comparison of thermal heating and supercritical extraction at 120°C**.**

The peak shape and the peak area for the extraction sample and the thermal heating sample are similar to the fresh ferrous sulfate sample. This indicated no dehydration took place for both thermal heating and extraction at this condition.

From Figure 4.6 in which the experimental temperature was 60°C, we do not observed the first peak in 40-80°C range. The first dehydration step (dehydration from $FeSO_4 \cdot 7H_2O$ to $FeSO_4 \cdot 4H_2O$) is completed at 60°C. The extraction sample peak is slightly smaller than the thermal sample peak. At 120°C (Figure 4.7), the first dehydration peak and the second dehydration peak have disappeared for the extraction sample. The extraction sample has lost six water molecules. The thermal heating sample however has not lost its six water molecules at 120°C. There is a small peak in 100-150°C range for the thermal heating sample. This peak is smaller than the fresh ferrous sulfate sample. It appears that the supercritical extraction process enhances the dehydration process under proper conditions. It is possible to recover water from a hydrated compound using supercritical carbon dioxide.

Dehydration Study of Calcium Sulfate ($CaSO_4 \cdot 2H_2O$)

The experimental procedures for calcium sulfate are the same as ferrous sulfate. The heating rates for the TGA in this study were set at 1°C /min and 10°C /min. The heating rates for the DSC were set at 5°C /min, 10°C /min and 15°C /min.

Plots of the percent weight remaining versus temperature for TGA thermograph are shown in Figure 4.8. An open pan was used in TGA process. Two dehydration steps are clearly seen at the low heating rate. In Figure 4.9, DSC curves for gypsum also clearly show two steps in the dehydration process. The peaks at the high heating rate

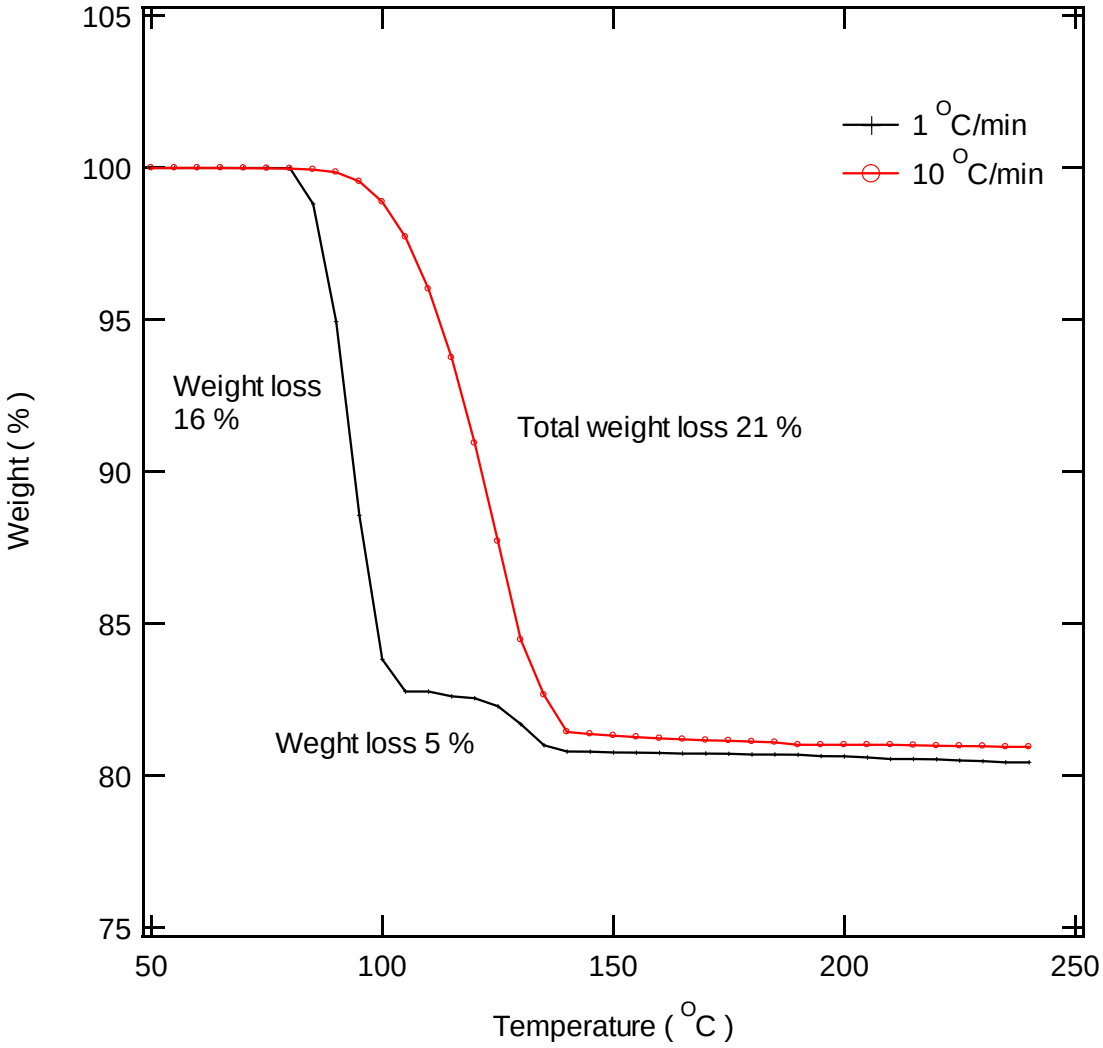

Figure 4.8: TGA results of calcium sulfate at different heating rates.

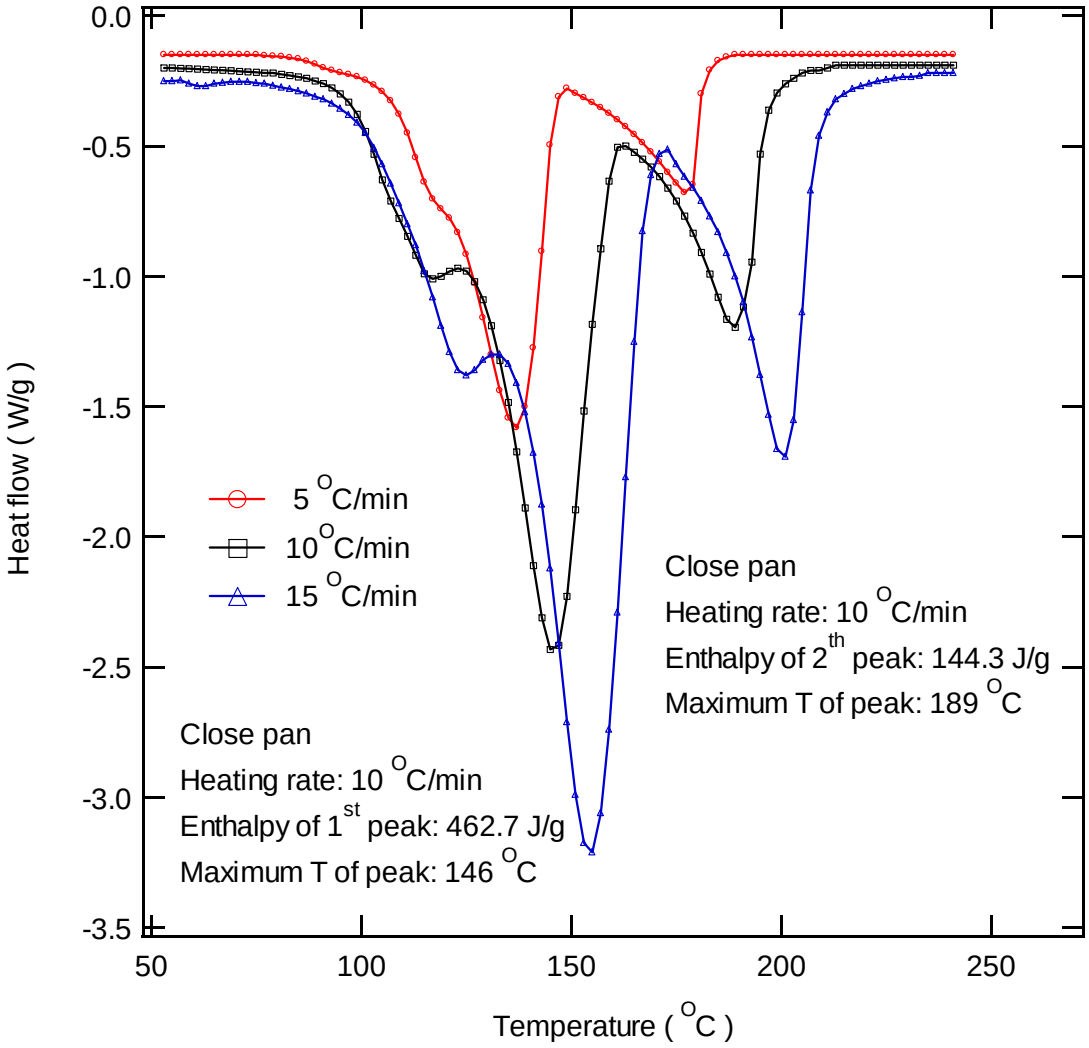

Figure 4.9: DSC results of calcium sulfate at different heating rate.

move to a higher temperature range. The sealed pan can encapsulate the gypsum, which can retard water evaporation. The temperature moves to higher range also because the temperature increases faster at higher heating rate.

The total enthalpy and the enthalpy to transition from one hydrate to another are similar at different heating rates. We obtained the enthalpy data using a closed DSC pan with a pinhole at a heating rate of 10°C /min. The maximum temperature is labeled. Sigmoidal baselines were used to determine the enthalpy for each step. The experimental data for enthalpy of transition from $CaSO_4 \cdot 2H_2O$ to $CaSO_4$ is 104.34 kJ/mol. The experimental data for enthalpy of transition from $CaSO_4 \cdot 2H_2O$ to $CaSO_4 \cdot 0.5H_2O$ is 79.58 kJ/mol. The experimental data for the enthalpy of transition from $CaSO_4 \cdot 0.5H_2O$ to $CaSO_4$ is 24.84 kJ/mol.

The enthalpy values for two dehydration steps were calculated and compared with the experimental results. The heat required for the various dehydration steps was estimated using the heats of formation of water and the various hydrates of calcium sulfate. The heats of formation and molar heat capacity of various compounds were shown in Table 4.1. The enthalpy of dehydration for each step can be calculated at the temperature that is the peak maximum temperature in DSC thermograph. Combining the enthalpy of vaporization of water, the total enthalpy for transition from $CaSO_4 \cdot 2H_2O$ to $CaSO_4$ is 111.19 kJ/mol. The enthalpy for transition from $CaSO_4 \cdot 2H_2O$ to $CaSO_4 \cdot 0.5H_2O$ is 81.20 kJ/mol. The enthalpy for transition from $CaSO_4 \cdot 0.5H_2O$ to $CaSO_4$ is 29.99 kJ/mol.

The experimental result for total enthalpy is –6% below the value calculated from the heats of formation and molar heat capacity of various compounds. The dehydration

enthalpy for each step has -2% and –17% difference from the calculated values from the heats of formation and molar heat capacity of various compounds.

References

1. Klaus S. Lackner, Christopher. H. Wendt. Carbon Dioxide Disposal in Carbonate Minerals. *Energy*, **1995**, **20**, 1153-1170.

2. Carlton C. Allen, Richard V. Morris, and David J. Lindstrom. *JSC Mars-1: Martian Regolith Simulant.* NASA Johnson Space Flight Center, Houston,TX, **1997**.

3. J. E. Macintyre (Ed.), Dictionary of Inorganic Compounds. (1992) London. New York, Chapman & Hall.

4. Diev. N. P., Abstract of Dehydration of Ferrous Sulfate, *Phys. Chem. Miner*.,**1995**,23,263-275.

5. Rodionov, A.I., Zapol'skii, A.K., Yakushev, V.I., Fedoritenko, I.I. Dehydration of Ferrous Sulfate Heptahydrate. Tr.-Mosk. Khim.-Tekhnol. *Inst. Im. D.I. Mendeleeva*, **1997**, 109, 51-56.

6. Y. Pelovski, V. Petkova, S. Nikolov. Study of the Mechanixm of the Thermochemical Decomposition of Ferrous Sulfate Monohydrate. *Thermochimica Acta* , **1996**, 274, 273-280.

7. N. Kanri, I. Gaballah, C. Mathieu, N. Neveux, O. Evrard. Kinetics of Dehydration of $FeSO_4.7H_2O$ under Different Atmospheres, EPC Congress 1999, The Minerals, Metals & Materials Society, **1999**.

8. D. L. Hudson-Lamb, C. A. Strydom and J. H. Potgieter. The Thermal Dehydration of Natural Gypsum and Pure Calcium Sulfate Dihydrate (gypsum). *Thermochimica Acta*, **1996**, 282,483.

9 Patricia M. Dove and Carol A. Czank. Crystal Chemical Controls on the Dissolution Kinetics of the Isostructural Sulfates: Celestite, Anglesite, and Barite . *Geochimica et Cosmochimica* Acta, **1995**, 59, 1907.

10 Reinhold, *Thermochemistry of the Chemical Substances*,90 Data, **1936**.

11 Perry, R.H.; Green, D.W, *Perry's Chemical Engineers' Handbook (7th Edition)*, McGraw-Hill, **1997**, 2-190, 2-194.

CHAPTER V

SOLUBILITY OF METAL-CHELATE COMPLEX IN SUPERCRITICAL CARBON DIOXIDE

Introduction

Since supercritical carbon dioxide is nonpolar and has a low dielectric constant, most solid metal salts do not dissolve directly. Therefore, modifiers or coordinating ligands (complexants) are required to increase solubilities of metal ions in the supercritical carbon dioxide phase. By addition of a complexing agent into the supercritical phase, the metal ion charge can to be neutralized and the lipophilic groups can be introduced to the metal-complex system. The addition of a complexing agent facilitates the solubilization of the metal complex into the supercritical carbon dioxide. Laintz et al. [1] first demonstrated that Cu^{2+} could be extracted by using the proper chelate. When metal ions are chelated with organic ligands, they may become quite soluble in supercritical carbon dioxide. The capability of extracting a metal in supercritical carbon dioxide depends largely on the effectiveness of the chelate. A variety of ligands can be used for supercritical fluid extraction of metal species. A suitable chelate should have relatively high solubility in supercritical carbon dioxide. At the same time, the chelate should form stable chelate-metal complex and this chelate-metal complex should be soluble in supercritical carbon dioxide. B-diketones, dithiocarbamates, organo-phosphate systems, and amines are the common ligands that have been used in the supercritical carbon dioxide system [2]. There are over fifty papers in the literature on supercritical fluid extraction of metal-chelate complexes [3].

Supercritical fluid extraction of Ni, Fe, Cu, Y, Ba, Li, Co, Mn, Pb, Zn, In, Ga, Cr, Ur, Th, La and Ac cations with chelating agent have been investigated [4-11]. Metal-complexes with fluorine-substituted ligands were found to be the most soluble, and metal-complexes with phenyl-substituted ligands were the least soluble [12].

Water in carbon dioxide microemulsions acts as a ligand for the extraction of metal ions [13]. A perfluoropolyether ammonium carboxylate surfactant was effective in forming water microemulsions droplets in supercritical carbon dioxide [14]. Water-based microemulsions are effective for extraction of metal ions from solids [13]. The nano-droplets of water suspended in carbon dioxide take advantage of both the high solubility of metal ions in water and the high diffusivity of carbon dioxide to penetrate pores that are inaccessible to bulk water.

The components of SiO_2, TiO_2, Al_2O_3, Fe_2O_3, MgO, CaO and K_2O have been identified in Martian soils. In this work, the solubility of minerals and compounds in supercritical carbon dioxide are determined as a function of temperature and pressure. The influence of parameters including extraction pressure, extraction temperature, concentration of ligand, concentration of water and ratio of ligand to metal on solubility of extraction metal in supercritical carbon dioxide was determined.

Materials and Methods

Materials

Copper (II) nitrate trihydrate ($Cu(NO_3)_2 \cdot 3H_2O$, FW=241.6 g/mol), nitric acid (HNO_3) and filter paper (Waterman qualitative No.2) were supplied from Fisher

Scientific Company. Water was deionized and purified by being passed through a Labconco WaterPros water purification system. High purity supercritical carbon dioxide was obtained from Air Liquide Products. Ammonium hydroxide (NH_4OH, 17%) was purchased from Labchem Inc. Fluorolink ($Cl(CF_2CF(CF_3)O)_nCF_2COOH$, PFPE-COOH, grade 7004, avg. MW=600) was obtained from Ausimont.

Methods

The experimental apparatus is a modified SFX220 supercritical fluid extraction system (Isco, Inc.), shown in Figure 5.1. The SFE220 extraction systems consist of an SFE220 extractor, an SFE200 controller, and one D series syringe pump. Both the pump and the extractor are connected to a SFE200 controller that controls all pumping and extraction operations. The 260D pump module operates up 500 bars, and has a cylinder capacity of 260 ml for extended operation. The pressure was varied from 100 to 400 bar in these studies. The pressure accuracy was ±2% of full scale. The temperature was varied between 60°C and 150°C.

To measure the amount of chelate and water, we modified the SFX220 system by adding a second pump. The chelate was dissolved in deionized water and placed in a reservoir. The desired amount of water and chelate was then introduced in the extraction system. Mg-chelate complex solubility, system parameters including pressure, temperature, quantity of ligand and water used were determined.

PFPE-NH^{4+} surfactant was formed by mixing the PFPE surfactant and ammonium hydroxide. PFPE-NH_4 surfactant of the form $[CF_3\text{-}(O\text{-}CF_2\text{-}CF(CF_3))_n\text{-}(O\text{-}CF_2)\text{-}COO]$-

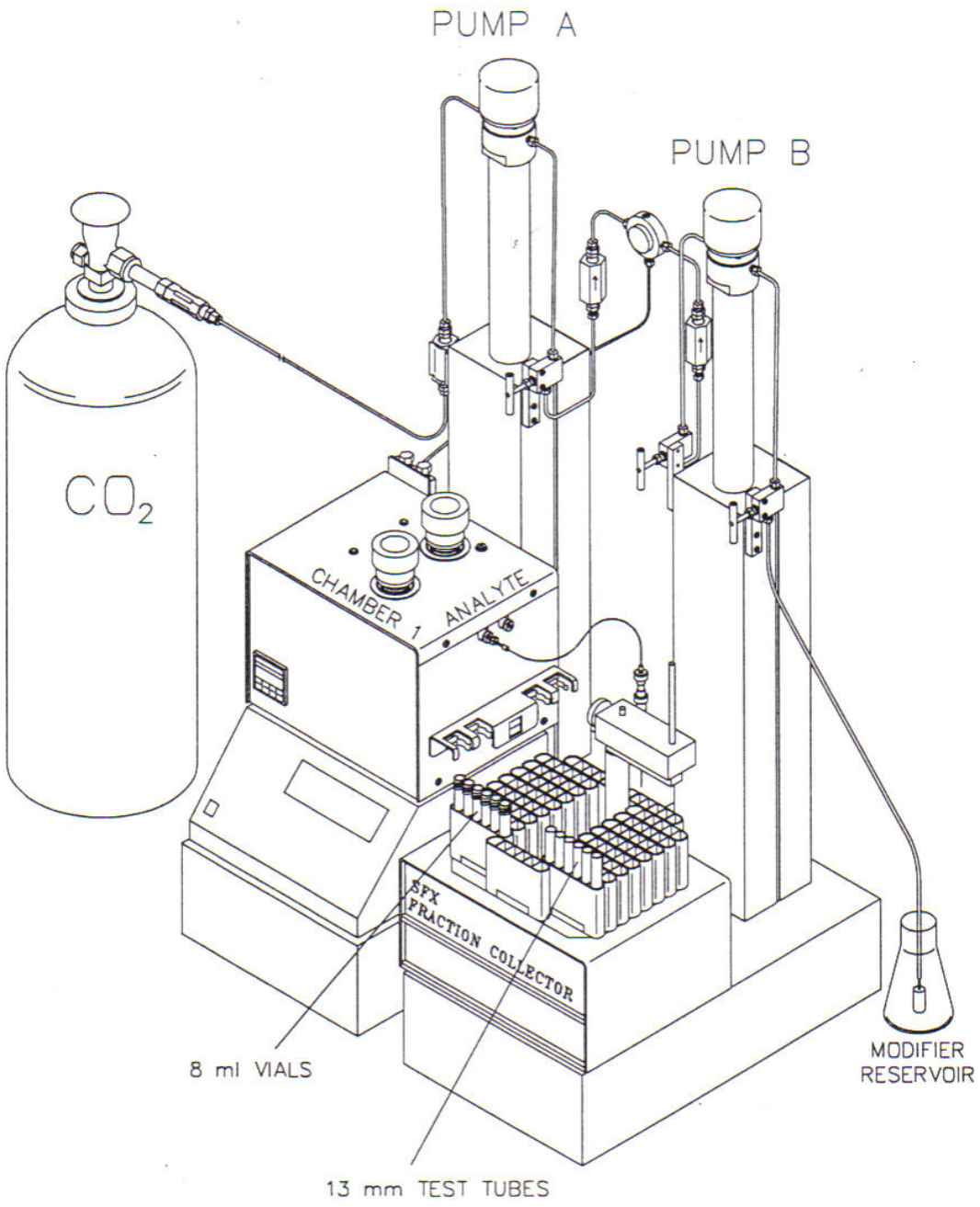

Figure 5.1: Modified SFX220 supercritical fluid extraction system (Isco, Inc.)

NH^{4+} was used in the extraction of copper ions. PFPE-NH_4 was synthesized from the neutralization of the acid (Ausimout) with aqueous ammonium hydroxide, followed by removal of water and excess ammonium under vacuum at 65^{o}C [14]. This surfactant was loaded into the reservoir.

A known amount of copper nitrate trihydrate was dissolved in deionized water. Half of the Waterman No.2 filter paper used as a substrate was spiked with 20 to 60 μl of the $Cu(NO_3)_2 \cdot 3H_2O$ solution(concentration of this solution is 34.9741g/L), mounted inside a stainless extraction cartridge (10 ml), and statically extracted using pure CO_2 for 30 min. The extraction temperature was 60°C. The extraction pressure was varied from 80 to 250 bar.

The filter paper was submerged in HNO_3 solution for 24 hours after extraction. A 100 ml solution with a pH of approximately 2 was prepared. This solution was transferred to a glass bottle with an air-tight lid. The filter paper was placed in the bottle and agitated for approximately 18 hours. The filter paper was then separated from the solution and the remaining solution was filtered. The pH was rechecked. The solution was then analyzed for cations using an AA (atomic absorption spectrometer). The mass of Cu^{2+} that remained on the filter paper was determined.

Results and Discussion

Solubility of Copper (II) Nitrate Trihydrate in Supercritical Carbon Dioxide

The Effect of Initial Amount of Cu in Filter Paper

The samples were prepared by spiking 20 μl, 30 μl, 45 μl of $Cu(NO_3)_2$ solution onto the filter paper. The measurements of extraction of $Cu(PFPECOO)_2$ in CO_2 were made at constant pressure (150 bar) and constant temperatures (60°C) for a 30 min static step. The results are shown in Table 5.1. Direct extraction of Cu ions by pure supercritical carbon dioxide is inefficient. This is because of the charge neutralization requirement and the weak interaction between solute and solvent. Using the chelating agent in the fluid phase to convert the charged species into metal chelate can significantly increase Cu^{2+} solubility in supercritical carbon dioxide.

Table 5.1: Extraction results of $Cu(NO_3)_2 \cdot 3H_2O$ in supercritical carbon dioxide.

The value of $Cu(NO_3)_2 \cdot 3H_2O$ solution added to filter paper	20 μL	30 μL	45 μL
Initial quantity of $Cu(NO_3)_2$(mg) in the filter paper by calculation	0.5434	0.8151	1.2227
Initial quantity of $Cu(NO_3)_2$(mg) in the filter paper by AA analysis	0.5293 ± 0.0063	0.8035 ± 0.0160	1.2049 ± 0.0140
$Cu(NO_3)_2$ (mg) remaining in the filter paper after extraction without chelat	0.5361 ± 0.0316	0.8307 ± 0.0063	1.2528 ± 0.0100
$Cu(NO_3)_2$ (mg) remaining in the filter paper after extraction with chelat	0.1332 ± 0.0096	0.3935 ± 0.0052	0.8060 ± 0.0130
$Cu(NO_3)_2$ (mg) removed after extraction with chelat	0.4102 ± 0.0096	0.4216 ± 0.0052	0.4167 ± 0.0130
$Cu(NO_3)_2$ removed percent (%) after extraction with chelat	75.5% ± 1.8	51.7% ± 6.5	34.1% ± 1.1

The percent removed is equal the quantity (mg) of Cu^{2+} removed from the filter paper after equilibrium extraction divided by the initial quantity of Cu^{2+} in the filter paper before extraction. As shown in Figure 5.2, 75.5%, 51.7% and 34.1% of Cu ions are removed after extraction, respectively, for filter paper being spiked 20 μl, 30 μl and 45 μl of (34.9741g/L) $Cu(NO_3)_2 \cdot 3H_2O$ solution. The initial weight of $Cu(NO_3)_2$ in the substrate are 0.5434mg, 0.8151mg and 1.227mg, respectively, for filter paper being spiked 20 μl, 30 μl and 45 μl of $Cu(NO_3)_2 \cdot 3H_2O$ solution. The amount of $Cu(NO_3)_2$ removed from each sample are same (0.41 mg) at these experimental conditions.

The Effect of Extraction Time

The measurement of the amount of $Cu(NO_3)_2$ extraced in supercritical carbon dixode at different times were made at constant pressure (150 bar) and constant temperatures (60°C). Filter paper samples were prepared by spiking 20 μl of $Cu(NO_3)_2 \cdot 3H_2O$ solution. The concentration of this solution is 34.9741g/L. The results are shown in Figure 5.3. The percents of Cu^{2+} removed from the filter paper after extraction are 75.7%, 72.9%, 75.0% and the amounts removed of $Cu(NO_3)_2$ are 0.411 mg, 0.400 mg, 0.408 mg for different extraction times at 30 min, 60 min and 90 min respectively. Base on these results, we assumed 30 min adequate to achieve equilibrium.

The Effect of Pressure

The extraction results for $Cu(NO_3)_2$ in supercritical carbon dixode at different pressures and constant temperatures (60°C) for a 30 min static step are shown in Figure 5.4. The samples were prepared by spiking 60 μl of $Cu(NO_3)_2 \cdot 3H_2O$ solution to the filter paper. The amount of $Cu(NO_3)_2$ extracted increases with increasing pressure.

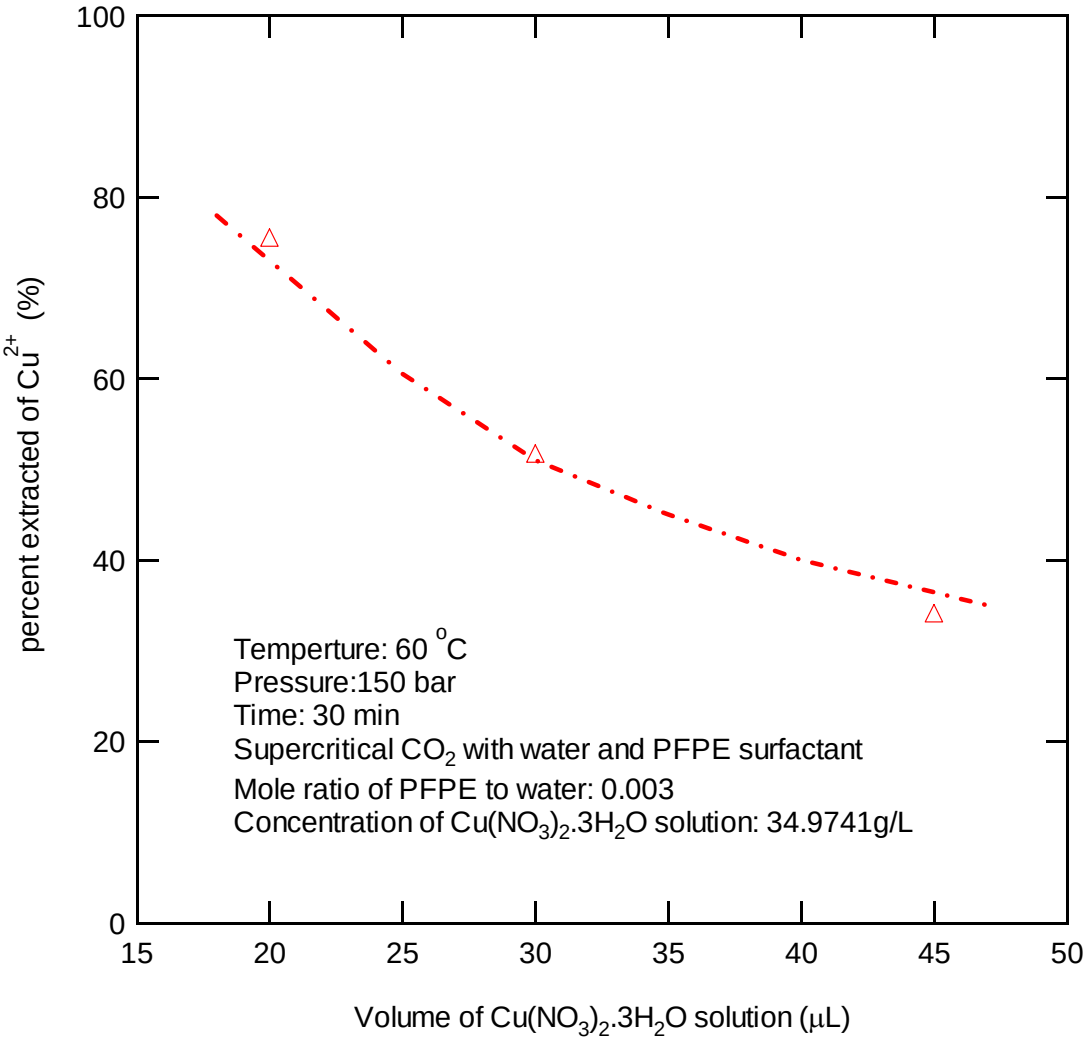

Figure 5.2: Equilibrium extraction of $Cu(NO_3)_2 \cdot 3H_2O$

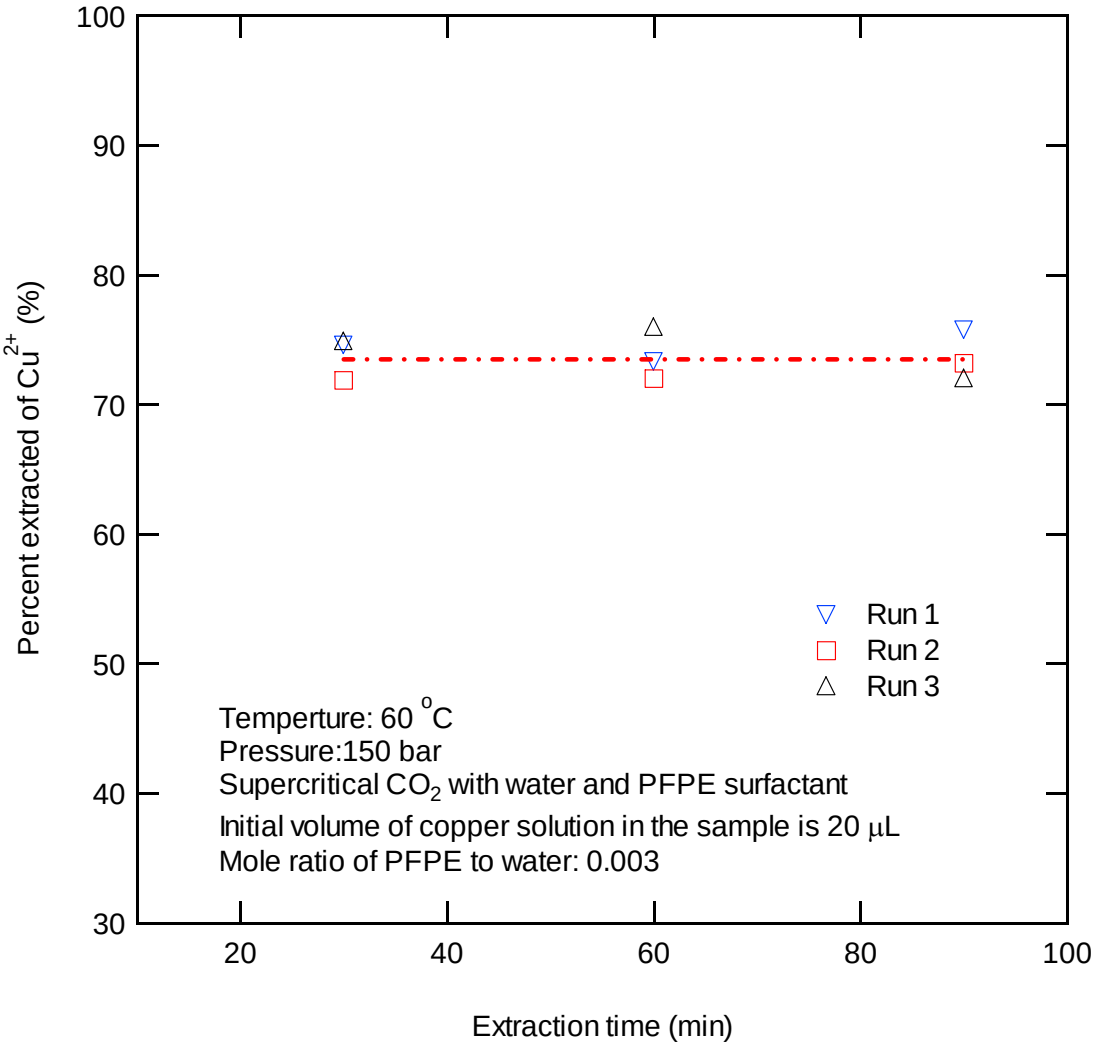

Figure 5.3: Effect of extraction time on equilibrium of $Cu(NO_3)_2 \cdot 3H_2O$ extraction in supercritical carbon dioxide.

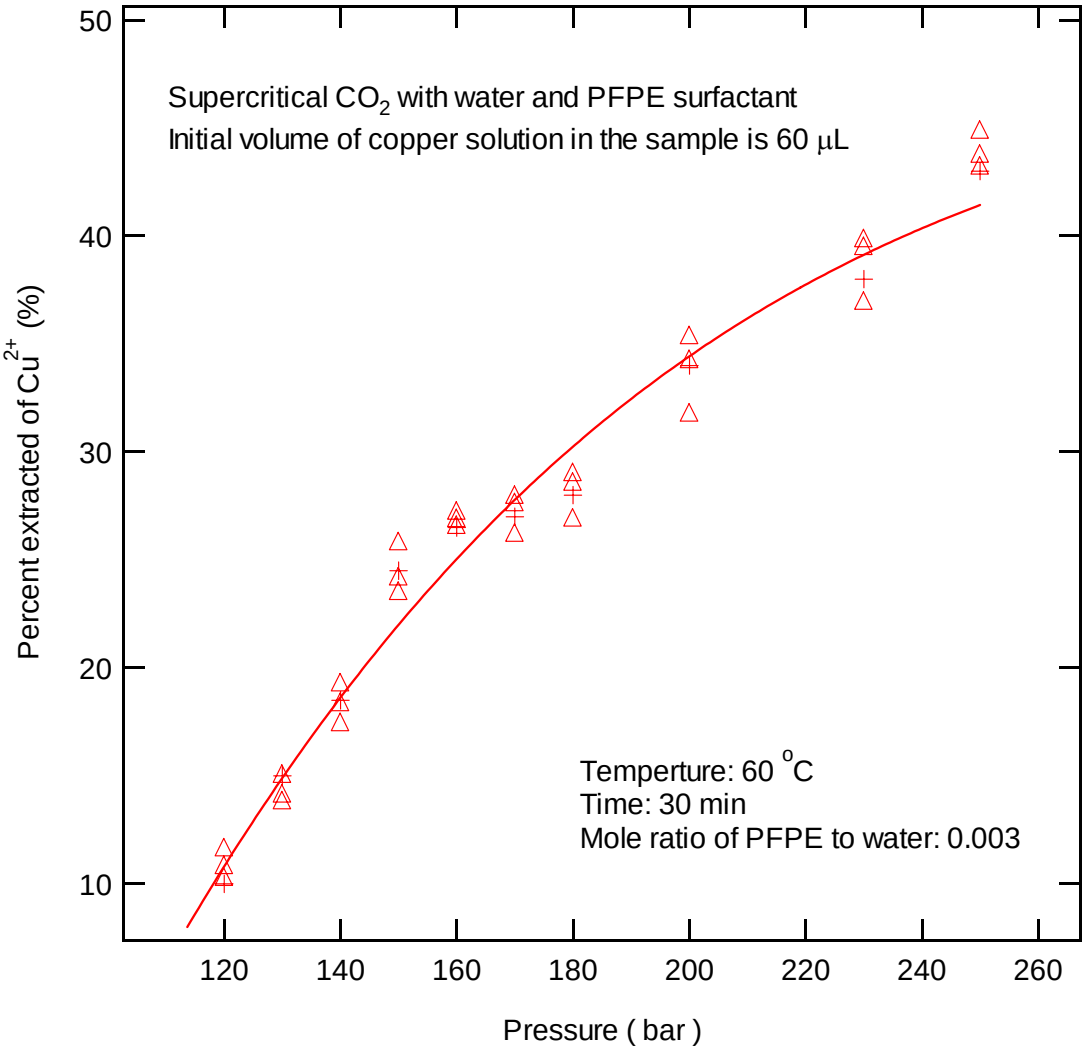

Figure 5.4: Equilibrium extraction of $Cu(NO_3)_2 \cdot 3H_2O$ in supercritical carbon dioxide as a function of pressure.

Solubility of $MgCl_2 \cdot 6H_2O$ in Supercritical Carbon Dioxide

The Effect of Extraction Time

It is necessary to determine the time for the system to achieve equilibrium when measuring solubility data. Extraction of $MgCl_2 \cdot 6H_2O$ in CO_2 at different times was made at constant pressure (150 bar) and constant temperature (60°C). The extraction samples were prepared by spiking 20μl of $MgCl_2 \cdot 6H_2O$ solution to the filter paper. The concentration of this solution is 8.1700g/100mL. The results are shown in Figure 5.5. The percents $MgCl_2 \cdot 6H_2O$ removed from the sample after extraction are 16.8%, 17.1% and 17.0% for different extraction times of 30 min, 60 min and 90 min respectively. $MgCl_2 \cdot 6H_2O$ % removed after extraction is the same at the different extraction times. $MgCl_2 \cdot 6H_2O$ removed from the filter paper after extraction does not change with further increasing time. This indicates that equilibrium is achieved within 30 min.

The Effect of Initial Amount of $MgCl_2 \cdot 6H_2O$ in Sample

The extraction samples were prepared by spiking 20 μl, 30 μl, and 45 μl of $MgCl_2 \cdot 6H_2O$ solution to the filter paper. The extraction condition is constant pressure (150 bar) and constant temperatures (60°C) for a 30 min static step. The amount of chelate and water loaded on the extraction cell are in excess compared to the moles of $MgCl_2$ spiked onto the sample. The results are shown in Figure 5.6. The percent removed is equal the quantity (mg) of Mg ions removed from the filter paper after equilibrium extraction divided by the initial weight of Mg ions in the filter paper before extraction. The amount of Mg ions removed were 16.1%, 10.6% and 7.3% after extraction, respectively, for filter paper being spiked 20 μl, 30 μl and 45 μl of $MgCl_2 \cdot 6H_2O$

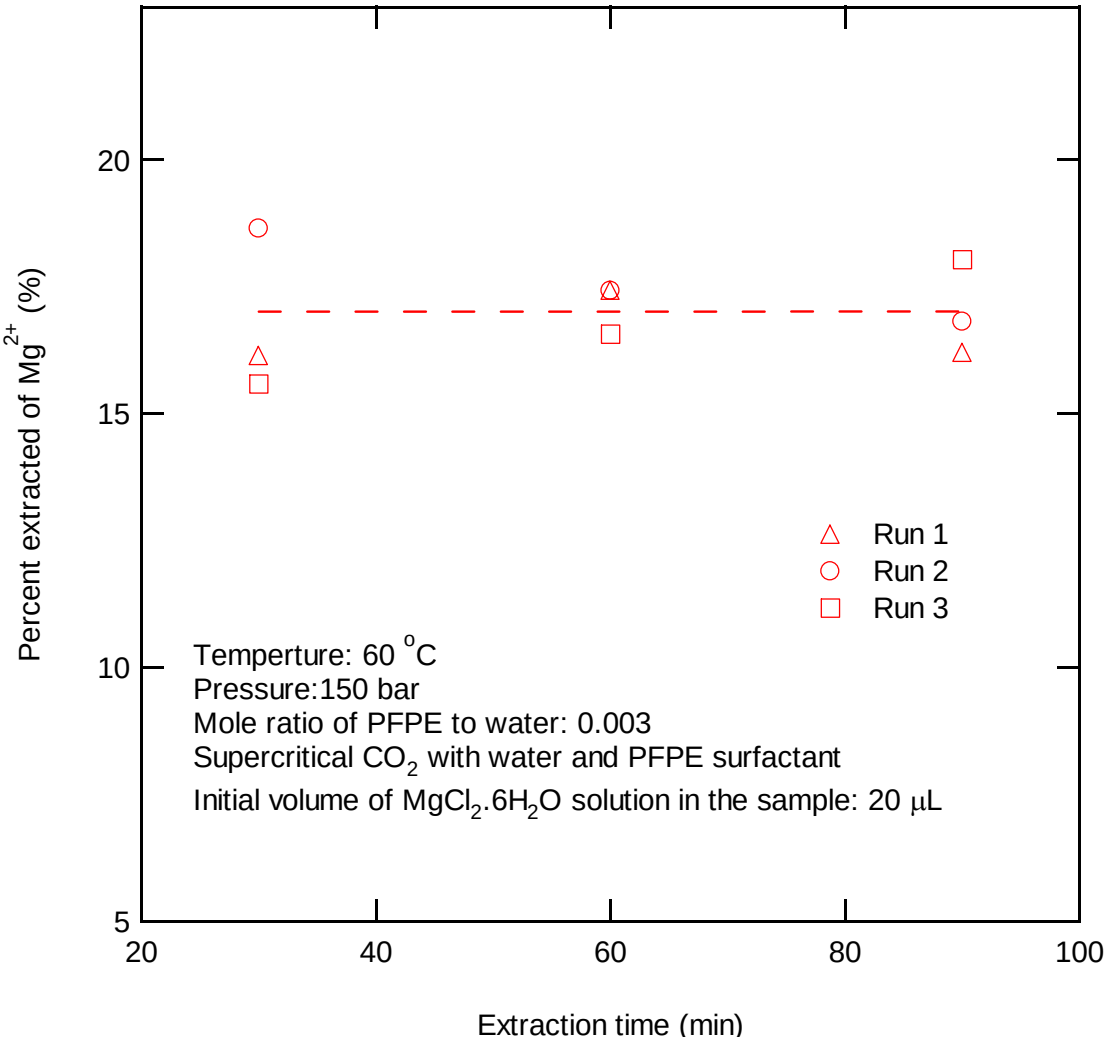

Figure 5.5: Effect of extraction time on equilibrium of $MgCl_2 \cdot 6H_2O$ extraction in supercritical carbon dioxide.

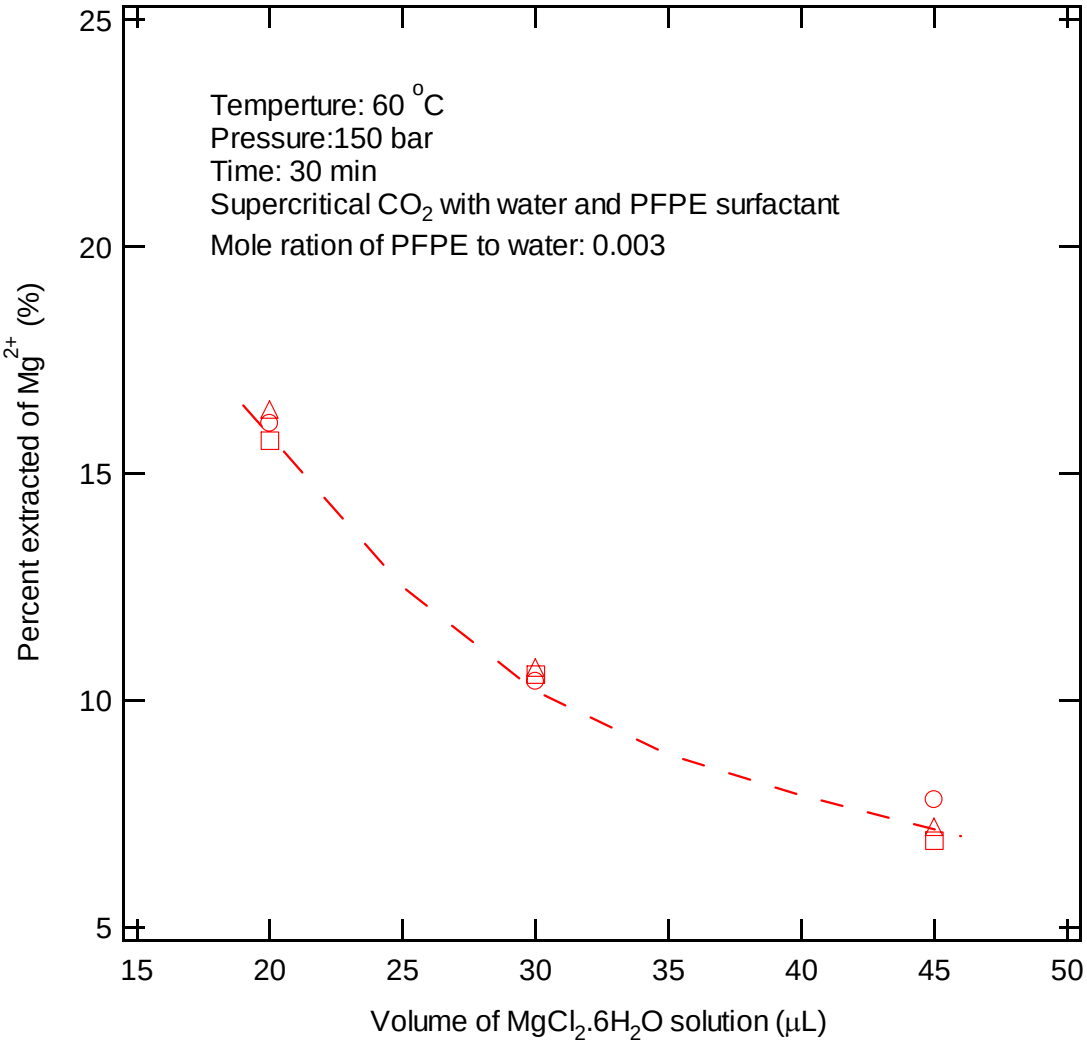

Figure 5.6: Equilibrium extraction of $MgCl_2 \cdot 6H_2O$ in supercritical carbon dioxide.

solution. The amounts of $MgCl_2 \cdot 6H_2O$ removed from each sample are 0.263 mg, 0.259 mg and 0.269 mg, respectively. The amount of $MgCl_2 \cdot 6H_2O$ removed after extraction is the same under the same conditions of temperature and pressure. The solubility of $MgCl_2 \cdot 6H_2O$ in supercritical carbon dioxide has a limit. Supercritical carbon dioxide cannot remove more Mg^{2+} by further increasing the amount $MgCl_2 \cdot 6H_2O$.

The effect of Molar Ratio of Chelate to Metal

The percent extracted at different ratios of chelate to metal is shown in Figure 5.7. The extraction condition is constant pressure (150 bar) and constant temperatures (60°C) for a 30 min static step. The extraction samples were prepared by spiking 10 μl of $MgCl_2 \cdot 6H_2O$ solution to the filter paper. PFPE-NH^{4+} surfactant was formed by mixing the PFPE surfactant and ammonium hydroxide. The average molecular weight of PFPE-NH^{4+} is 672[14]. As the mole ratio of chelate to metal increases from 0.4 to 4, the percentage metal removed only increases 10%. The percentage extracted doesn't change appreciably with further increase in the ratio. The supercritical carbon dioxide has a weak solvent interaction with conventional surfactants. This disadvantage limits the use of supercritical carbon dioxide as a solvent for metal extraction. Yazdi and Beckman [16] have shown that highly fluorinated ligands greatly enhance the solubility of metal complexes. But the ligand has to be in large excess. Our extraction results have shown that good extraction percentages are possible at very low metal-chelate ratios because water can form a stable emulsion in the supercritical carbon dioxide phase. Johnston [17] and Eastoe [18] first showed that stable water nanoemulsion droplets can be formed in supercritical carbon dioxide with droplet size range from 3 nm to 10 nm.

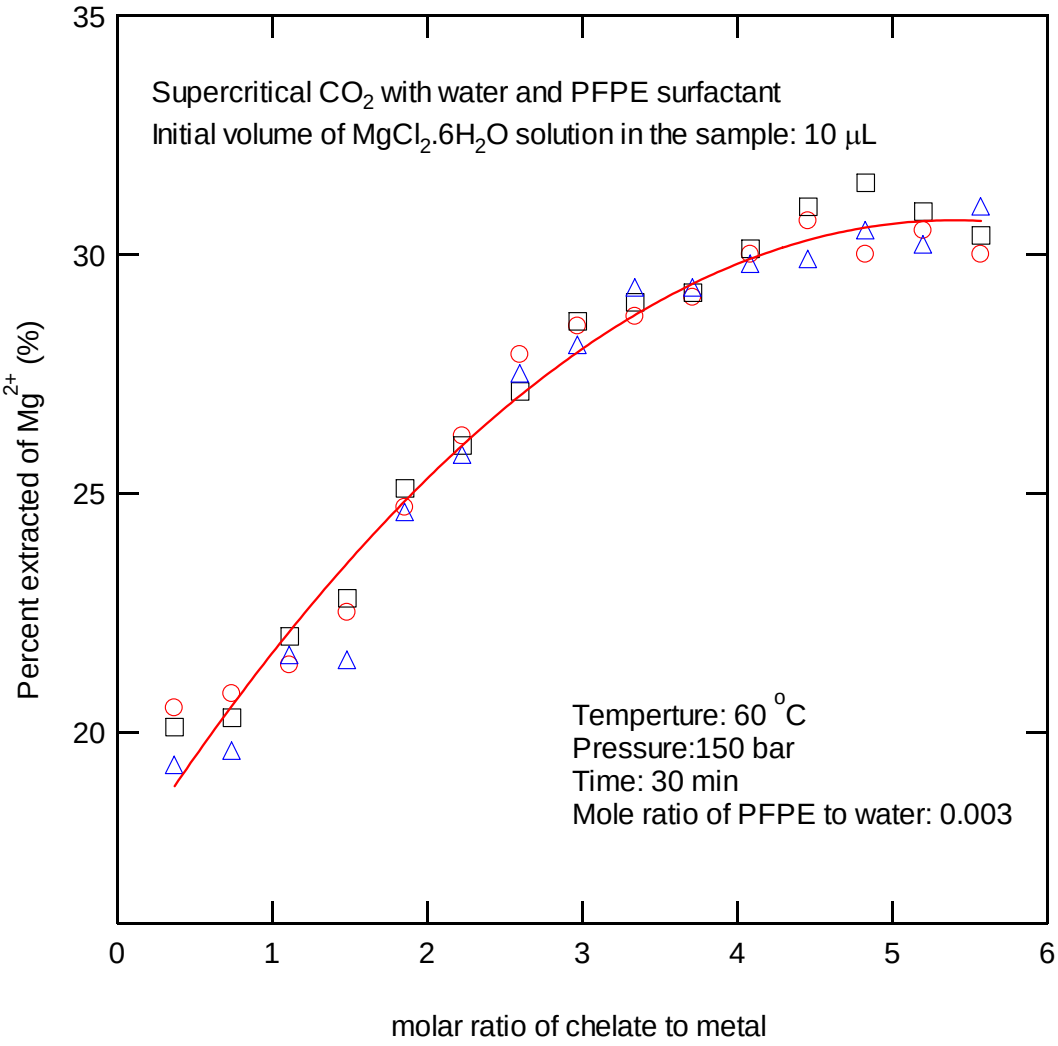

Figure 5.7: Effect of the molar ratio of chelate to metal on equilibrium extraction

Johnston and Lee [19] also showed that stable water–in–carbon dioxide emulsion droplets about 10 nm in diameter have been formed with perfluoropolyether ammonium carboxylate (PFPE-NH_4). High extraction percentages of metal in supercritical carbon dioxide take advantage of the high solubility of metal in nanodroplets of water suspended in the supercritical carbon dioxide phase. This process takes advantage of the high diffusivity of carbon dioxide by penetrating pores inaccessible to the bulk water. Therefore, using a small amount of water in the metal extraction can decreases dramatically the amount of chelate used.

The Effect of Amount of Chelate and Water

The equilibrium extraction of $MgCl_2 \cdot 6H_2O$ in supercritical carbon dioxide with different amounts of chelates is shown in Figure 5.8. The extraction condition is constant pressure (150 bar) and constant temperatures (60°C) for a 30 min static step. The chelate weight percent is equal to the mass of chelate divided by the sum of the mass of carbon dioxide, chelate and water. The water weight percent is equal to the mass of water divided by the sum of the mass of carbon dioxide, chelate and water. No metal was extracted in the absence of chelate, as the metal is insoluble in pure carbon dioxide. As the chelate weight percent increased between 0 to 1%, the percent metal removed after extraction increased from 0 up to 30%. Further increase of the chelate has no significant effect on the equilibrium extraction. The addition of a complexing agent makes the solubilization of the chelate-metal complex in the supercritical carbon dioxide possible. Results also show that once the amount of chelate added reaches about 1%, further increases of additional chelate have no significant effect.

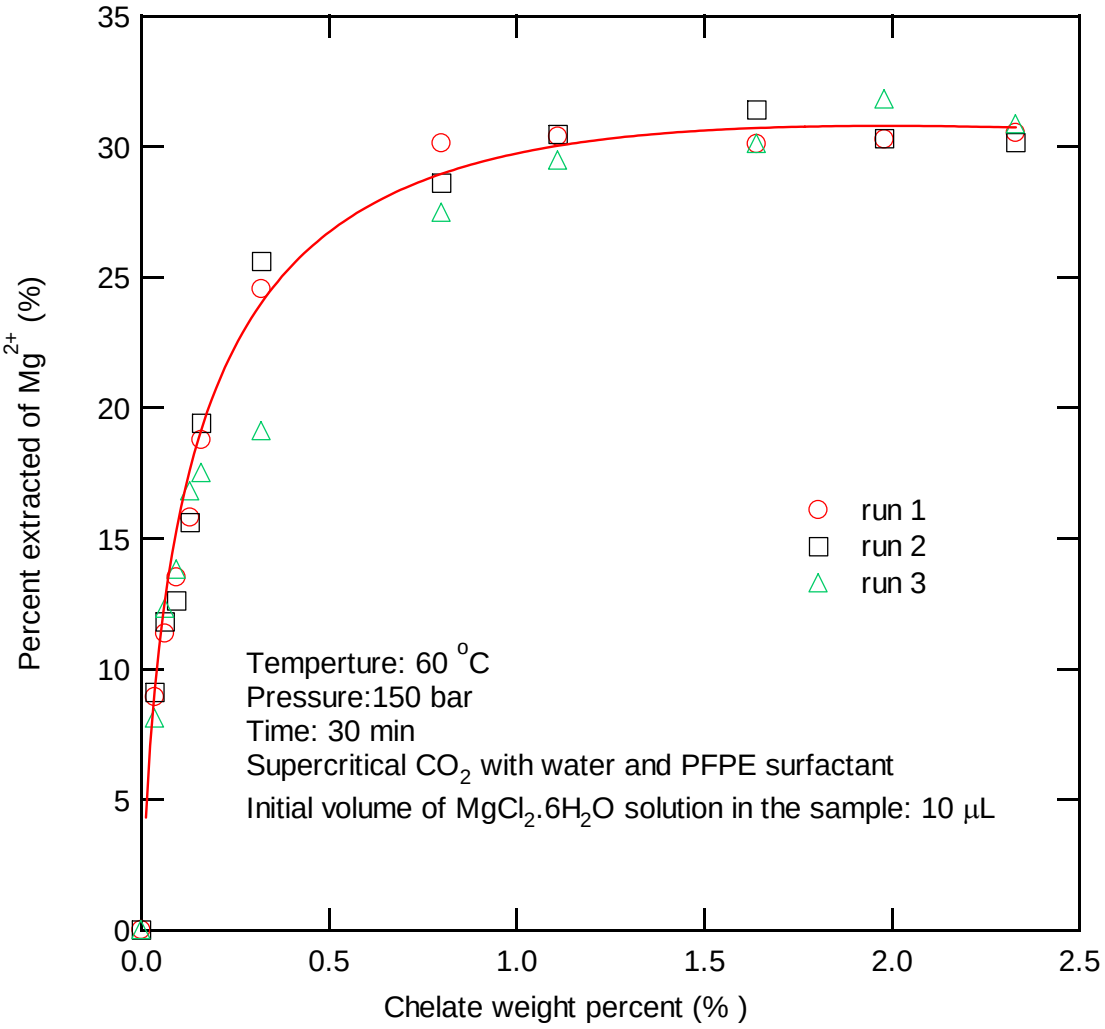

Figure 5.8: The effect of chelate concentration on equilibrium extraction**.**

The equilibrium extraction of $MgCl_2 \cdot 6H_2O$ in supercritical carbon dioxide with different concentrations of water is shown in Figure 5.9. Only a small amount of metal is extracted in the absence of water. The percent metal-removed is about 5% when water weight percent is zero. In this case, the surfactant only serves as a chelate to solubilize the metal in the carbon dioxide phase. Adding a small amount of water increases equilibrium extraction dramatically (percent metal-removed increases up to 31%). Further increases of water (water weight percent > 0.2%) have no significant effect on the percent of metal extracted. A small amount of water is important to the extraction. In our experiments, the best extraction percentage (31%) is obtained in the presence of water (0.2%) and chelate (1%). These results are explained by the formation of the water- carbon dioxide microemulsions in supercritical carbon dioxide (Figure 5.10). Water-in-carbon dioxide emulsions are formed as a medium for the extraction. The water- carbon dioxide micro-emulsion consists of a small amount of water and surfactant that covers the water core. Ordinarily a surfactant (such as perfluoropolyether ammonium carboxylate) consists of two main entities; a hydrophilic head group and a hydrophobic tail group. The head group has an affinity for the polar water environment and will attach to the water core. Parts of surfactant attached to the water core are attracted to the metal ions. Once the minimum surfactant and water for forming the water-carbon dioxide microemulsions is reached, increasing the surfactant and water has little or no effect on the efficiency of extraction.

The Effect of Extraction Pressure and Temperaure

Determination of the solubility for $MgCl_2 \cdot 6H_2O$ at different pressures and temperatures was performed using 1.5% of chelate and 0.4% of water. The extraction samples were

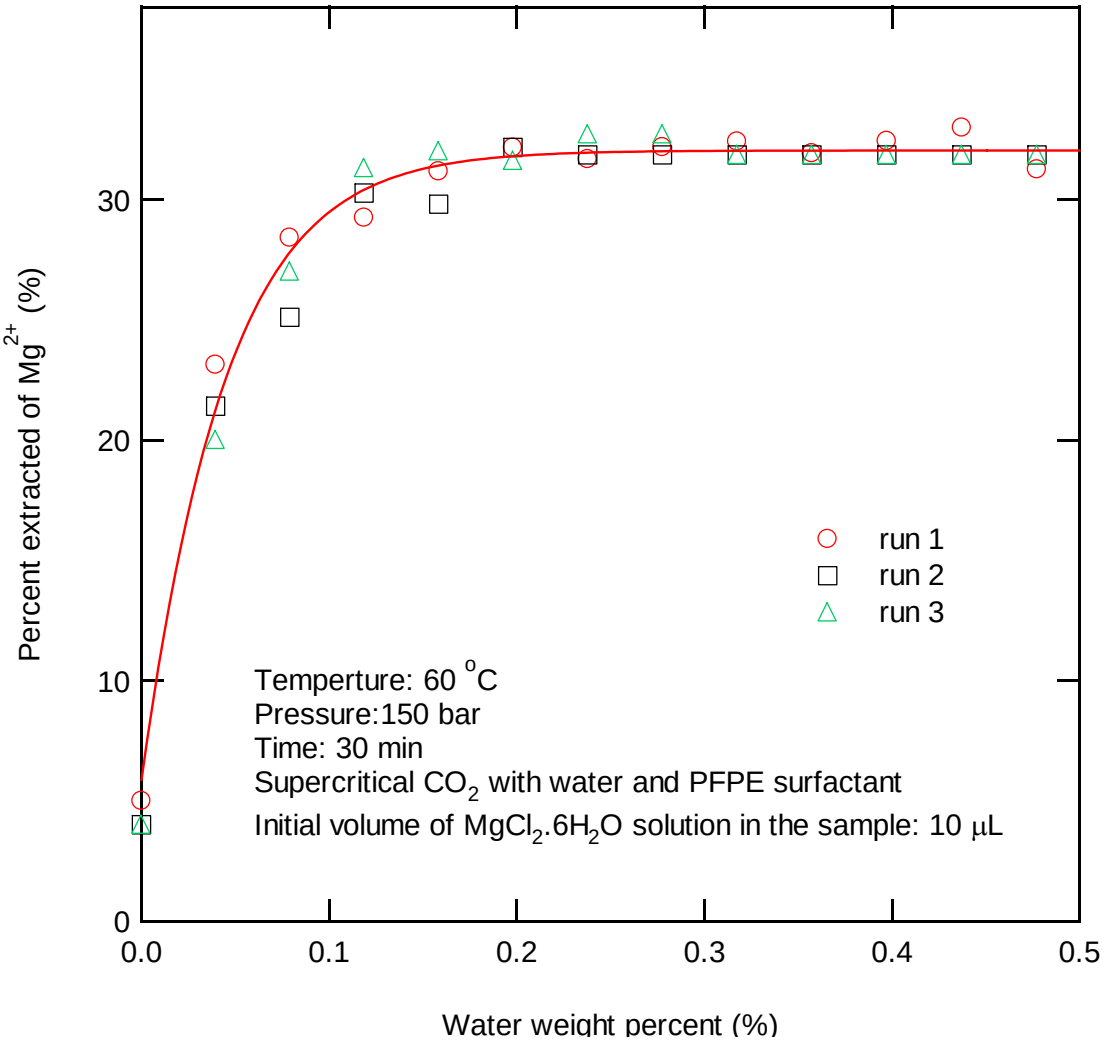

Figure 5.9: The effect of water concentration on equilibrium extraction**.**

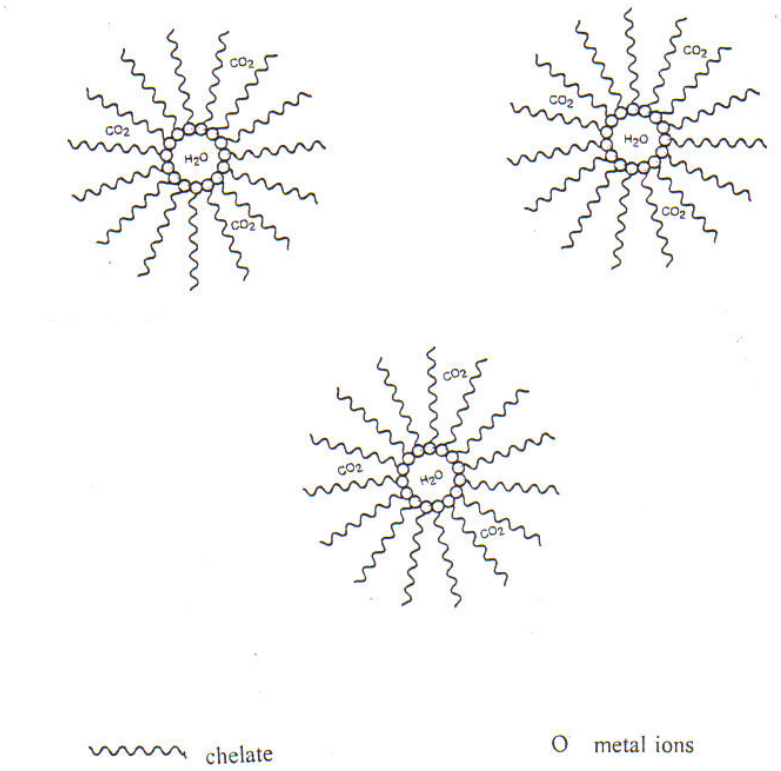

Figure 5.10: The water-carbon dioxide micro-emulsion in supercritical CO_2 phase.

prepared by spiking 10 μl (8.170 g/100ml) of $MgCl_2 \cdot 6H_2O$ solution to the filter paper (Whatman No.2). Figure 5.11 shows the solubility as a functon of pressure. Each data point is the average of three experimental runs. The solubility increases with increasing pressure at constant temperature. At constant pressure, the solubility increases with high temperature.

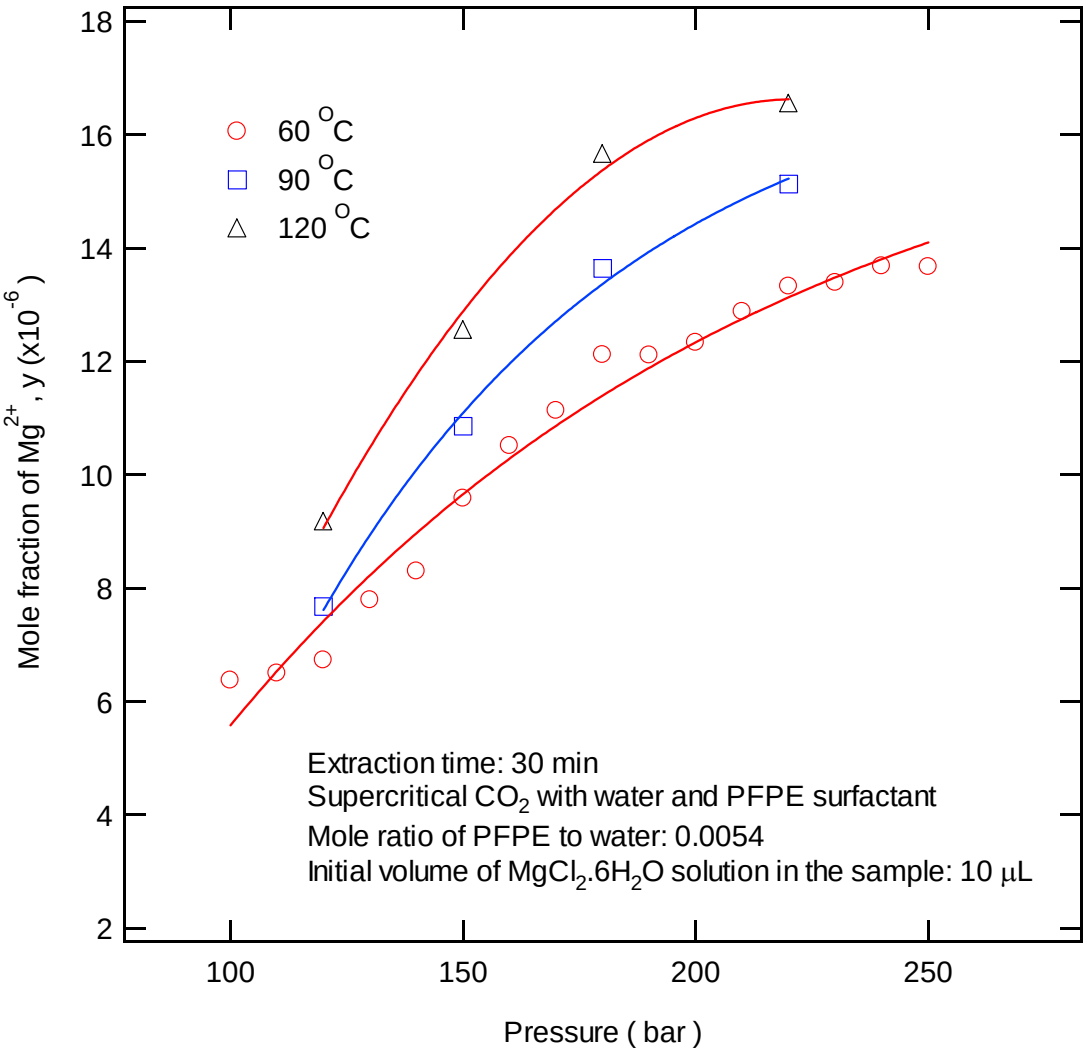

Figure 5.11: The effect of pressure and temperature on the solubility of Mg^{2+} in supercritical carbon dioxide

References

1. Laintz, K. E., Yu, J., Wai, C. M., Smith, R. D., Extraction of Metal Ions with Sodium Bis(trifluoroethyl)dithiocarbamate Chelation and Supercritical Fluid Chromatography. *Anal. Chem.*, **1992**, 64, 311-315.

2. Laintz, K. E., Wai, C. M., Yonker, C. R., Smith, R. D., Extraction of Metal Ions from Liquid and Solid Materials by Supercritical Carbon Dioxide. *Anal. Chem.*,**1992**, 64, 2875-2878.

3. C. M. Wai and Shaofen Wang. Supercritical Fluid Extraction: Metals as Complexes. *Journal of chromatography A.*, **1997,** 785, 369-384.

4. Cowey CM, Bartle KD, Burford MD, Clifford AA, et al. Solubility of Ferric and a Nickel Complex in Supercritical Fluids. *J. Chem. Eng. Data.,* **1995**, 40, 1217-1221.

5. Glennon JD, Hutchinson S, Walker A, Harris SJ, McSweeney CC, New Fluorinated Hydroxamic Acid Reagents for the Extraction of Metal Ions with Supercritical CO_2. *Journal of Chromatography A.*, **1997**, 770, 85-91.

6. Cross W, Akgerman A., Erkey C. Determination of Metal-chelate Complex Solubilities in Supercritical Carbon Dioxide. *Ind. Eng. Chem. Res.,* **1996**, 35, 1765-1770.

7. Murphy JM, Erkey C, Copper (II) Removal from Aqueous Solutions by Chelation in Supercritical Carbon Dioxide Using Fluorinated B-diketones. *Ind. Eng. Chem. Res*., **1997**, 36, 5371-5376.

8. Wai CM, Wang S, Yu JJ, Solubility Parameters and Solubilities of Metal Dithiocarbamates in Supercritical Carbon Dioxide. *Anal. Chem.*, **1996**, 68, 3516-3519.

9. Murphy JM, Erkey C. Thermodynamics of Extraction of Copper (II) from Aqueous Solutions by Chelation in Supercritical Carbon Dioxide. *Environ. Sci. Technol.,* **1997**, 31, 1674-1679.

10. Brennecke, J. F. and C. A. Eckert, Phase Equilibria for Supercritical Fluid Process Design. *AICHE J.*, **1989**, 35(9), 1409.

11. C. M. Wai and Shaofen Wang. Supercritical Fluid Extraction: Metals as Complexes. *Journal of Chromatography A.*, **1997**, 785, 369-384.

12. Neil G. Smart, Carleson T., Kast T., et al., Solubility of Chelating Agents and Metal-containing Compound in Supercritical Fluid Carbon Dioxide. *Talanta,***1997**, 44, 137-150.

13. M. Z. Yates, D. L. Apodaca, M. L. Campbell, *Metal Extractions Using Water in Carbon Dioxide Microemulsions*. The royal society of chemistry. 25-26, **2001.**

14. C. Ted Lee, Jr., Pettros A. Psathas, and Keith P. Johnston, Water-in –carbon Dioxide Emulsions: Formation and Stability. *Langmuir* **1999**, 15, 6781-6791.

15. Anthony F. Lagalante, Brian N. Hansen, and Thomas J. Bruno, Solubilities of Copper(II) and Chromium(III) Diketonates in Supercritical Carbon Dioxide. *Inorg. Chem.*, **1995**, 34, 5781-5785.

16. Ali V. Yazdi, Eric J. Beckman. Design of Highly CO_2-Soluble Chelating Agents. 2. Effect of Chelate Structure and Process Parameters on Extraction Efficiency. *Ind. Eng. Chem. Res.*, **1997**, 36, 2368-2374

17. Johnston, K. P.; Harrison, K. L.; Clarke M. J.; Howdle, S. M.; Heitz, M. P.; Bright, F. V.; Carlier, C.; Randolph T. W., Water-in-Carbon Dioxide Microemulsions: An Environment for Hydrophiles Including Proteins. *Science* **1996**, 271.624

18. Julian Eastoe;Beatrice M.H.Cazelles. Water-CO_2 Micro-emulsions Studied by Small-angle Neutron Scattering. *Langmuir*., **1997,** 13, 6980

19. Ted Lee, Jr.;Petros A.. Water-in-carbon Dioxide Emulsions: Formation and Stability. *Langmuir*., **1999**, 15,678.

CHAPTER VI

THERMODYNAMIC MODELING OF METAL-CHELATE COMPLEX SOLUBILITY IN SUPERCRITICAL CARBON DIOXIDE

Introduction

To model supercritical extraction processes, the solubility data as a function of pressure and temperature range are required. There are several ways to obtain the solubility data of metal-chelate in supercritical carbon dioxide. However, obtaining experimental solubility data over a wide range of temperature and pressure is not always feasible. Therefore, the ability to correlate and predict the solubility of metal-chelate in supercritical carbon dioxide is important. Thermodynamic models are used to correlate the solubility data for a metal-chelate in supercritical carbon dioxide. Experimental data are needed to determine the parameters of the models [1].

The solubility of metal-chelate in supercritical carbon dioxide is modeled using equations for phase equilibria. Solubility data can be estimated using standard thermodynamic models incorporating conventional mixing rules. A suitable equation of state is needed in this calculations process. The equation of state methods provide one of the most useful techniques used to modeling phase equilibria of multicomponent system [2]. The Peng-Robinson equation has been the most widely used [3]. However, the theoretical parameters for this method are not always available. Critical temperature, Tc, critical pressure, Pc, solid molar volume, v_s, and sublimation pressure, p^{sat} are needed for the pure metal-chelate complex. We used the nonlinear least squares method to fit these unknown properties and the interaction coefficient k_{ij} from experimental solubility data.

The nonlinear least square method is a mathematical procedure for fitting the model to a given set of data points by minimizing the sum of the squares of the offsets ("the residuals") of the data points from the model.

We used a thermodynamic model incorporating conventional mixing rules and the Peng-Robinson equation of state (EOS) to model the chelate complex solubility in supercritical carbon dioxide.

Thermodynamic Modeling

The solubility of a metal-chelate in supercritical fluid is determined by the equation of phase equlibrium. When the metal-chelate phase (solid phase) and supercritical fluid phase are in equilibrium, we have following equilibrium relations for component i:

$$f_i^F = f_i^S \; ; \; T_i^F = T_i^S \; ; \; P_i^F = P_i^S \tag{6-1}$$

where f_i^F is the fugacity of component i in the supercritical fluid phase and f_i^S is that in the solid phase.

For the binary system, consider the solubility of a metal-chelate (2) in supercritical carbon dioxide (1) at temperature, T and pressure, P. Recall the fugacity definition of metal-chelate in the supercritical carbon dioxide phase:

$$f_2^F = p \, \phi_2^F \, y_2 \tag{6-2}$$

where P is the pressure, ϕ_2^F is the fugacity coefficient and y_2 is the solubility (mole fraction) in a supercritical carbon dioxide. Because we assume that the solid solute is pure, the fugacity of solute in the solid state is equal to the pure solid fugacity.

The fugacity of metal-chelate in the solid phase is given by:

$$f_2^S = f_2^{pureS} = p_2^{Sat}\phi_2^S\left(\int_{p_2^{Sat}}^{p}\frac{v_2^S}{RT}dp\right) \tag{6-3}$$

where p_2^{Sat} is the saturated vapor pressure, ϕ_2^S is the fugacity coefficient at saturation pressure, R is the gas constant, T is the absolute temperature, and v_2^S is the solid-state molar volume of the solute.

Assuming that the molar volume of solid-state solute is constant over the pressure range and the saturated vapor of the solid solute vapor system behaves as an ideal gas. The sublimation fugacity coefficient ϕ_2^S can be assumed to be unity because the sublimation pressure is very low. We can derive y_2 by combining equation 6-2 and 6-3.

$$y_2 = \frac{f_2^F}{p\phi_2^F} = \frac{f_2^s}{p\phi_2^F} = \frac{p_2^{Sat}\phi_2^S}{p\phi_2^F}\exp\left(\int_{p_2^{Sat}}^{p}\frac{v_2^S}{RT}dp\right) = \frac{p_2^{Sat}}{p}\frac{1}{\phi_2^F}\left[\frac{v_2^S(p-p_2^{Sat})}{RT}\right] \tag{6-4}$$

To calculate fugacity coefficients ϕ_2^F (the fugacity coefficient of component 2 in the supercritical fluid phases), we use equation of state. In the equation of state methods, fugacity coefficients ϕ_2^F,

$$\ln\phi_2^F = \frac{1}{RT}\int_V^{\infty}\left[\left(\frac{\partial P}{\partial n_2}\right)_{T,V,n1} - \frac{RT}{V}\right]dV - \ln\frac{PV}{nRT} \tag{6-5}$$

To use equation 6-5, we need a suitable equation of state that holds for the entire range of possible mole fractions at the system condition. We used the Peng-Robinson equation of state that follows:

$$p = \frac{RT}{v-b} - \frac{a(T)}{v(v+b)+b(v-b)} \tag{6-6}$$

$$b = 0.07780\frac{R\ T_C}{P_C} \tag{6-7}$$

$$a(T) = a(T_C)\alpha(T)\,, \tag{6-8}$$

$$a(T_C) = 0.45724\frac{(RT_C)^2}{P_C} \tag{6-9}$$

$$\alpha(T) = [1+\beta(1-\sqrt{T/T_c})]^2 \tag{6-10}$$

$$\beta = 0.37464 + 1.54226\omega - 0.26992\,\omega^2 \qquad 0 \le \omega \le 0.5 \tag{6-11}$$

$$\omega = -1.0 - \log P^{sat} \qquad \text{at } T_r = 0.7 \tag{6-12}$$

Assuming a one-fluid theory of the mixture, we extend equation 6-6 to the binary system. The common procedure is writing mixing rules that are quadratic in mole fraction. For a binary mixture,

$$b = y_1^2 b_1 + 2\,y_1 y_2 b_{12} + y_2^2 b_2 \tag{6-13}$$

$$a = y_1^2 a_1 + 2\,y_1 y_2 a_{12} + y_2^2 a_2 \tag{6-14}$$

$$b_{12} = \frac{1}{2}(b_1 + b_2) \tag{6-15}$$

$$a_{12} = (1-k_{12})\sqrt{a_1 a_2} \tag{6-16}$$

Using the mixing rules for binary system,

$$\left(\frac{\partial P}{\partial n_2}\right)_{T,V,n1} = \frac{RT}{v-b} + \frac{nRT\,b_2}{(v-nb)^2} - \frac{2n(y_1 a_{12} + y_2 a_2)}{v^2 + 2nbv - n^2 b^2} + \frac{2n^2 a(v-nb)b_2}{(v^2+2nbv-n^2b^2)^2} \tag{6-17}$$

Combining equation (6-17) with (6-5), the supercritical fluid phase fugacity coefficient is given by:

$$\ln \phi_2^F = \frac{b_2}{b}\left(\frac{Pv}{RT} - 1\right) - Ln\frac{P(v-b)}{RT} - \frac{a}{2\sqrt{2}bRT}\left[\frac{2(y_1 a_{12} + y_2 a_2)}{a} - \frac{b_2}{b}\right]\ln\frac{v+(1+\sqrt{2})b}{v+(1-\sqrt{2})b} \tag{6-18}$$

The Nonlinear Least Squares Fitting

Critical temperature, *Tc*, critical pressure, Pc, solid molar volume, v_s, and sublimation pressure, p^{sat} and interaction coefficient, k_{ij} need to be determined for the pure metal-chelate complex to calculate the metal-chelate complex solubility in supercritical carbon dioxide. These pure property data are not available for the metal-chelate complexes. We used the nonlinear least squares to fit the unknown pure component properties and the interaction coefficient k_{ij}. The nonlinear least square method is a mathematical procedure for finding the best-fitting of a model to a given set of experimental data points by minimizing the sum of the squares of the offsets ("the residuals") of the data points from the model. Suppose that the data points are (p_1, y_1), (p_2, y_2),… (p_n, y_n). Where p is the independent variable pressure and y is the dependent variable solubility. The model $y=f(p)$ has the error e from each data point, i.e., $e_1=y_1-f(p_1)$, $e_2=y_2-f(p_2)$,… $e_n=y_n-f(p_n)$. According to the method of nonlinear least squares, the best fit has the property that

$$S = \sum_{i=1}^{n} e_i = \sum_{i=1}^{n} [y_i - f(p_i)]^2 = \min \qquad (6\text{-}19)$$

In our case, we used the thermodynamic model described previously to correlate chelate-complex solubility in supercritical carbon dioxide. Critical temperature (*Tc*), critical pressure (P_c), solid molar volume (v_s) and sublimation pressure (P^{sat}) for chelate complex are not available. These unknown pure component properties and the interaction coefficient k_{ij} were used as fit parameters. A trial and error method was used to obtain these parameters which best satisfy our system of equations. To obtain these modeling parameters, a set of experimental solubility data at a constant temperature and varying

pressure were used to fit these unknown parameters by minimizing the follow equation using nonlinear least squares:

$$f(T, p, T_c, p_c, p^{sat}, v_s, k_{ij}) = \sum_i [(y_{i,\mathrm{model}} - y_{i,\mathrm{experiment}}) / y_{i,\mathrm{experiment}}]^2 \quad (6\text{-}20)$$

Program Description

We used the Marquardt-Levenberg least squares (MLLS) method to fit the above equation to the experimental data and determine the unknown parameters. This method uses the Gauss-Newton technique and nonlinear regression together to find the best fit. The program includes main program, function program, nonlinear regression program, and statistical analysis of regression program. The nonlinear regression program and statistical analysis of regression programs are provided by Constantinides [4]. The model equations of this problem are given as function in the program.

Results and Discussion

We used the nonlinear least squares method to fit the parameters (*Tc*, *Pc*, *Vs*, P^{sat} and k_{12}) of an organic compound/carbon dioxide system and inorganic compound/ carbon dioxide system to verify the feasibility of this model-fitting technique. We used naphthalene as an example of the organic compound/ carbon dioxide system. The solubility data of naphthalene in carbon dioxide are provided by Paulaitis [5]. The experimentally measured critical temperature *Tc*, critical pressures *Pc* and molar volume v_s of naphthalene are provided by Reid [7] are shown in Table 6-1(a). Antoine's equation for the vapor pressure of the naphthalene is [8]:

$$\log_{10}^{P(bar)} = 8.722 - \frac{3783}{T}, (T = K) \qquad (6\text{-}21)$$

Table 6.1(a): Critical property and other parameters for naphthalene.

Tc (K)[7]	*Pc* (MPa)[7]	v_s(m^3/mol)[7]	P^{sat} (Pa)[8]	k_{12}[2]
748.4	4.05	1.25E-4	240.0	0.103

The interaction coefficient k_{12} (carbon dioxide /naphthalene) is fit from binary vapor-liquid equilibrium data. k_{12}=0.103 in the Peng-Robinson equation is obtained from binary vapor-liquid equilibrium data at 410.9 K [2].

The fitted values of *Tc*, *Pc*, v_s, P^{sat} and k_{12} are shown in Table 6-1(b). The values for critical temperature (*Tc*), critical pressure (*Pc*), molar volume of the solid (v_s) and

Table 6.1(b): Estimated values of critical property and other parameters for naphthalene using experimental data [(1)]

	Tc (K)	*Pc* (MPa)	v_s (m^3/mol)	P^{sat} (Pa)	k_{12}
Estimated results at 333.55 K	748.9	4.04	1.03E-4	245.3	0.089
Estimated results at 303.15 K	750.1	3.95	1.12E-4	243.3	0.105
% difference from Table 6.1(a) at 333.55 K	0.07	-0.3	-17.6	2.2	-13.6
% difference from Table 6.1(a) at 303.15 K	0.2	-2.5	-10.4	1.4	1.9

[(1)] All parameters estimated by Marquardt-Levenberg least squares (MLLS) method from experimental data. The solubility data of naphthalene in carbon dioxide are provided by Paulaitis [5].

sublimation pressure (P^{sat}) are very close at different experimental temperature. These values agree with the experimental [7] and reference values [2,8]. The critical temperature (*Tc*) and critical pressure (*Pc*), v_s and P^{sat} are within 0.2% of *Tc*, 2.5% of *Pc*, 17.6% of v_s and 2.2% of P^{sat} values provided by R. C. Reid et al. [7,8]. The estimated value of the interaction coefficient k_{12} is slightly larger at the lower experimental temperature. It also agrees with reference [2] value of 0.103. The experimental data of naphthalene and fitted results are shown in the Figure 6.1. Figure 6.1 shows good agreement between experimental and calculated results using estimated parameter values. The solubility of naphthalene in carbon dioxide predicted by this model is very good.

For an inorganic compound/carbon dioxide system, we used the experimental data of cupric acetylacetonate by Cross et al [6]. as an example to verify the feasibility of this model. Critical properties and other parameter values from their study are list in Table 6.2. Among these values, solid molar volume and solid vapor pressure are measured

Table 6.2: Critical property and other parameters for cupric acetylacetonate.

	Tc (K)	*Pc* (MPa)	v_s (m^3/mol)	P^{sat} (Pa)	k_{12}
Properties of Cu-acetylacetonate [6]	577.3[(1)]	5.54[(1)]	8.74E-4[(2)]	0.48[(2)]	0.179[(1)]
Estimated results of Cu-acetylacetonate[(3)]	603	6.86	7.36E-4	0.49	0.219
% difference	4.5	23.8	-4.4	2.1	22.4

[(1)]Estimated by Cross [6] using experimental data.
[(2)] Independently determined parameters [6].
[(3)] All parameters estimated by Marquardt-Levenberg least squares (MLLS) method from experimental data. The solubility data of cupric acetylacetonate in carbon dioxide are provided by Cross [6].

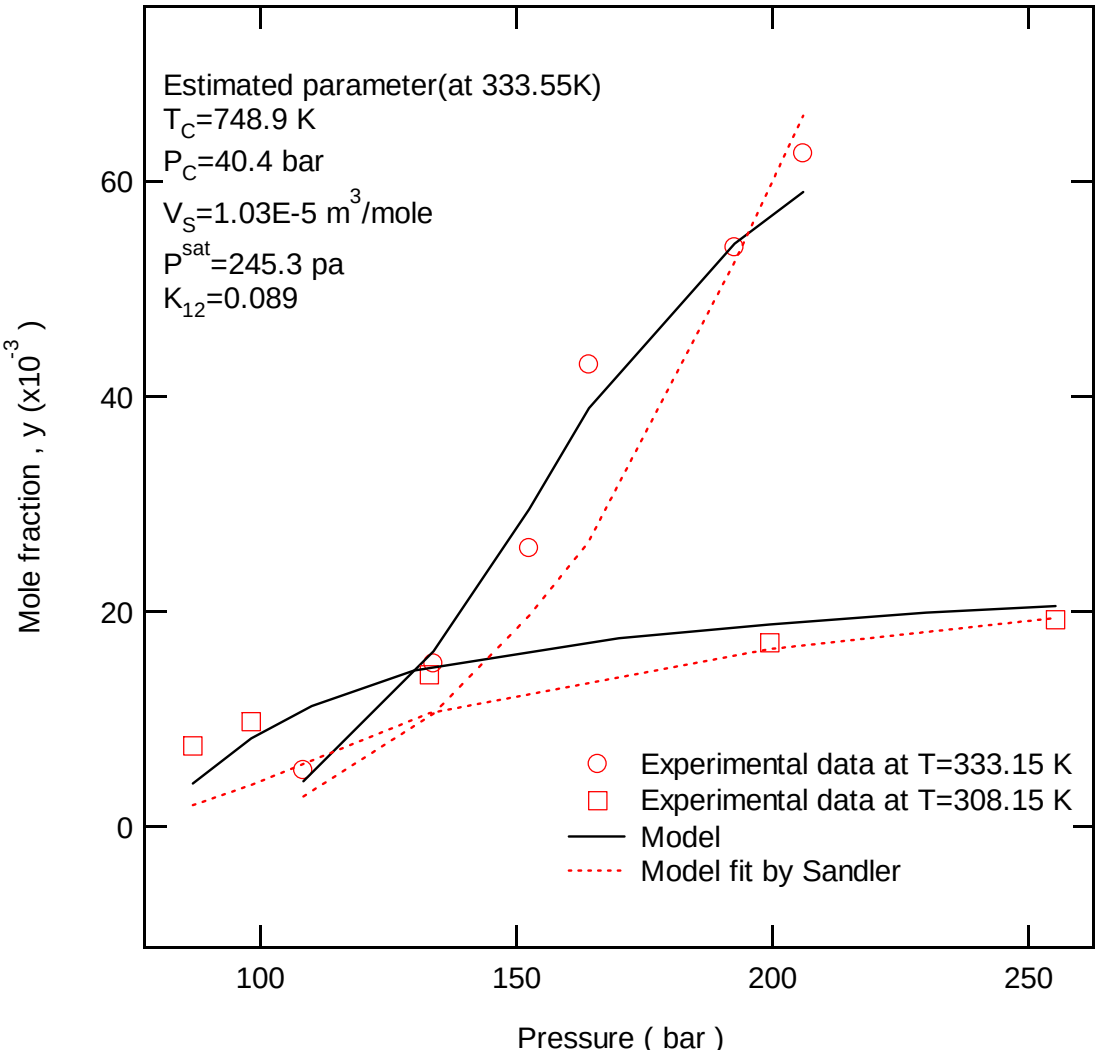

Figure 6.1: Solubility of naphthalene in supercritical carbon dioxide as a function of pressure. (Experimental data from McHugh and Paulaitis [5])

directly from their experiments, critical temperature (*Tc*), critical pressure (*Pc*) and interaction coefficient (k_{12}) are fit from their solubility experimental data [6]. In our study, solid molar volume, solid vapor pressure, critical temperature (*Tc*), critical pressure (*Pc*) and interaction coefficient (k_{12}) were used as fit parameters. The results are shown in Table 6.2. Our fitted values of critical temperature (*Tc*), molar volume of the solid (v_s), sublimation pressure (P^{sat}) correspond well (within 4.5%) with the values provided by Cross [6]. Our estimated values of the critical pressure (*Pc*) and interaction coefficient (k_{12}) have 23.8% and 22.4% differences from Cross's values. We estimated all five parameters (*Tc*, *Pc*, v_s, P^{sat} and k_{12}) in our method, while Cross estimated three parameters (*Tc*, *Pc* and k_{12}) having previously determined v_s and P^{sat} independently. Our estimated values of parameters correspond well with Cross. The experimental and calculated results using our estimated parameter value are in good agreement. The estimated solubility of cupric acetylacetonate using our estimated parameters is very good as shown in Figure 6.2.

The estimated solubility and supercritical properties of the pure solid phase are very good using this model for both organic/carbon dioxide system and inorganic/ carbon dioxide systems. We used this model to correlate the experimental data (solubility of Cu-chelate and Mg-chelate complex) over the temperature and pressure range. The experimental data of $Cu(PFPECOO)_2$ and model results are shown in the Figure 6.3. The experimental data of $Mg(PFPECOO)_2$ and model results are shown in the Figure 6.4. The values of the critical temperature (T_c), critical pressure (P_c), molar volume of the solid (v_s) and sublimation pressure (P^{sat}) and interaction coefficient k_{12} are shown in Table 6.3. A static extraction was carried out at 60°C for 30 minutes using the SFE220

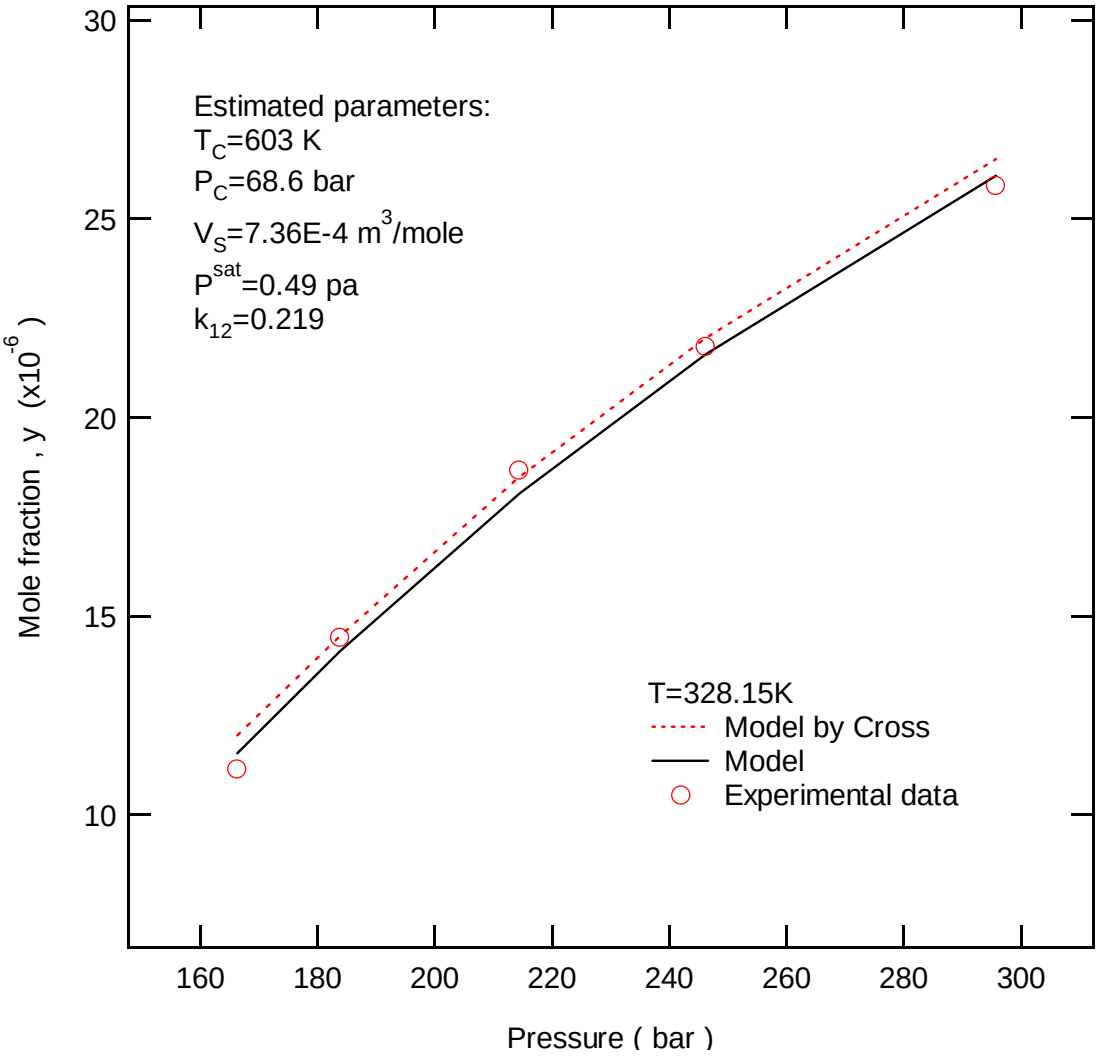

Figure 6.2: Solubility of cupric acetylacetonate in supercritical carbon dioxide as a function of pressure.

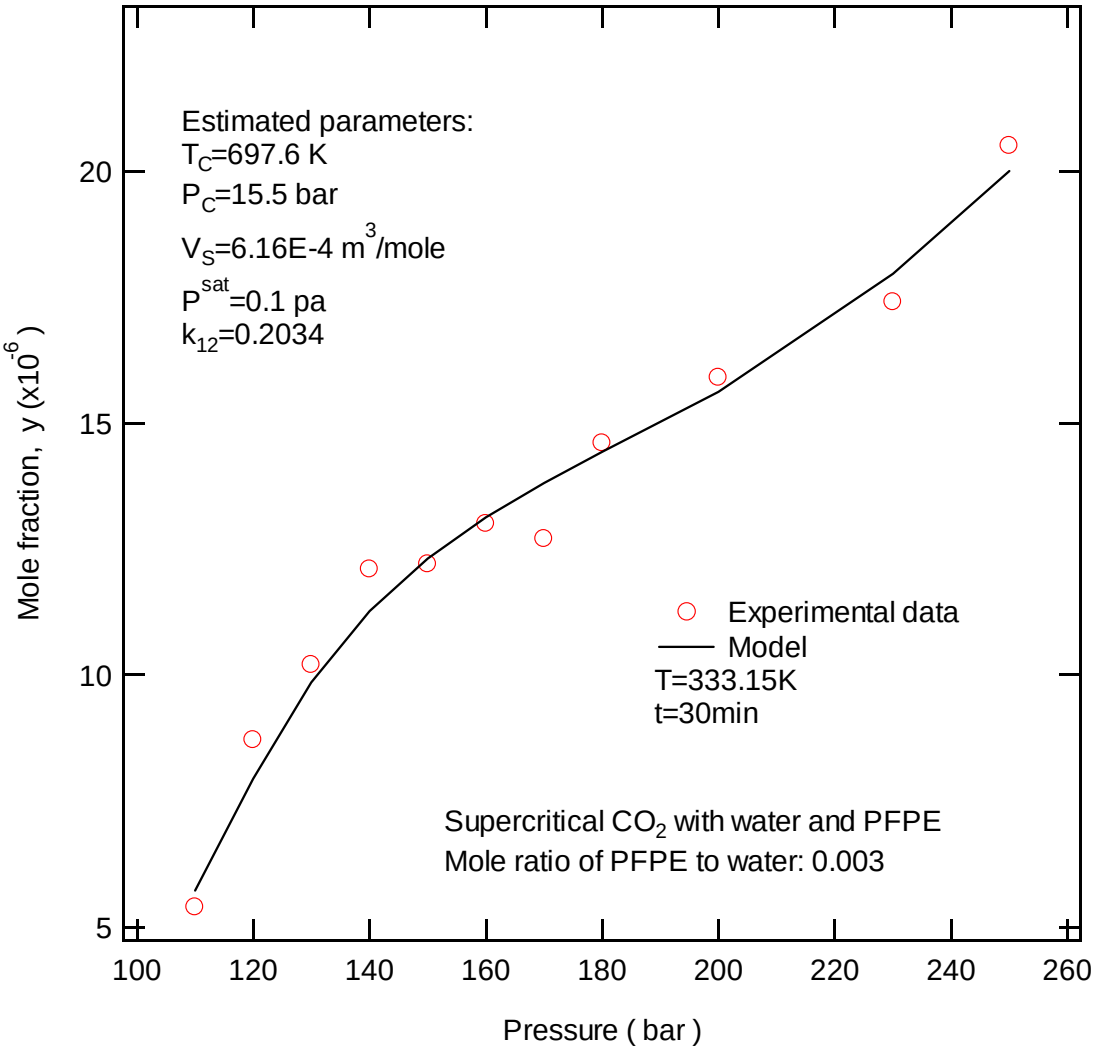

Figure 6.3: Solubility of $Cu(PFPECOO)_2$ in supercritical carbon dioxide as a function of pressure.

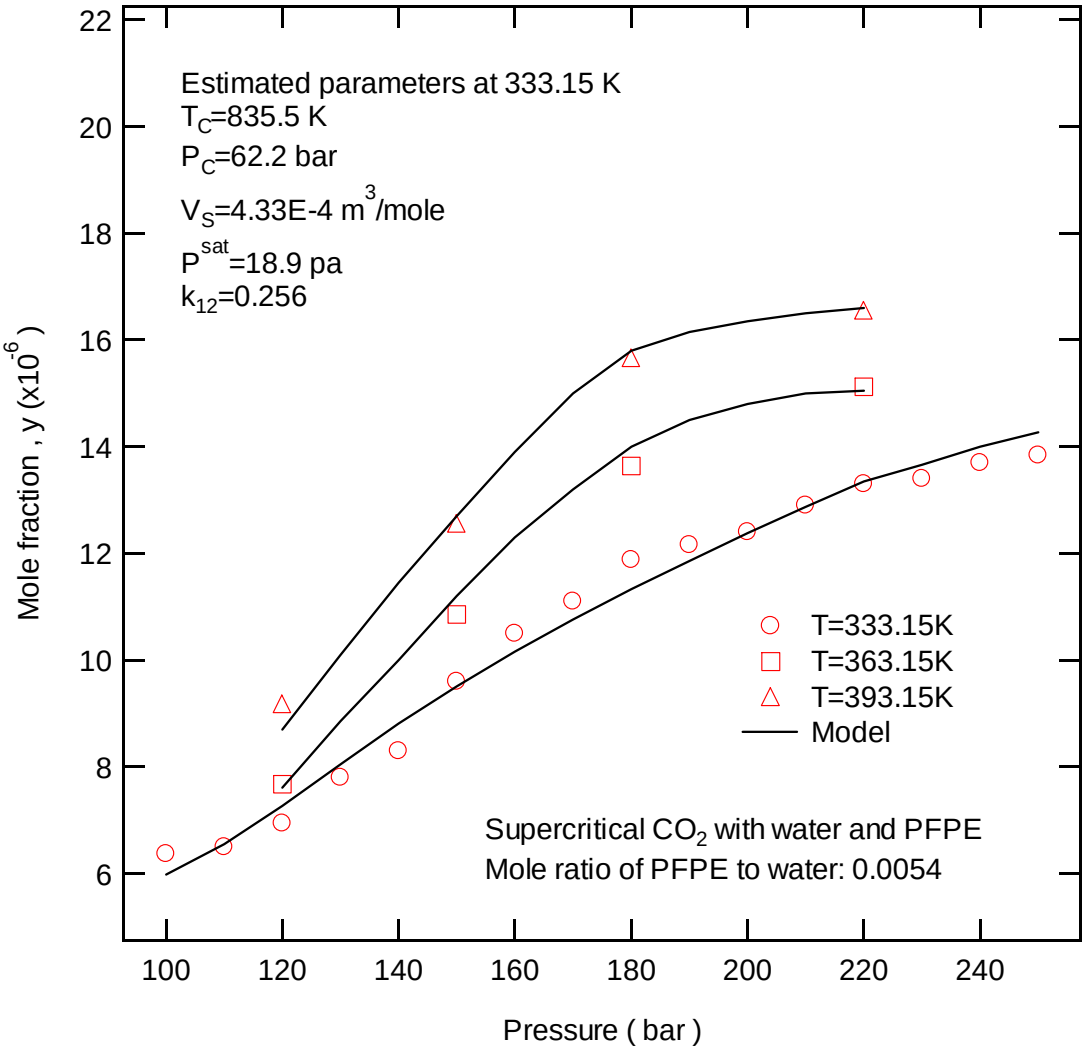

Figure 6.4: Solubility of $Mg(PFPECOO)_2$ in supercritical carbon dioxide as a function of pressure.

Table 6.3: Summary of property parameters fits on Cu-$(PFPECOO)_2$ and Mg-$(PFPECOO)_2$[(1)]

	Tc (K)	*Pc* (MPa)	v_s (m^3/mol)	P^{sat} (Pa)	k_{12}
Estimated results of Cu-$(PFPECOO)_2$	697.6	1.55	6.16E-4	0.1	0.203
Estimated results of Mg-$(PFPECOO)_2$ at 333.15 K	835.5	6.22	4.33E-4	18.9	0.256
Estimated results of Mg-$(PFPECOO)_2$ at 363.15 K	833.8	6.01	4.28E-4	22.1	0.187
Estimated results of Mg-$(PFPECOO)_2$ at 393.15 K	836.9	6.36	4.36E-4	25.5	0.131

(1) All parameters estimated by Marquardt-Levenberg least squares (MLLS) method from experimental data

extraction systems. PFPE-NH^{4+} surfactant and water was used to increase Cu ions solubility in supercritical carbon dioxide. The solubility of the Cu-chelate in carbon dioxide was determined.

The amount of chelate and water added to the extraction cell are in excess compared to the moles of copper ions added onto the sample. Determination of the solubility for Mg-chelate at different pressures and temperatures was performed using 1.5% of chelate and 0.4% of water. Figures 6.3 and 6.4 show the experimental and calculated results using our estimated parameters are in good agreement for both Cu-chelate and Mg-chelate. Solubility of Cu-chelate and Mg-chelate complexes in supercritical carbon dioxide can be predicted at the experimental conditions using Peng-

Robinson equation of state. For Mg-chelate/carbon dioxide system, we get values for critical temperature (*Tc*), critical pressure (*Pc*) and molar volume of the solid (v_s) that are very close at different experimental temperatures. While a poor initial guess will still converge in our method, it may require a large number of iterations, and sometimes exceeds the maximum limit of iterations defined in the function. The estimated value of the sublimation pressure (P^{sat}) increases slightly with increasing the temperature. The estimated value of the interaction coefficient k_{12} decreases with increasing temperature (shown in Figure 6.5). For a binary system, k_{12} is often nearly independent of temperature. However, our results indicate that k_{12} depends on temperature for the metal/chelate/water/ carbon dioxide system.

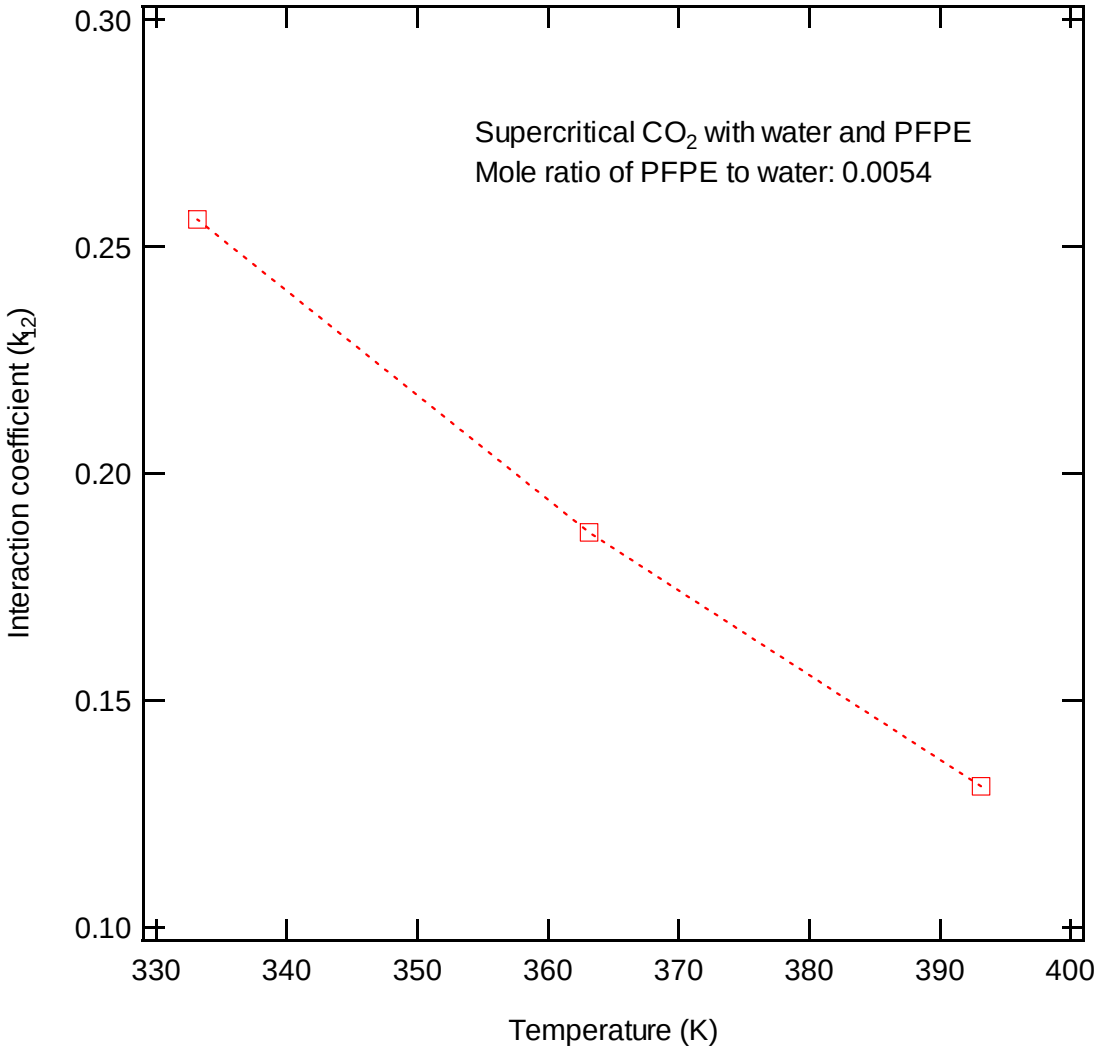

Figure 6.5: Model estimate value of interaction coefficients for Mg/chelate/CO_2 system as a function of temperature

References

1. Ralf Dohrn; Gerd Brunner. High-pressure Fluid-phase Equilibrium: Experimental Methods and Systems Investigated (1988-1993). *Fluid Phase Equilibrium*, **1995**,106, 213-282.

2. John M. Prausnitz and Rudiger N. Lichtenthaler. Molecular Thermodynamics of Fluid-phase Equilibria. Third edition. Prentice Hall International Series in the Physical and Chemical Engineering Sciences. 713, 720, data, **1999**.

3. K. D. Bartle, A. A. Clifford, S. A. Jafar, and G. F., Shilstone, Solubilities of Solids and Liquids of Low Volatility in Supercritical Carbon Dioxide. *J. Phys. Chem. Ref. Data*, **1991**, 20(4), 713-756.

4. Alkis Constantinides and Navid Mostoufi. Numerical Methods for Chemical Engineers with Matlab Applications. **1999**, Prentice Hall International Series in the Physical and Chemical Engineering Sciences. 500.

5. Stanleyi. Sandler. Chemical and Engineering Thermodynamics. Wiley Series in Chemical Engineering. P171, P466, data, **1989**.

6. Cross W, Akgerman A., Erkey C.. Determination of Metal-chelate Complex Solubilities in Supercritical Carbon Dioxide. *Ind. Eng. Chem. Res*., **1996**, 35, 1765.

7. R. C. Reid, J. M. Prausnitz, and B. E. Poling, The Properties of Gases and Liquids,**1986**, 4th ed., McGraw-Hill, New York, Appendix A and other sources.

8. R.C. Weast. Handbook of Chemistry and Physics, **1987**, Chemical Rubber Publishing Co., Cleveland, C-357, D-214.

CHAPTER VII

CONCLUSIONS AND RECOMMENDATIONS

Conclusions

The objective of this investigation was to develop a supercritical extraction process for extracting useful materials from in-situ resources on Mars. We did the initial screening to determine the soluble species of inorganic minerals that may be present in the Martian regolith. The results show no appreciable extraction for $CaCl_2$, $AgNO_3$, NH_4SO_4, NaI, $K_2Cr_2O_7$, $(NH_4)_2MoO_4$, $CuCl_2$ and $FeCl_3$. Simulated Martian soils, $CaSO_4 \cdot 2H_2O$, $FeSO_4 \cdot 7H_2O$, $CoCl_2 \cdot 6H_2O$, $CuSO_4 \cdot 5H_2O$, $FeCl_2 \cdot 4H_2O$, $MnSO_4 \cdot 5H_2O$, $Ni(NO_3)_2 \cdot 5H_2O$, $Fe(NH_4)_2(SO_4)_2 \cdot 12H_2O$, $Fe(NO_3)_3 \cdot 9H_2O$, $Fe(NH_4)2(SO_4)_2 \cdot 6H_2O$ and $CuCl_2 \cdot 2H_2O$ show significant weight change in supercritical extraction process. The supercritical extraction process removes more water than heating at one atmosphere nitrogen. We confirmed, therefore, that it is possible to recover water from hydrated species using supercritical carbon dioxide.

We did further tests on hydrated species (ferrous sulfate and calcium sulfate) to determine their dehydration behavior in supercritical carbon dioxide. For ferrous sulfate, the first three waters are removed over the temperature range of 40-80^{o}C, the next three between 100-150^{o}C, and the last water between 200-350^{o}C. We use DSC to estimate the enthalpy for the dehydration process. The best result was obtained at a heating rate of 2.5^{o}C/min using an open pan. The total enthalpy change from $FeSO_4 \cdot 7H_2O$ to $FeSO_4$ is 390.9 kJ/mol. The transition enthalpies for the three dehydration steps are 145.7 kJ/mol,

180.4 kJ/mol and 64.8 kJ/mol corresponding. These values are within –2.5%, -8.8%, 1.2% and 3.4% calculated using heating formation and heat capacity. For calcium sulfate, 1.5 molar waters are removed over the temperature range of 80-100^{o}C, and 0.5 molar water are removed between 100-140^{o}C. We obtained the best enthalpy data using a closed DSC pan with a pin hole heating at a rate of 10°C /min. The total enthalpy of transition from $CaSO_4 \cdot 2H_2O$ to $CaSO_4$ is 104.34 kJ/mol. The transition enthalpies for the two dehydration steps are 79.58 kJ/mol and 24.84 kJ/mol. These values are within –6%, -1%, and -17% calculated using heating formation and heat capacity.

To enhance the solubility of metal in carbon dioxide, we used a small amount of water and a surfactant. The surfactant was a high performance perfluoropolyether. We studied the solubility of copper (II) nitrate trihydrate ($Cu(NO_3)_2 \cdot 3H_2O$). Combining water and surfactant enhances the solubility of Cu^{2+} in supercritical carbon dioxide. The solubility of copper (II) nitrate trihydrate as a function of pressure was measured using excess water and surfactant at 60^{o}C. The solubility increases as the pressure increases.

The influence of parameters including extraction pressure, extraction temperature, amount of chelate used, amount of water used, molar ratio of chelate to metal on the solubility of chloride hexahydrate($MgCl_2 \cdot 6H_2O$) were examined. Equilibrium is reached within 30 min. The amount of Mg^{2+} removed from the sample did not change with different initial loading. The best extraction results were obtained when the molar ratio of chelate to metal is greater than 5, chelate concentration greater than 1% by weight and water concentration greater than 0.15% by weight. Once the minimum surfactant and water ratio is reached, increasing the surfactant and water has an insignificant effect on the solubility. The solubility of $MgCl_2 \cdot 6H_2O$ at different pressures and temperatures was

detemined using the optimum concentration of water and chelate. The solubility increases with increasing temperature and pressure.

Finally, we used a thermodynamic model incorporating conventional mixing rules and the Peng-Robinson equation of state (EOS) to model chelate complex solubility in supercritical carbon dioxide. We confirmed this modeling approach by fitting naphthalene/carbon dioxide (organic compound/carbon dioxide system) and cupric acetylacetonate/carbon dioxide (inorganic compound/carbon dioxide system) data provided by Paulaitis [1] and Cross [2]. We obtained the model parameters (Tc, Pc, v_s, P^{sat} and k_{12}) for Cu-$(PFPECOO)_2$ and Mg-$(PFPECOO)_2$ by fitting experimental data using the Marquardt-Levenberg least squares (MLLS) method. Good agreement between experimental and calculated results was achieved. The solubility estimated with the experimental data by this model is quite well. For the system, Mg-$(PFPECOO)_2/CO_2/H_2O$, we determined Tc, Pc, v_s, P^{sat} and k_{12} from the experimental solubility data. At different temperature, we found K_{12} to be a function of temperature.

Recommendations

Measure exit CO_2 in screening for soluble species and dehydration studies

Currently, the solubility screening and dehydration studies of hydrated species were performed using an ISCO SFX220 supercritical fluid extraction system. The supercritical carbon dioxide is pumped through the extraction cell at a flow rate about 1 ml/min. Approximately one gram of sample was weighted and placed in the extraction cell. The extraction cell was weighed before and after extraction to detect mass change.

Analyses water in the exit carbon dioxide steam will give the material balance. Therefore, it may further confirm the results.

Reaction studies

Another possible path to obtain water in Martian soil would be through the reaction of serpentine (magnesium silicate hydroxide) with supercritical carbon dioxide. Serpentine can react with carbon dioxide at 350^{o}C as [3].

$$Mg_3Si_2O_5(OH)_4 + 3CO_2 = 3MgCO_3 + 2SiO_2 + 2H_2O \quad (3\text{-}1)$$

In our work, our ISCO SFX220 supercritical fluid extraction system has a limit of 150^{o}C. We can study this reaction in supercritical carbon dioxide if the extraction system is modified to a sufficiently high temperature.

Determined the solubility of metal-chelate using a different substrate

The current substrate for our experiment is filter paper. The samples were spiked with an amount of the metal solution onto the filter paper and then were mounted inside a stainless extraction cartridge. Other substrates might be used.

Model development

Although the fit to the experimental data was good using the thermodynamic model, the major disadvantage of this method is the lack of parameters for the pure metal-chelate complex. It will be very useful if that parameter were directly measured independently or estimated using a group contribution approach.

References

1. Stanleyi. Sandler. Chemical and Engineering Thermodynamics. Wiley Series in Chemical Engineering. P171, P466, data, **1989**.

2. Cross W, Akgerman A., Erkey C. Determination of Metal-chelate Complex Solubilities in Supercritical Carbon Dioxide. *Ind. Eng. Chem. Res*., **1996**, 35, 1765.

3. Ron Zevenhoven. Mineral Carbonation for Long-term CO_2 Storage:an Exergy Analysis. *Int.J. Thermodynamics*, **2004**, **7**, 23.

APPENDIX

APPENDIX A: EXPERIMENTAL SETTINGS AND ACCURACIES

Table A.1: ISCO SFX220 supercritical fluid extraction system settings and accuracies

Flow Rate:	1 cc/min
Flow Rate Accuracy:	± 0.5%(maximun 0.5μl/min seal leakage)
Temperature:	25°C ~ 145°C
Temperature Accuracy:	± 0.5% measuring range
Pressure:	50bar ~ 280bar
Pressure Accuracy:	± 2% of full scale

Table A.2: Differential Scanning Calorimeters and Thermo Gravimetric Analysis setting and accuracies

Differential Scanning Calorimeters		Thermo Gravimetric Analysis	
N_2 flow Rate:	90 cc/min	Weight Sensitivity:	0.1 mg
Heating Rate:	10°C /min	N_2flowRate:	120cc/min
Temperature Accuracy:	± 0.1°C	Heating Rate:	10°C /min
Calorimetric Sensitivity:	± 0.2μW		
Baseline Noise:	± 0.1μW		

APPENDIX B. DATA OF SCREENING FOR SOLUBLE SPECIES OF SIMULATED MARTIAN REGOLITH AND INORGANIC COMPOUNDS IN SUPERCRITICAL CARBON DIOXIDE EXTRACTION

Minerals	Pressure (bar)	Extraction cell and sample before extraction (mg)	Extraction cell and sample after extraction (mg)
Simulated Martian regolith at 120 °C	60	166.1275 166.1545 166.1745	165.9102 166.0170 166.0363
	90	165.9730 166.0741 166.2946	165.8547 165.9440 166.1334
	150	166.0356 165.7495 166.2946	165.9019 165.6638 166.1264
	250	166.0567 166.2946 166.3946	165.9850 166.1534 166.2534
Simulated Martian regolith at 35 °C	60	166.1462 165.2981 166.0480	166.0879 165.2145 166.0017
	90	166.1783 165.7814 166.1454	166.1186 165.7297 166.0850
	150	166.0675 166.1638 165.6905	166.0012 166.1005 165.6602
	250	166.0184 166.1987 166.0740	165.9630 166.1352 166.0130
$Fe(NH_4)_2(SO_4)_2 \cdot 12H_2O$ at 35 °C	60	166.0055 166.1917 166.2015	165.9745 166.1500 166.1590
	90	166.3069 165.8050 166.1564	166.2543 165.7843 166.1275
	150	166.0776 166.0546 166.1730	165.9554 165.9503 166.0600
	250	166.1572 165.8694 166.2648	166.0357 165.7937 166.1190
$FeSO_4 \cdot 7H_2O$ at 35 °C	60	165.8957 166.0365 166.3005	165.7492 165.8600 166.0375

	90	166.0746 165.9862 166.2050	165.7565 165.6804 165.8389
	150	166.0964 166.3847 166.1576	165.7800 165.9505 165.8350
	250	166.3305 166.1204 166.2110	165.9177 165.7354 165.9000
$FeSO_4 \cdot 7H_2O$ at 60 °C	200	166.0735 166.1877 166.1359	165.8513 165.9647 165.8988
$FeSO_4 \cdot 7H_2O$ at 100 °C	200	166.3561 166.1233 166.0673	165.8729 165.7513 165.7585
$FeSO_4 \cdot 7H_2O$ at 150 °C	200	166.2871 166.1770 166.1116	165.8211 165.7952 165.7577
$Fe(NO_3)_3 \cdot 9H_2O$ at 35 °C	60	166.0457 166.0472 166.1603	165.9793 165.9875 166.0879
	90	166.2508 166.1643 166.3766	166.0982 166.0590 166.2375
	150	165.9938 166.0448 166.0748	165.8956 165.8932 165.9477
	250	166.0648 166.2578 166.1705	165.9293 166.1195 166.0513
$Fe(NH_4)_2(SO_4)_2 \cdot 6H_2O$ at 35 °C	90	166.1266 166.1096 166.3773	166.0723 166.0556 166.2977
	150	166.1184 166.2176 165.9665	166.0492 166.1411 165.9188
$Fe(NH_4)_2(SO_4)_2 \cdot 6H_2O$ at 60 °C	90	166.1750 166.1756 166.0667	166.0476 166.0513 165.9697
$Fe(NH_4)_2(SO_4)_2 \cdot 6H_2O$ at 90 °C	90	166.3767 166.1985 166.0768	166.1451 165.9873 165.8820
Serpentine at 35 °C	150	165.8788 166.1047 166.3901	165.8779 166.1050 166.3900

Serpentine at 120 °C	60	166.1750 166.0084 166.1095	166.1417 165.9776 166.0840
	90	166.0983 165.9896 166.2659	166.0665 165.9545 166.2358
	120	166.1976 166.1754 166.1945	166.1683 166.1439 166.1443
Serpentine at 140 °C	60	165.6738 166.0365 166.2746	165.6502 166.0075 166.2458
	90	166.1957 166.0084 166.1856	166.1652 165.9740 166.1619
	120	166.0078 166.1954 166.1187	165.9764 166.1623 166.0956
NH_4HF_2 at 35 °C	150	166.1785 166.1421 165.8966	166.1287 166.1023 165.8590
$CoCl_2 \cdot 6H_2O$ at 35 °C	150	166.1768 166.1725 166.2657	166.0484 166.0360 166.1184
$CuSO_4 \cdot 5H_2O$ at 35 °C	150	166.3647 166.0472 165.7832	166.1494 165.8959 165.6673
$FeCl_2 \cdot 4H_2O$ at 35 °C	150	165.5892 166.1351 166.3846	165.5478 166.0283 166.2520
$MnSO_4 \cdot 5H_2O$ at 35 °C	150	166.0746 166.1735 166.2865	165.9845 166.1004 166.1718
$Ni(NO_3)_2 \cdot 5H_2O$ at 35 °C	150	166.1284 166.1987 166.1438	166.0262 166.1041 166.0372
$CaSO_4 \cdot 2H_2O$ at 35 °C	150	166.1689 166.3745 166.0488	166.1284 166.3224 166.0071
$CaCl_2$ at 35 °C	150	166.2734 166.1638 166.0947	166.2702 166.1601 166.0837
$AgNO_3$ at 35 °C	150	166.1845 166.0352 166.2730	166.1842 166.0355 166.2730

NH_4SO_4 at 35 °C	150	166.0583 166.2740 166.2835	166.0284 166.2564 166.2646
NaI at 35 °C	150	166.0856 166.0462 166.1648	166.0832 166.0465 166.1650
$K_2Cr_2O_7$ at 35 °C	150	166.0128 166.1854 166.1842	166.0047 166.1742 166.1746
$(NH_4)_2MoO_4$ at 35 °C	150	166.0389 166.1947 166.1264	166.0048 166.1706 166.1104
$CuCl_2$ at 35 °C	150	166.0934 166.1945 166.1379	166.0930 166.1958 166.1375
$FeCl_3$ at 35 °C	150	166.2037 166.1804 166.1258	166.2037 166.1800 166.1255

APPENDIX C: DSC AND TGA DATA OF SIMULATED MARTIAN REGOLITH

Temperature (°C)	Heat flow (W/g)	Time (min)	Weight % (35°C)	Weight % (120°C)
30	-0.29	0	100.00	100.0
35	-0.29	2	99.70	98.00
40	-0.29	4	99.30	96.50
45	-0.30	6	99.10	95.10
50	-0.32	8	99.10	94.00
55	-0.33	10	99.00	93.50
60	-0.34	12	99.00	93.40
65	-0.36	14	99.00	93.40
70	-0.38	16	99.00	93.30
75	-0.40	18	99.00	93.30
80	-0.42	20	99.00	93.30
85	-0.45	22	99.00	93.30
90	-0.48	24	99.00	93.20
95	-0.51	26	99.00	93.20
100	-0.55	28	99.00	93.20
105	-0.60	30	99.00	93.20
110	-0.66	32	99.00	93.20
115	-0.70	34	99.00	93.10
120	-0.75	36	99.00	93.10
125	-0.79	38	99.00	93.10

130	-0.82	40	98.99	93.00
135	-0.83	42	98.99	93.00
140	-0.83	44	98.99	93.00
145	-0.82	46	98.98	93.00
150	-0.80	48	98.98	92.99
155	-0.78	50	98.98	92.99
160	-0.75	52	98.97	92.99
165	-0.73	54	98.97	92.99
170	-0.71	56	98.97	92.99
175	-0.69	58	98.97	92.99
180	-0.67	60	98.97	92.99
185	-0.64			
190	-0.62			
195	-0.60			
200	-0.58			
205	-0.55			
210	-0.53			
215	-0.51			
220	-0.49			
225	-0.48			
230	-0.46			
235	-0.44			
240	-0.42			
245	-0.40			
250	-0.39			
255	-0.38			
260	-0.37			
265	-0.37			
270	-0.36			
275	-0.35			
280	-0.34			
285	-0.34			
290	-0.33			
295	-0.32			
300	-0.31			
305	-0.31			
310	-0.30			
315	-0.29			
320	-0.29			
325	-0.29			
330	-0.29			
335	-0.29			
340	-0.29			
345	-0.29			

APPENDIX D: TGA DATA OF FERROUS SULFATE CALCIUM SULFATE

T (°C)	Weight % of ferrous sulfate at 1 °C/min	Weight % of ferrous sulfate at 5 °C/min	Weight % of ferrous sulfate at 10 °C/min	T (°C)	Weight % of calcium sulfate at 1 °C/min	Weight % of calcium sulfate at 10 °C/min
30	99.78	99.70	99.72	50	100.00	100.00
40	97.23	98.39	98.70	55	100.00	100.00
50	88.27	96.15	97.88	60	100.00	100.00
60	85.49	94.64	97.83	65	100.00	100.00
70	85.32	94.39	97.80	70	100.00	99.99
80	84.79	93.89	97.60	75	100.00	99.98
90	83.38	92.74	96.39	80	99.99	99.97
100	80.81	90.86	93.99	85	98.81	99.94
110	77.21	87.81	88.43	90	94.94	99.85
120	72.90	82.66	81.16	95	88.57	99.55
130	70.55	77.03	78.35	100	83.83	98.88
140	69.92	75.58	77.53	105	82.77	97.72
150	69.37	75.03	77.05	110	82.77	96.01
160	68.98	74.69	76.68	115	82.61	93.75
170	68.93	74.43	76.39	120	82.55	90.94
180	68.84	74.21	76.13	125	82.29	87.71
190	68.74	74.00	75.90	130	81.70	84.47
200	68.62	73.81	75.68	135	81.00	82.66
210	68.37	73.25	75.46	140	80.80	81.44
220	67.86	72.58	75.19	145	80.79	81.37
230	67.37	72.13	74.57	150	80.77	81.32
240	66.74	71.53	73.92	155	80.76	81.27
250	66.14	70.92	73.64	160	80.75	81.23
260	65.75	70.45	73.43	165	80.73	81.20
270	65.34	70.12	72.97	170	80.73	81.17
280	64.37	69.43	71.92	175	80.72	81.15
290	63.55	68.62	71.57	180	80.70	81.12
300	63.48	68.47	71.55	185	80.70	81.10
310	63.45	68.41	71.53	190	80.69	81.02
320	63.41	68.35	71.50	195	80.65	81.02
330	63.32	68.29	71.48	200	80.64	81.02
340	63.23	68.23	71.45	205	80.60	81.02
350	63.22	68.20	71.42	210	80.55	81.02
				215	80.55	81.00
				220	80.54	80.99
				225	80.50	80.98
				230	80.48	80.97
				235	80.44	80.95
				240	80.44	80.95

APPENDIX E: DSC DATA OF FERROUS SULFATE AND CALCIUM SULFATE

T (°C)	Heat flow (W/g) [1]	Heat flow (W/g) [2]	T (°C)	Heat flow (W/g) [3]	Heat flow (W/g) [4]	Heat flow (W/g) [5]
0	-0.27	-0.365	53	-0.15	-0.2	-0.25
5	-0.28	-0.427	55	-0.15	-0.2	-0.25
10	-0.29	-0.538	57	-0.15	-0.202	-0.2477
15	-0.29	-1.35	59	-0.15	-0.203	-0.26
20	-0.3	-2.577	61	-0.15	-0.205	-0.27
25	-0.3019	-1.856	63	-0.15	-0.206	-0.27
30	-0.3562	-1.071	65	-0.15	-0.208	-0.26
35	-0.3495	-1.464	67	-0.15	-0.209	-0.257
40	-0.3631	-2.073	69	-0.15	-0.211	-0.253
45	-0.3762	-2.878	71	-0.15	-0.213	-0.253
50	-0.3928	-3.55	73	-0.15	-0.215	-0.253
55	-0.44	-3	75	-0.15	-0.217	-0.258
60	-0.4564	-2.482	77	-0.153	-0.22	-0.26
65	-0.5064	-2.068	79	-0.155	-0.22	-0.268
70	-0.8843	-1.761	81	-0.157	-0.225	-0.275
75	-1.597	-1.453	83	-0.161	-0.229	-0.28
80	-0.6831	-1.151	85	-0.166	-0.235	-0.289
85	-0.6339	-0.923	87	-0.175	-0.24	-0.298
90	-0.7161	-0.689	89	-0.186	-0.25	-0.31
95	-0.8484	-0.589	91	-0.2	-0.26	-0.32
100	-1.084	-0.557	93	-0.21	-0.277	-0.337
105	-1.757	-0.514	95	-0.219	-0.2997	-0.356
110	-4.644	-0.387	97	-0.226	-0.332	-0.38
115	-3.515	-0.339	99	-0.235	-0.378	-0.41
120	-4.495	-0.308	101	-0.248	-0.444	-0.45
125	-3.569	-0.292	103	-0.266	-0.532	-0.506
130	-1.926	-0.2814	105	-0.291	-0.63	-0.57
135	-0.4877	-0.2803	107	-0.326	-0.711	-0.644
140	-0.3133	-0.2795	109	-0.378	-0.778	-0.72
145	-0.2985	-0.279	111	-0.451	-0.847	-0.8
150	-0.2923	-0.2785	113	-0.5454	-0.919	-0.88
155	-0.2862	-0.2781	115	-0.6386	-0.99	-0.98
160	-0.2833	-0.2777	117	-0.703	-1.01	-1.08
165	-0.2814	-0.2773	119	-0.7417	-1	-1.19
170	-0.2803	-0.277	121	-0.7765	-0.981	-1.29
175	-0.2795	-0.277	123	-0.8321	-0.969	-1.36
180	-0.279	-0.28	125	-0.9162	-0.98	-1.38
185	-0.2785	-0.289	127	-1.0277	-1.02	-1.36
190	-0.2781	-0.327	129	-1.16	-1.09	-1.32
195	-0.2777	-0.403	131	-1.302	-1.19	-1.3
200	-0.2773	-0.556	133	-1.439	-1.323	-1.3
205	-0.2770	-0.905	135	-1.544	-1.484	-1.336

210	-0.2770	-0.962	137	-1.581	-1.674	-1.409
215	-0.2767	-0.919	139	-1.502	-1.889	-1.521
220	-0.2763	-0.659	141	-1.275	-2.11	-1.676
225	-0.2756	-0.588	143	-0.9052	-2.31	-1.876
230	-0.2741	-0.649	145	-0.4966	-2.432	-2.121
235	-0.2755	-1.019	147	-0.3116	-2.416	-2.407
240	-0.2737	-1.071	149	-0.2786	-2.228	-2.711
245	-0.2764	-1.028	151	-0.2982	-1.896	-2.989
250	-0.2897	-0.974	153	-0.3148	-1.517	-3.175
255	-0.3272	-0.904	155	-0.3329	-1.184	-3.211
260	-0.3809	-0.828	157	-0.3531	-0.894	-3.06
265	-0.4473	-0.769	159	-0.3751	-0.635	-2.74
270	-0.5308	-0.705	161	-0.3997	-0.504	-2.29
275	-0.6331	-0.643	163	-0.4263	-0.5	-1.771
280	-0.7507	-0.58	165	-0.4558	-0.524	-1.251
285	-0.8732	-0.508	167	-0.4878	-0.55	-0.826
290	-0.9790	-0.451	169	-0.5227	-0.58	-0.6115
295	-1.0390	-0.388	171	-0.5608	-0.617	-0.53
300	-1.0350	-0.336	173	-0.6016	-0.661	-0.513
305	-0.9741	-0.3	175	-0.6431	-0.711	-0.57
310	-0.8954	-0.2617	177	-0.6786	-0.769	-0.617
315	-0.8670	-0.2557	179	-0.6491	-0.834	-0.66
320	-1.0070		181	-0.2999	-0.908	-0.71
325	-1.1350		183	-0.209	-0.991	-0.77
330	-1.1280		185	-0.173	-1.08	-0.83
335	-0.5824		187	-0.159	-1.165	-0.91
340	-0.2634		189	-0.15	-1.196	-1
345	-0.2617		191	-0.15	-1.117	-1.1
350	-0.2557		193	-0.15	-0.945	-1.234
			195	-0.15	-0.531	-1.378
			197	-0.15	-0.3624	-1.531
			199	-0.15	-0.296	-1.662
			201	-0.15	-0.261	-1.692
			203	-0.15	-0.24	-1.551
			205	-0.15	-0.22	-1.138
			207	-0.15	-0.21	-0.67
			209	-0.15	-0.21	-0.46
			211	-0.15	-0.2	-0.37
			213	-0.15	-0.19	-0.32
			215	-0.15	-0.19	-0.3
			217	-0.15	-0.19	-0.28
			219	-0.15	-0.19	-0.27
			221	-0.15	-0.19	-0.26
			223	-0.15	-0.19	-0.25
			225	-0.15	-0.19	-0.245
			227	-0.15	-0.19	-0.24

			229	-0.15	-0.19	-0.235
			231	-0.15	-0.19	-0.235
			233	-0.15	-0.19	
			235	-0.15	-0.19	
			237	-0.15	-0.19	
			239	-0.15	-0.19	
			241	-0.15	-0.19	

[1]Ferrous sulfate using closed pan at 10 °C /min
[2]Ferrous sulfate using open pan at 10 °C /min
[3]Calciun sulfate using closed pan at 5 °C /min
[4]Calciun sulfate using closed pan at 10 °C /min
[5]Calciun sulfate using closed pan at 15 °C /min

APPENDIX F: EQUILIBRIUM EXTRACTION DATA OF Cu(NO3)2·3H2O IN SUPERCRITICAL CARBON DIOXIDE[1].

Pressure (bar)	Time (min)	Cu^{2+} Concentration (mg/L)		
		Run 1	Run 2	Run 3
[2] 150	30	1.871	1.952	2.070
150	60	1.967	1.958	2.063
150	90	1.783	1.950	1.975
[3] 120	30	19.521	19.826	19.704
130	30	18.768	19.041	18.972
140	30	18.240	18.036	17.833
150	30	16.897	16.751	16.390
160	30	16.222	16.077	16.153
170	30	15.990	15.914	16.303
180	30	15.781	15.682	16.147
200	30	14.282	14.526	15.072
230	30	13.928	13.369	13.288
250	30	12.545	12.423	12.179

[1]Extraction temperature is 60 °C. Mole ration of PFPE to water is 0.006. The concentration of copper solution is 34.9741g/L.
[2] Initial volume of copper solution is 20 μl.
[3] Initial volume of copper solution is 60 μl.
Caculation example:

The samples were prepared by spiking 20 μl of $Cu(NO_3)_2$ solution onto the substrate. The concentration of this solution is 34.9741g/L. The measurements of extraction of $Cu(PFPECOO)_2$ in CO_2 were made at constant pressure (150 bar) and constant temperatures (60°C) for a 30 min static step. Analyzed value for Cu^{2+} using an

AA (atomic absorption spectrometer) is 1.871 mg/l. The molar mass of $Cu(NO_3)_2 \cdot 3H_2O$ is 241.6. The molar mass of $Cu(NO_3)_2$ is 187.6. The molar mass of Cu is 63.6.

Initial $Cu(NO_3)_2 \cdot 3H_2O$ on the substrate: 20 μl × 34.9741g/L = 0.6995 mg
Initial $Cu(NO_3)_2$ on the substrate: 0.6995 mg × 187.6 ÷ 241.6 = 0.5434 mg
Initial Cu^{2+} on the substrate: 0.5434 mg × 63.6 ÷ 187.6 = 0.1842 mg
Cu^{2+} on the substrate after extraction: 25 ml × 1.871 mg/l =0.04678 mg
Cu^{2+} removed after extraction: 0.1842-0.04678=0.1374 mg
Cu^{2+} removed % after extraction: 0.1374÷ 0.1842 × 100% = 74.6 %

APPENDIX G-1: Equilibrium extraction data of $MgCl_2 \cdot 6H_2O$ in supercritical carbon dioxide (T=60°C, P=150 bar,V=20 μl).

t(min)	Mg^{2+}Concentration (mg/L)		
	Run 1	Run 2	Run 3
30	6.484	6.291	6.522
60	6.383	6.383	6.445
90	6.476	6.429	6.337

APPENDIX G-2: Equilibrium extraction data of $MgCl_2 \cdot 6H_2O$ as a function of molar ratio of chelate to metal in supercritical carbon dioxide (T=60°C, P=150 bar, V=10μl).

Molar ratio of chelate to metal	Mg^{2+}Concentration (mg/L)		
	Run 1	Run 2	Run 3
0.37	3.072	3.087	3.118
0.74	3.060	3.079	3.107
1.11	3.037	3.014	3.029
1.48	2.995	2.983	3.033
1.86	2.909	2.894	2.913
2.23	2.852	2.859	2.867
2.60	2.786	2.816	2.801
2.97	2.763	2.759	2.778
3.34	2.755	2.743	2.732
3.71	2.739	2.736	2.732
4.09	2.705	2.700	2.713
4.46	2.678	2.666	2.709
4.83	2.705	2.647	2.686
5.20	2.686	2.670	2.697
5.57	2.705	2.689	2.666

APPENDIX G-3: Equilibrium extraction data of $MgCl_2 \cdot 6H_2O$ as a function of chelate concentration in supercritical carbon dioxide (T=60°C, P=150 bar, V=10µl).

Chelate %	Mg^{2+}Concentration (mg/L)		
	Run 1	Run 2	Run 3
0	3.864	3.864	3.864
0.04	3.519	3.512	3.551
0.06	3.425	3.408	3.389
0.09	3.342	3.377	3.331
0.13	3.254	3.261	3.215
0.16	3.139	3.114	3.188
0.32	2.916	2.875	3.126
0.80	2.700	2.759	2.803
1.11	2.690	2.687	2.726
1.64	2.701	2.651	2.701
1.98	2.694	2.693	2.635
2.33	2.685	2.699	2.672

APPENDIX G-4: Equilibrium extraction data of $MgCl_2 \cdot 6H_2O$ as a function of water concentration in supercritical carbon dioxide (T=60°C, P=150 bar, V=10µl).

Water %	Mg^{2+}Concentration (mg/L)		
	Run 1	Run 2	Run 3
0	3.671	3.709	3.709
0.039	2.970	3.037	3.091
0.08	2.766	2.894	2.821
0.12	2.734	2.695	2.655
0.16	2.659	2.713	2.628
0.20	2.622	2.621	2.643
0.24	2.640	2.633	2.600
0.28	2.621	2.633	2.600
0.32	2.612	2.633	2.633
0.36	2.631	2.633	2.633
0.40	2.611	2.633	2.633
0.44	2.590	2.633	2.633
0.48	2.657	2.633	2.633
0.52	2.616	2.633	2.633
0.56	2.621	2.633	2.593
0.60	2.621	2.633	2.600

APPENDIX G-5: Equilibrium extraction data of $MgCl_2 \cdot 6H_2O$ as a function of pressure in supercritical carbon dioxide (T=60°C, V=10μl).

Pressure (bar)	Mg^{2+}Concentration (mg/L)		
	Run 1	Run 2	Run 3
100	3.481	3.440	3.502
110	3.383	3.362	3.447
120	3.285	3.292	3.245
130	3.123	3.086	3.032
140	2.967	2.932	2.926
150	2.683	2.727	2.748
160	2.488	2.512	2.552
170	2.415	2.320	2.368
180	2.2043	2.164	2.120
190	2.0400	2.026	2.203
200	2.0311	2.083	1.963
210	1.9204	1.892	1.852
220	1.8005	1.767	1.728
230	1.6873	1.729	1.708
240	1.6444	1.627	1.584
250	1.6124	1.569	1.563

Extraction of $MgCl_2 \cdot 6H_2O$ in CO_2 at different times was made at constant pressure (150 bar) and constant temperature (60°C). The extraction samples were prepared by spiking 20μl of $MgCl_2 \cdot 6H_2O$ solution to the filter paper. The concentration of this solution is 8.1700g/100mL. The molar mass of $MgCl_2 \cdot 6H_2O$ is 203. The molar mass of $MgCl_2$ is 95. The molar mass of Mg is 24. The molar mass of chelate is 600. Mole ratio of chelate to metal is 5. Molar ratio of chelate to water is 0.003 (1g chelate/10ml water).

Initial $MgCl_2 \cdot 6H_2O$ on the substrate: 20 μl × 81.700g/L = 1.6340 mg
= 0.008049 mmol

Initial $MgCl_2$ on the substrate: 1.6430 mg × 95 ÷ 203 = 0.7647 mg
= 0.008049 mmol

Initial Mg^{2+} on the substrate: 0.5434 mg × 24 ÷ 95 = 0.1932 mg
= 0.008049 mmol

Chelate used: Mole ratio of chelate to metal × n_{Mg} = 5 × 0.008049 = 0.04025 mmol

$= 0.04025 \times 600 = 24.15$ mg

Water used: $n_{chelate} \div$ molar ratio of chelate to water $= 0.04025\text{mmol} \div 0.003$

$= 13.42$ mmol $= 13.42 \times 18 = 241.5$ mg

CO_2 used: $n_{CO2} = 0.1276$ mol $= 5.6144$ g

Chelate % $= 24.15 \times (24.15+241.5+5614.4) \times 100\% = 0.41\%$

Water % $= 241.5 \times (24.15+241.5+5614.4) \times 100\% = 4.1\%$